

Poultry Litter Ash as an Alternative Fertilizer Source for Corn

Clara Ray Ervin

Dissertation submitted to the faculty of the Virginia Polytechnic Institute and State University in
partial fulfillment of the requirements for the degree of

Doctor of Philosophy In
Crop and Soil Environmental Sciences

Mark S. Reiter, Committee Chair
Brooks Whitehurst
Rory O. Maguire
Wade E. Thomason
Charlie W. Cahoon, Jr.
Garnett Whitehurst

September 5, 2019

VIRGINIA POLYTECHNIC INSTITUTE AND STATE UNIVERSITY
Eastern Shore Agricultural Extension and Research Center; Painter, Virginia

Keywords: corn, electron scanning microscopy (ESM), phosphorus (P), poultry litter (PL),
poultry litter ash (PLA), potassium (K), nitrogen (N), and X-ray absorption near edge structure
spectroscopy (XANES).

Poultry Litter Ash as an Alternative Nutrient Source for Corn Production

Clara Ray Ervin

ABSTRACT

Poultry litter ash (PLA) is a co-product from manure-to-energy systems that originated in response to increased poultry litter (PL) volumes generated in concentrated poultry production regions. Investigating PLA as a crop fertilizer is an alternative solution to balancing poultry and crop regional nutrient cycling in the Commonwealth of Virginia. As the expanding world population places pressure on the poultry industry to meet consumption demands, increased PL production presents an obstacle to identify alternative uses for increased volumes. Currently, Virginia produces 44 million broilers with PL produced predominately in the Shenandoah Valley and Eastern Shore. Likewise, a growing world population places pressure on crop production areas and subsequently finite natural resources used for crop fertilization. Poultry litter ash is an alternative phosphorus (P) and potassium (K) source enhancing transportation logistics, repurposing PL nutrients, and offers dual purpose as a fertilizer and an energy source when compared to PL.

Three PLA products [(fluidized bed bulk (FB Bulk), fluidized bed fly (FB Fly), and combustion Mix (CMix)], two manufactured co-products [(granulated poultry litter ash (GPLA), and ash coated urea (ACU)] were evaluated as P, K, and N sources for corn (*Zea Mays L.*) production in comparison to industry fertilizers [(PL, triple superphosphate (TSP), muriate of potash (KCL), and urea). A comprehensive examination of elemental composition, P speciation, P and K solubility, improved functionality into granulized forms, and field testing were conducted to discern PLA potential as an alternative fertilizer source.

Poultry litter ash products were evaluated by total elemental analysis, backscatter-electron dispersive (BSED) microscopy, and X-ray absorption near edge structure (XANES) spectroscopy. Poultry litter ash elemental concentrations were highly variable ranging from 50.6 to 102.0 g P kg⁻¹ and 62.6 to 120.0 g K kg⁻¹ and were comparatively higher than PL concentrations. Phosphorus structures that provided and controlled P solubility were Ca and Ca-Mg-phosphate compounds. Spectroscopy confirmed Ca structures as predominately monetite (dicalcium phosphate anhydrous; CaHPO₄; log K ° 0.30) and brushite (dicalcium phosphate dihydrate; CaHPO₄·2H₂O; 0.63 log K °) species that were supported by BSED and elemental stoichiometric ratios (Ca:P; 1.12 to 1.71:1). Additionally, GPLA acidified from FB Fly had higher brushite and monetite percentages described by spectra models, translating into a more soluble Ca-phosphate species when compared to FB Fly original P species.

Granulated poultry litter acidulation trials successfully identified a desired granulation point of 29% (14.5 g acid to 50 g PLA) phosphoric acid (75% H₃PO₄) acidulation. Acidulation dose response relationships created simple linear regression (SLR) equations that sufficiently (R² > 0.80) described changes in total measurable P and water soluble P, pH, and exothermic reaction temperatures to increasing H₃PO₄ acidulation. Solubility tests included: sequential extraction, particle size effect on solubility, carbon effect on water soluble P, and Mehlich-1 extraction of PLA sources that confirmed decreased P solubility. A majority PLA P was found in bound plant unavailable fractions (87.7 to 97.7% P of total P). Granulated poultry litter ash had improved P plant available P of 36.0% P of total P. Carbon (C) effects on PLA P were examined by ashing PLA samples in a muffle furnace at 550 °C. Differences in total carbon content negatively impacted FB Bulk and CMix total P (1.30 and 4.56 g P kg⁻¹); however, muffle furnace temperatures increased FB Fly total P by 6.74 g P kg⁻¹.

All fertilizer products were investigated under field conditions in separate P, K and N corn studies across Virginia coastal plain soils to determine fertilizer effects on corn plant parameters [(most mature leaf (V6), corn ear leaf (R1), and grain (R6)]. Poultry litter P treatments, averaged over rate, recorded highest yield in both years. At eight of nine field sites, FB Bulk resulted in numerically or significantly higher Mehlich-1 concentrations than other P sources post-harvest. Although Mehlich-1 P increased, yield and plant parameters did not; which leads to the conclusion that PLA sources increased soil residual P that did not translate into immediate plant availability recorded within a growing season. Across plant efficacy parameters examined, PLA K is a comparable nutrient source and improved plant parameters when compared to control. Eighteen out of twenty-one plant parameters examined found similar ACU and urea effects on N concentrations. Therefore, ACU is a comparable N source to urea. When compared to industry fertilizer sources, we concluded that PLA is a slowly available P source, decreased P availability negatively affected early plant growth, K is a comparable nutrient source and improved plant parameters compared to control, and ACU effectively provided N to maintain sufficient corn growth. In conclusion, PLA co-products serve as a densified nutrient source that may provide plant available nutrients if processed to aid in nutrient distribution to grain producing areas.

Poultry Litter Ash as an Alternative Nutrient Source for Corn Production

Clara Ray Ervin

ABSTRACT GENERAL AUDIENCE ABSTRACT

Poultry litter ash (PLA) is a co-product from manure-to-energy systems that originated in response to increased poultry litter (PL) volumes generated in concentrated poultry production regions. Investigating PLA as an alternative crop fertilizer is essential to balancing poultry and crop regional nutrient cycling in the Commonwealth of Virginia. As the expanding world population places pressure on the poultry industry to meet consumption demands, heightened PL production presents an obstacle to identify alternative uses for increased volumes. Currently, Virginia produces 44,683,904 broilers with PL produced predominately in the Shenandoah Valley and Eastern Shore. Likewise, a growing world population places pressure on crop production areas and subsequently finite natural resources used for fertilization vital to maintaining crop yields. Poultry litter ash, a co-product from manure-to-energy systems, is an alternative phosphorus (P) and potassium (K) source enhancing transportation logistics, repurposing PL nutrients, and offers dual purpose as a fertilizer and an energy source when compared to PL.

In this dissertation, three PLA products [(fluidized bed bulk (FB Bulk), fluidized bed fly (FB Fly), and combustion Mix (CMix)], two manufactured co-products [(granulated poultry litter ash (GPLA), and ash coated urea (ACU)] were evaluated as P, K, and N source for corn (*Zea Mays L.*) production in comparison to industry fertilizers (PL, triple superphosphate (TSP), muriate of potash (KCL), and urea). Each of the following chapters provides a comprehensive examination of the following topics: elemental composition, P speciation, P and K solubility,

improved functionality into granulized forms, and field testing designed to provide parameters to conclude PLA potential as an alternative P, K and N source.

In the second chapter, PLA products were evaluated by total elemental analysis, backscatter-electron dispersive (BSED) microscopy, and X-ray absorption near edge structure (XANES) spectroscopy. Poultry litter ash elemental concentrations are highly variable and are comparatively higher than PL concentrations. Phosphorus structure and species identified Ca as the primary element controlling P structure and subsequent solubility. The third component of this dissertation is granulation trials investigating phosphoric acid effects on granulizing and increasing total and water soluble P. Our results identified 29% (14.5 g acid to 50 g PLA) phosphoric acid acidulation for desired granule size. The third dissertation component examines PLA solubility. The results demonstrated PLA decreased P water solubility when compared to industry fertilizer sources. Granulated poultry litter ash demonstrated improved P plant availability due to the granulation process.

The final and fourth dissertation components investigated PLA sources under field conditions in separate P, K and N corn studies across Virginia coastal plain soils to determine fertilizer effects on corn plant parameters. Minority of plant parameters tested revealed P control yielded numerically higher P concentrations than PLA P sources tested. Poultry litter P treatments, averaged over rate, recorded highest yield in both years. At eight of nine field sites, FB Bulk resulted in numerically or significantly higher Mehlich-1 concentrations than other P sources post-harvest. Although Mehlich-1 P concentrations increased, yield and plant parameters did not; which leads to the conclusion that PLA sources increased soil residual P that did not translate into immediate plant availability recorded within a growing season. Across plant efficacy parameters examined, PLA K is a comparable nutrient source and improved plant

parameters when compared to controls. The majority of plant parameters examined found similar ACU and urea effects on N concentrations. Therefore, ACU is a comparable N source to urea. When compared to industry fertilizer sources, field results concluded that PLA is a slowly available P source, decreased P availability negatively affected early plant growth, K is a comparable nutrient source and improve plant parameters compared to control, ACU effectively provides N to maintain sufficient corn growth. In conclusion, PLA co-products serve as a densified nutrient source that may provide plant available nutrients if processed to aid in nutrient distribution to grain producing areas.

Dedication

This dissertation is dedicated in memory of my grandpa the late Troy D. Korn. “Let us not forget that the cultivation of the earth is the most important labor of man. When tillage begins, other arts follow. The farmers, therefore, are the founders of human civilization” (Webster, D.). Additional dedication to my parents John and Jill Ervin. And special dedication to my future husband, Blake Millsaps, with whom I will share this degree.

Acknowledgements

Foremost I would like to express my sincere gratitude to my major professor, Mark S. Reiter, Ph.D., for the present opportunity, mentorship, and guidance during my research program. Additional thanks to my committee members: Drs. Rory Maguire, Wade Thomason, Charlie Cahoon, and Garnett Whitehurst. A special thanks to Dr. Brooks Whitehurst for weekly phone calls, jokes, and superior alchemy knowledge. A huge thanks for assistance, companionship, and good humor by Kim Mills and John Mason of the Virginia Tech ESAREC Soils research team. Thanks are also due to my undergraduate advisors Dr. Sandy Maddox, Amy Johnson, and Stephen Edwards at the University of Mount Olive. The guidance and opportunities provided at UMO were irreplaceable. A special thanks to my fellow graduate students, friends, and family for supporting me through my Ph.D. work. Thanks are also due to my parents, John and Jill Ervin, for instilling faith and a work ethic that has carried me through my doctorate program. Blake Millsaps and the Millsaps family for their support. Additional, thanks to collaborating farmers across the Commonwealth for the opportunity to conduct field trials on their property as well as many thanks for being the 2% of the population that grows our food. Many thanks to the faculty and staff at the Eastern Shore AREC. Drs. Amy Shober (University of Delaware) and Kirk Scheckel (U.S. EPA) for the awesome opportunity to utilize XANES spectroscopy on our fertilizer products. Steve McCartney of the Virginia Tech Institute for Critical Technology and Applied Science (ICTAS) for assistance in conducting electron microscopy work. Athena Tilley of the VT soil testing lab. Last but certainly not least, Dr. Ozzie Abaye for her unwavering student mentorship and sincere devotion to agriculture research.

Table of Contents

List of Tables.....	xviii
List of Figures	xxii
Abbreviations List	xxiv
Chapter 1: Poultry Litter Ash Literature Review	1
Introduction	1
Agriculture Production Systems effect on Regional Nutrient Cycling.....	1
Background of the Chesapeake Bay.....	3
Manure-to-Energy Systems.....	6
Finite Mineral Fertilizer Resources.....	7
Poultry Litter Ash Fertilizer Characteristics	9
References	15
Chapter 2: Poultry Litter Ash and Co-Products Elemental and Chemical Composition.....	19
Abstract	19
Introduction	21
Materials and Methods.....	28
Poultry Litter Ash Sources	28
Elemental and Chemical Composition Analysis.....	29
Electron Microscopy Elemental Analysis and Physical Structure Identification	29
Poultry Litter Ash Phosphorus Speciation via XANES Spectroscopy	30
Statistical and Data Analysis.....	32
Results and Discussion	32
Elemental and Chemical Composition Analysis.....	32
Electron Microscopy Elemental Analysis and Physical Structure Identification	34
Poultry Litter Ash Phosphorus Speciation via XANES Spectroscopy	39
Conclusion.....	42
References	45
Chapter 3: Granulated Poultry Litter Ash Acidulation and Physical Characteristics	72
Abstract	72
Introduction	74
Materials and Methods.....	78
Poultry Litter Ash Acidulation.....	78
Bulk Granular Manufacturing.....	79
Physical Characteristic Analysis	80
Statistical Analysis	81
Results and Discussion	81
Poultry Litter Ash Acidulation.....	81
Granulated Poultry Litter Ash-Bulk Granular Manufacturing.....	84

Physical Evaluation of Granulated Poultry Litter Ash.....	86
Conclusions	88
Chapter 4: Delineating Factors influencing Poultry Litter Ash Nutrient Solubility	107
Abstract	107
Introduction	109
Materials and Methods.....	115
P Solubility Using Sequential Extractions	115
Phosphorus Species and Solubility Identification via XANES Spectroscopy	116
Poultry Litter Ash and Industry Fertilizer Mehlich-1 P Extractions.....	117
Muffle Furnace Protocol	118
Particle Size Effect on Water Soluble Phosphorus	118
Statistical Analysis	118
Results and Discussion	119
Poultry Litter Ash and Industry Standard Fertilizer Characteristics prior to Sequential Extraction	119
Poultry Litter Ash and Industry Standards Fertilizers Characteristics after Sequential Extraction	119
X-ray Absorption Near Edge Structure Spectroscopic PLA P Species Solubility.....	122
Poultry Litter Ash and Industry Fertilizers Mehlich-1 P Extractions	125
Muffle Furnace.....	127
Particle Size Effect on Water Soluble Phosphorus	128
Conclusions	129
References	131
Chapter 5: Poultry Litter Ash as an Alternative Nutrient Source for Corn Production	149
Abstract	149
Introduction	151
Materials and Methods.....	155
Experimental Design.....	155
Sample Analysis	156
Statistical Analysis	157
Results and Discussion	157
Phosphorus	157
Phosphorus Source and Rate Effects on Corn Yield.....	157
Phosphorus Source and Rate Effect on Plant Tissue and Grain P Concentrations	159
Phosphorus Sources Effect on Mehlich-1 Soil Test P after Harvest.....	162
Potassium	165
Potassium Source Effect on Corn Yield.....	165

Potassium Source Effect on Plant Tissue and Grain K Concentrations	165
Potassium Source Effect on Mehlich-1 Soil Test K after Harvest	166
Nitrogen.....	167
Nitrogen Source Effect on Corn Yield.....	167
Nitrogen Source Effect on Plant Tissue and Grain N Concentrations	167
Conclusions	169
References	171
Chapter 6: Conclusions	206

List of Tables

Table 2.1 Phosphorus K-XANES spectra phosphate standards used in linear combination fitting.	49
Table 2.2a Total elemental analysis of broiler litter converted into poultry litter ash (PLA) via fluidized bed combustion system in Rhodesdale, MD producing fluidized bed fly (FB Fly), fluidized bed bulk (FB Bulk), granulated poultry litter ash (GPLA), and ash coated urea (ACU) and from combustion thermo-conversion system in Lancaster county, PA producing combustion mix (CMix).	50
Table 2.2b Total elemental analysis of broiler litter converted into poultry litter ash (PLA) via fluidized bed combustion system in Rhodesdale, MD producing fluidized bed fly (FB Fly), fluidized bed bulk (FB Bulk), granulated poultry litter ash (GPLA), and ash coated urea (ACU) and from combustion thermo-conversion system in Lancaster county, PA producing combustion mix (CMix).	51
Table 2.2c Total elemental analysis of broiler litter converted into poultry litter ash (PLA) via fluidized bed combustion system in Rhodesdale, MD producing fluidized bed fly (FB Fly), fluidized bed bulk (FB Bulk), granulated poultry litter ash (GPLA), and ash coated urea (ACU) and from combustion thermo-conversion system in Lancaster county, PA producing combustion mix (CMix).	52
Table 2.3 Electron scanning microscopy back scatter overview elemental analysis of broiler litter converted into poultry litter ash (PLA) via fluidized bed combustion system in Rhodesdale, MD producing fluidized bed fly (FB Fly), fluidized bed bulk (FB Bulk), granulated poultry litter ash (GPLA), and ash coated urea (ACU) and from combustion thermo-conversion system in Lancaster county, PA producing combustion mix (CMix).	53
Table 2.4 Electron scanning microscopy back scatter electron dispersive physical structure identification providing average elemental analysis of fluidized bed bulk (FB Bulk) selected structures.	54
Table 2.5 Electron scanning microscopy back scatter electron dispersive physical structure identification providing average elemental analysis of fluidized bed fly (FB Fly) selected structures.	55
Table 2.6 Electron scanning microscopy back scatter electron dispersive physical structure identification providing average elemental analysis of combustion mix (CMix) selected structures.	56
Table 2.7 Electron scanning microscopy back scatter electron dispersive physical structure identification providing average elemental analysis of granulated poultry litter ash (GPLA) selected structures.	57
Table 2.8 Linear combination fitting weight percentage of standards describing spectra poultry litter ash P spectra fitting.	58
Table 2.9 Selected poultry litter ash elemental properties that were used for XANES analysis. .	59
Table 3.1 GPLA-Acd1 acidulation ratio calculations.	95
Table 3.2 GPLA-Acd2 acidulation ratio calculations.	96
Table 3.3 EPA 3050B digested fertilizer total elemental analysis of fluidized bed fly (FB Fly), granulated poultry litter ash-bulk (GPLA-B), and granulation poultry litter ash-acidulation 2 (GPLA-Acd2).	97

Table 3.4 Fertilizer physical characteristics of granulated poultry litter ash-bulk (GPLA-B) compared to industry standard triple superphosphate (TSP) and original poultry litter ash (PLA), fluidized bed fly (FB Fly).....	98
Table 4.1 Sequential extraction operationally defined P fractions and data notation explanation.	136
Table 4.2 Phosphorus K-XANES spectra phosphate standards used in linear combination fitting.	137
Table 4.3 Poultry litter ash and co-products total elemental analysis via EPA 3050 B.	138
Table 4.4 Experiment 1: Sequential poultry litter ash, triple superphosphate (TSP), and poultry litter (PL) extraction delineating operationally defined P fractions.....	139
Table 4.5 Experiment 2: Sequential poultry litter ash, granulated poultry litter ash (GPLA), and triple superphosphate (TSP) extraction delineating operationally defined P fractions...	140
Table 4.6 Experiment 3: Sequential poultry litter ash poultry litter extraction delineating operationally defined K fractions.....	141
Table 4.7 Experiment 4: Sequential poultry litter ash poultry litter extraction delineating operationally defined K fractions.....	142
Table 4.8 Linear combination fitting (LCF) weight percentage of standards describing poultry litter ash P spectra fitting.	143
Table 4.9 Selected poultry litter ash elemental properties that were used for XANES analysis.	144
Table 4.10 Poultry litter ash and triple superphosphate Mehlich-1 fertilizer extraction.	145
Table 4.11 Muffle furnace (550 °C) effect on poultry litter ash carbon loss and changes in total and water soluble P.	146
Table 4.12 Poultry litter ash particle size distribution and particle size effect on water soluble P.	147
Table 4.13 Poultry litter ash particle size effect on water soluble P.	148
Table 5.1 Poultry litter ash corn field site locations, soil series, nutrient concentrations, and studies conducted in Virginia in 2017 and 2018.....	174
Table 5.2 Total elemental analysis of broiler litter converted into poultry litter ash (PLA) via fluidized bed combustion system in Rhodesdale, MD producing fluidized bed fly (FB Fly), fluidized bed bulk (FB Bulk), granulated poultry litter ash (GPLA), and ash coated urea (ACU) and from combustion thermo-conversion system in Lancaster county, PA producing combustion mix (CMix).	175
Table 5.3 Poultry litter ash phosphorus (P), potassium (K), and nitrogen (N) field study treatments in 2017 and 2018 for Virginia corn field studies.	176
Table 5.4 Corn yield response to P control, poultry litter (PL), triple superphosphate (TSP), combustion mix (CMix), and fluidized bed bulk (FB Bulk) sources averaged over P rate in 2017.	177
Table 5.5 Corn yield response to P control, poultry litter (PL), triple superphosphate (TSP), combustion mix (CMix), and fluidized bed bulk (FB Bulk) sources averaged over P rate in 2017 sites.	178
Table 5.6 Corn yield response to P control, poultry litter (PL), triple superphosphate (TSP), granulated poultry litter ash (GPLA), and fluidized bed bulk (FB Bulk) sources averaged over rate in 2018.	179
Table 5.7 Corn yield response to P control, poultry litter (PL), triple superphosphate (TSP), granulated poultry litter ash (GPLA), and fluidized bed bulk (FB Bulk) sources averaged over rate in 2018 sites.	180

Table 5.8a Most mature V6 corn leaf (MM), corn ear leaf (CE), and corn grain P concentrations as effected by P sources ((fluidized bed bulk (FB Bulk), combustion mix (CMix), poultry litter (PL), and triple superphosphate (TSP)) averaged over rate in 2017.	181
Table 5.8b Most mature V6 corn leaf (MM), corn ear leaf (CE), and corn grain P concentrations as effected by P sources ((fluidized bed bulk (FB Bulk), combustion mix (CMix), poultry litter (PL), and triple superphosphate (TSP)) averaged over rate in 2017.	182
Table 5.9 Most mature V6 corn leaf (MM), corn ear leaf (CE), and corn grain P concentrations as effected by phosphorus (P) rate 0, 9.8, 19.6, and 29.3 kg P ha ⁻¹ averaged over P sources in 2017.	183
Table 5.10 Most mature V6 corn leaf (MM), corn ear leaf (CE), and corn grain phosphorus (P) concentrations as effected by P sources including: P control, fluidized bed bulk (FB Bulk), granulated poultry litter ash (GPLA), poultry litter (PL), and triple superphosphate (TSP) averaged over P rate in 2018.	184
Table 5.11 Most mature V6 corn leaf (MM), corn ear leaf (CE), and corn grain phosphorus (P) concentrations as effected by P rate 0, 9.8, 19.8, 29.3 kg P ha ⁻¹ averaged over P sources in 2018.	185
Table 5.12 Mehlich-1 soil test (0-15 cm) phosphorus (P) levels as effected by P sources ((fluidized bed bulk (FB Bulk), combustion mix (CMix), poultry litter (PL), and triple superphosphate (TSP)) averaged over P rate in 2017.	186
Table 5.13 Mehlich-1 soil test (0-15 cm) phosphorus (P) levels as effected by P sources ((fluidized bed bulk (FB Bulk), combustion mix (CMix), poultry litter (PL), and triple superphosphate (TSP)) averaged over P rate in 2017 sites.	187
Table 5.14 Mehlich-1 soil test (0-15 cm) phosphorus (P) levels as effected by P rate 0, 9.8, 19.6, 29.3 kg P ha ⁻¹ averaged over P sources in 2017.	188
Table 5.15 Mehlich-1 soil test (0-15 cm) phosphorus (P) levels as effected by P rate 0, 9.8, 19.6, 29.3 kg P ha ⁻¹ averaged over P sources in 2017 sites.	189
Table 5.16 Mehlich-1 soil test (0-15 cm) phosphorus (P) levels as effected by P sources ((fluidized bed bulk (FB Bulk), granulated poultry litter ash (GPLA), poultry litter (PL), and triple superphosphate (TSP)) averaged over P rate in 2018.	190
Table 5.17 Mehlich-1 soil test (0-15 cm) phosphorus (P) levels as effected by P sources ((fluidized bed bulk (FB Bulk), granulated poultry litter ash (GPLA), poultry litter (PL), and triple superphosphate (TSP)) averaged over P rate in 2018 sites.	191
Table 5.18 Corn yield response to potassium (K) sources K control, fluidized bed fly (FB Fly), fluidized bed bulk (FB Bulk), combustion mix (CMix), poultry litter (PL), and muriate of potash (KCL) in 2017 and 2018.	192
Table 5.19 Corn yield response to potassium (K) sources K control, fluidized bed fly (FB Fly), fluidized bed bulk (FB Bulk), combustion mix (CMix), poultry litter (PL), and muriate of potash (KCL) in 2017 and 2018.	193
Table 5.20a Most mature V6 corn leaf (MM), corn ear leaf (CE), and corn grain K concentrations as effected by potassium (K) sources K control, fluidized bed fly (FB Fly), fluidized bed bulk (FB Bulk), combustion mix (CMix), poultry litter (PL), and muriate of potash (KCl) in 2017.	194
Table 5.20b Most mature V6 corn leaf (MM), corn ear leaf (CE), and corn grain K concentrations as effected by potassium (K) sources K control, fluidized bed fly (FB Fly), fluidized bed bulk (FB Bulk), combustion mix (CMix), poultry litter (PL), and muriate of potash (KCl) in 2017.	195

Table 5.21 Most mature V6 corn leaf (MM), corn ear leaf (CE), and corn grain K concentrations as effected by potassium (K) sources K control, fluidized bed fly (FB Fly), fluidized bed bulk (FB Bulk), combustion mix (CMix), poultry litter (PL), and muriate of potash (KCl) in 2018.	196
Table 5.22 Mehlich-1 soil test (0-15 cm) potassium (K) concentrations by poultry litter ash K sources including: K control, fluidized bed fly (FB Fly), fluidized bed bulk (FB Bulk), combustion mix (CMix), poultry litter (PL), and muriate of potash (KCl).	197
Table 5.23 Mehlich-1 soil test (0-15 cm) potassium (K) concentrations by poultry litter ash K sources including: K control, fluidized bed fly (FB Fly), fluidized bed bulk (FB Bulk), combustion mix (CMix), poultry litter (PL), and muriate of potash (KCl).	198
Table 5.24 Corn yield response to nitrogen (N) sources including: N control, ash coated urea (ACU), and urea (CO(NH ₂) ₂) utilized as starter and side dress N in 2017.	199
Table 5.25 Corn yield response to nitrogen (N) sources including: N control, ash coated urea (ACU), and urea (CO(NH ₂) ₂) utilized as starter and side dress N in 2017 sites.	200
Table 5.26 Corn yield response to nitrogen (N) sources including: N control, ash coated urea (ACU), urea (CO(NH ₂) ₂), urea starter with ACU at side dress (Urea/ACU), and ACU starter with urea at side dress (Urea/ACU) in 2018.	201
Table 5.27 Corn yield response to nitrogen (N) sources including: N control, ash coated urea (ACU), urea (CO(NH ₂) ₂), urea starter with ACU at side dress (Urea/ACU), and ACU starter with urea at side dress (Urea/ACU) in 2018 sites.	202
Table 5.28a Corn plant tissue (most mature (MM), corn ear leaf (CE), and grain) response to nitrogen (N) sources including: N control, ash coated urea (ACU), and urea (CO(NH ₂) ₂) utilized as starter and side dress N in 2017 sites.	203
Table 5.28b Corn plant tissue (most mature (MM), corn ear leaf (CE), and grain) response to nitrogen (N) sources including: N control, ash coated urea (ACU), and urea (CO(NH ₂) ₂) utilized as starter and side dress N in 2017 sites.	204
Table 5.29 Corn plant tissue (most mature (MM), corn ear leaf (CE), and grain) response to nitrogen (N) sources including: N control, ash coated urea (ACU), and urea (CO(NH ₂) ₂) utilized as starter and side dress N in 2018 sites.	205

List of Figures

Figure 2.1 Diagram illustrating protocol implemented to examine poultry litter ash (PLA) samples via electron microscopy (ESM) backscatter electron dispersive (BSED) analysis. First, two regions (a) were chosen for overview elemental analysis of each sample. Then specific structures (b) within each region were identified for multipoint structural analysis.....	60
Figure 2.2 Fluidized bed bulk (FB Bulk) backscatter electron dispersive (BSED) elemental analysis of multipoint identified structures (Pts. 1.1, 1.2, and 1.3).	61
Figure 2.3a Fluidized bed fly (FB Fly) backscatter electron dispersive (BSED) elemental analysis of multipoint identified structures (Pts. 2.1 and 2.2).	62
Figure 2.3b Fluidized bed fly (FB Fly) backscatter electron dispersive (BSED) elemental analysis of multipoint identified structures (Pt 2.3).....	63
Figure 2.3c Fluidized bed fly (FB Fly) backscatter electron dispersive (BSED) elemental analysis of multipoint identified structures (Pt 2.4).....	64
Figure 2.4a Combustion mix (CMix) backscatter electron dispersive (BSED) elemental analysis of multipoint identified structures (Pt 3.1).....	65
Figure 2.4b Combustion mix (CMix) backscatter electron dispersive (BSED) elemental analysis of multipoint identified structures (Pts. 3.2, 3.3, and 3.4).	66
Figure 2.5 Granulated poultry litter ash (GPLA) backscatter electron dispersive (BSED) elemental analysis of multipoint identified structures (Pts. 4.1 and 4.2).....	67
Figure 2.6 Linear combination fitting (LCF) results of P K-edge X-ray absorption near-edge structure (XANES) spectra of fluidized bed fly (FB Fly) poultry litter ash. The spectra of the reference standards represent the relative proportion of each standard describing sample spectra species.	68
Figure 2.7 Linear combination fitting (LCF) results of P K-edge X-ray absorption near-edge structure (XANES) spectra of fluidized bed bulk (FB Bulk) poultry litter ash. The spectra of the reference standards represent the relative proportion of each standard describing sample spectra species.	69
Figure 2.8 Linear combination fitting (LCF) results of P K-edge X-ray absorption near-edge structure (XANES) spectra of combustion mix (CMix) poultry litter ash. The spectra of the reference standards represent the relative proportion of each standard describing sample spectra species.	70
Figure 2.9 Linear combination fitting (LCF) results of P K-edge X-ray absorption near-edge structure (XANES) spectra of granulated poultry litter ash (GPLA) poultry litter ash. The spectra of the reference standards represent the relative proportion of each standard describing sample spectra species.....	71
Figure 3.1 Diagram adapted from Sastry and Fuerstenau (1972) illustrating granulation via coalescence.	99
Figure 3.2 Diagram adapted from Sastry and Fuerstenau (1972) depicting nucleation, the first step in fertilizer granulation.....	100
Figure 3.3 Granulated poultry litter ash (GPLA-Acd1) phosphoric acid (H ₃ PO ₄) effect on temperature (°C) recorded at one and two minutes during mixing.	101
Figure 3.4 Phosphoric (H ₃ PO ₄) acidulation effect on water soluble P (WSP), total P (TP) and pH for granulated poultry litter acidulation trial 1 (GPLA-Acd1).....	102

Figure 3.5 Total and water soluble P solubilized by phosphoric acid (H₃PO₄) acidulation for granulated poultry litter ash acidulation trial 1 (GPLA-Acd1). Solubilized P in this calculation is defined as P amount previously unavailable that was increased by H₃PO₄. The calculation subtracts original P amount from original FB Fly of WSP 0.62 and TP 50.63 g P kg⁻¹ as well as subtracts P amount from each H₃PO₄ acidulation percentage. 103

Figure 3.6 Granulated Poultry Litter Ash acidulation trial 2 (GPLA-Acd2) visual effect on granule size. 104

Figure 3.7 Granulated Poultry Litter Ash acidulation trial 2 (GPLA-Acd2) effect on granule size. 105

Figure 3.8 Granulated poultry litter ash acidulation trial 2 (GPLA-Acd 2) effect on water soluble (WSP) and total phosphorus (TP) (g P kg⁻¹). 106

Abbreviations List

ACU	Ash Coated Urea
BE	Binding Energy
BSED	Back Scatter Electron Dispersive
CMix	Combustion Mix
DRP	Dissolved Reactive Phosphorus
ESAREC	Eastern Shore Agricultural Research and Extension Center
ESM	Electron Scanning Microscopy
FB Bulk	Fluidized Bed Bulk
FB Fly	Fluidized Bed Fly
GPLA	Granulated Poultry Litter Ash
GPLA-Acd1	Granulated Poultry Litter Ash Acidulation 1
GPLA-Acd2	Granulated Poultry Litter Ash Acidulation 2
GPLA-B	Granulated Poultry Litter Ash Acidulation Bulk
K	Potassium
KCl	Potassium Chloride
KP	Potassium Phosphate
LCF	Linear Combination Fitting
N	Nitrogen
P	Phosphorus
PL	Poultry Litter
PLA	Poultry Litter Ash
RP	Rock Phosphate

SLR	Simple Linear Regression
TMA	Turkey Manure Ash
TP	Total Phosphorus
TSP	Triple Superphosphate
WSP	Water Soluble Phosphorus
XANES	X-ray Absorption Near Edge Structure Spectroscopy

Chapter 1: Poultry Litter Ash Literature Review

Introduction

The United States' integrated poultry industry is expanding research and infrastructure to meet growing world populations and consumption demands. Increasing poultry production heightens needs to balance agronomic and environmental poultry litter (PL) utilization and nutrient distribution (Sharpley, 1994; Sims et al., 1998; Slaton et al., 2004). Commonly, PL generated is sold or used as a fertilizer within localized areas of poultry production because PL is not easily transported due to bulkiness, low nutrient density, and associated transportation costs beyond nutrient concentrated areas (Sharpley, 1994; Pelletier et al., 2001). Examining regional agricultural nutrient cycling across production areas revealed obvious disproportional nutrient cycling between concentrated livestock and crop production areas (Sims et al., 1998; Slaton et al., 2004). Crop regions remained in a nutrient deficit status as nutrients removed in grain are rarely returned, albeit only from inorganic fertilizers, as surplus manure nutrients build in livestock production regions due to transportation difficulties (Slaton et al., 2004).

Agriculture Production Systems effect on Regional Nutrient Cycling

Disrupted nutrient distribution within the USA is caused by large distances between crop and livestock production areas. Major crop production regions remain nutrient deficit as surplus nutrients from manure build in livestock production regions due to transportation difficulties. For instance, in 2016, poultry produced on the DELMARVA peninsula consumed more than 3.11 million metric tons of grain consistently exceeding grain amounts produced in the region, causing average corn (*Zea Mays L.*) and soybean (*Glycine max L.*) imports to total 354,000 and 202,000 metric tons, respectively (Delmarva Poultry Industry, 2017). Phosphorus associated with imported grains is metabolized into meat and eggs and is exported for consumption, while undigested P is found in considerable quantities in PL (9 to 22 g P kg⁻¹ total P) (Havlin et al.,

2014). Unlike grain, PL is rarely shipped 80 to 160 km beyond original source due to low bulk density per nutrient value of PL 0.37 g cm^3 and ~ 9 to 22 g P kg^{-1} total P vs. triple superphosphate (TSP) 1.09 g cm^3 and approximately $201.0 \text{ g P kg}^{-1}$, causing PL to be land applied in close proximity to poultry production (Pelletier et al., 2001; Reiter and Daniel 2013; Havlin 2014). Maguire et al. (2007) conducted a mass balance estimate of P generated from livestock manures, and identified that 78% of US counties fall into lowest manure P production of less 0 to 15 kg P ha^{-1} while 22% of counties produced greater than $15 \text{ kg manure P ha}^{-1}$. The authors conclude that mass balance calculations demonstrated that animal production and subsequent manure P generated is concentrated in a small percentage of counties across the US (Maguire et al. 2007). Due to PL undesirable low bulk density, rarely PL nutrients are redistributed to crop production regions where soils are left in a nutrient deficit relying on mined and synthetic fertilizers (i.e. Coastal Plain regions of Virginia) to replace grain removed nutrients.

In high density poultry production regions, such as the Shenandoah Valley and Eastern Shore, poultry operations produce high PL volumes contributing to concentrated nutrient areas. The Shenandoah Valley Region (Rockingham, Page, Shenandoah, and Augusta counties) and the Eastern Shore (Accomack county) accounted for 80% of broiler chickens in Virginia with surrounding tributaries feeding into the Chesapeake Bay watershed (USDA, 2017). On average, broilers produced 0.562 kg of PL per bird according to Coufal et al. (2006). The anticipated increase in PL production prompted economic analysis by Pelletier et al. (2001) examining economic feasibility and PL transportation logistics to redistribute nutrients from concentrated to nutrient deficit areas within the Commonwealth. Pelletier et al. (2001) concluded PL can be transported and applied at competitive cost to commercial fertilizers within the breakeven

transportation distance outside of poultry production regions. Results calculated PL transported 122 to 161 km from the Shenandoah Valley would cost a subsidy program \$3.97 a metric ton⁻¹ (in 2019 due to inflation rate transportation would cost approximately \$5.75 metric ton⁻¹) (Pelletier et al., 2001). Concluding remarks recommended research investigating alternative PL uses that could provide a solution for increased PL volumes beyond a transportation subsidy program (Pelletier et al., 2001). In effort to redistribute PL nutrients, manure-to-energy systems have been investigated as an alternative method to convert PL into poultry litter ash (PLA) condensing P nutrients 4 to 10 times while creating a green energy source (Crozier et al., 2009; Pagliari et al., 2009; Codling, 2013; Middleton, 2015). Densifying nutrients into PLA increases shipping potential; however, PLA fine particulate physical characteristics compounded with confirmed decreased nutrient solubility are major obstacles for PLA adoption as a viable fertilizer which can aid in PL nutrient redistribution (Codling, 2006; Middleton, 2015).

Background of the Chesapeake Bay

The Chesapeake Bay watershed spans 165,800 square kilometers encompassing forested, urban, suburban, and agricultural land spanning five physiographic provinces, six states, one district, and eight major watersheds feeding into the sensitive Bay (Gellis et al., 2009). In the Bay watershed region, (Pennsylvania, Virginia, Maryland, New York, Delaware, West Virginia, and the District of Columbia) agricultural land use accounts for 22% of watershed area (EPA, 2010a). According to the Bay Watershed Model, agriculture across the region contributes 44% total N and P loads to the Bay and 65% total sediment loads (EPA, 2010a). The primary concern involving PL is chemical alterations to water quality caused by nutrient runoff or leaching. Excessive nitrate or P can promote eutrophication. Eutrophication is a natural process that accumulates nutrients in surface waters for aquatic growth (Mueller and Helsel, 2016). However, when N and P exceed threshold concentrations in freshwater, excessive algae growth occurs that

later decomposes and reduces oxygen concentrations in water, subsequently causing fish kills. Increased nutrient loading in watersheds is associated with synthetic fertilizer use and confined animal feeding operations (CAFO) that generate large nutrient rich manure quantities (Howarth et al., 2002). Virginia's agricultural N and P pollution has decreased from 9,403,877 kg N and 2,188,129 kg P per year⁻¹ in 2009 to 7,184,903 kg N and 1,460,567 kg P per year⁻¹ in 2017 (Chesapeake Bay Program, 2017). A study examining soil P concentrations influenced by agricultural uses including cash grain, dairy, lawn, and prairie grass landscapes found dairy and cash grain soils with highest mean P concentrations of 75 and 168 mg P kg⁻¹ (Bennett et al., 2005). Examining links between P inputs and exports across the United States, the National Research Council compiled a dataset to increase P source and balance awareness (Metson et al., 2017). On agricultural land across the United States, a net P accumulation rate of 7.5% year⁻¹ created 0.19 Tg P surplus with fertilizer contributing 74% total P agricultural inputs (Metson et al., 2017). Nationally, 92.4% total P applied (1.85 Tg inorganic P and 0.65 Tg manure P) was removed with crop harvest; however, removal rates varied across the U.S. influenced by proximity to CAFO (Metson et al., 2017). The Fertilizer Institute (TFI) reported Virginia's critical P levels according to Bray 1P extractions as 30 ppm (The Fertilizer Institute, 2015). Contrasting TFI critical P levels, the current relative frequency (41.6%) of P concentrations in Virginia is greater than 50 ppm P (The Fertilizer Institute, 2015). The TFI study indicates that a majority of Virginia soils are below threshold concentration's of P. A long-term PL rotation drawdown study on a legacy P soil (Mehlich 1 VH >55 ppm P) in the mid-Atlantic, found that it would take 14 years to reduce Mehlich-1 P concentrations to where P replacement by fertilizer would be needed (Fleming-Wimer et al., 2018). As noted in the study "Very High" soil P is an economic benefit for crop producers as P fertilizer will not be needed for over a decade;

however, limited PL transportation and necessity to land apply PLA complicates nutrient distribution and often exacerbates soil test P concentrations (Pelletier et al., 2001; Fleming-Wimer et al., 2018).

The National Estuarine Eutrophication Assessment report concluded 40% of the nation's estuaries expressed eutrophic conditions and Howarth et al., (2002) predicted by 2020 two out of every three estuaries will have impaired uses (Bricker et al., 1999). Global P fluctuation is estimated by P concentrations in ocean sediment. Estimates of P fluxes before heightened agricultural and industrial production were 8 Tg P yr⁻¹ while current estimates are 22 Tg P yr⁻¹ (Howarth et al., 2002). The National Estuarine Eutrophication Assessment report found 84 of the 138 estuaries studied exhibited moderate to high eutrophic conditions (Bricker et al., 1999). The mid-Atlantic region home to the Chesapeake Bay and surrounding tributaries rated high overall for eutrophic conditions (Bricker et al., 1999).

Recognizing the Chesapeake Bay's vulnerability, state and federal governments in 1988 enacted the Chesapeake Bay Preservation Act addressing non-point source pollution management (VA DEQ). Despite passing the act in 1988, EPA designated the Chesapeake Bay watershed as an "impaired water body" due to sediment and nutrients draining into the Bay (Phillips and Lindsey, 2012). As an impaired water body the EPA mandated the Chesapeake Bay and local waters to adhere a Total Maximum Daily Load (TMDL) which defined maximum amounts of pollution a body of water can receive and still meet water quality standards (EPA, 2010b). The TMDL identified N, P, and sediment as sources of pollution and defined threshold levels from all sources across the Chesapeake Bay watershed as 84.3 million kg N (185.9 million lbs. N), 5.6 million kg P (12.5 million lbs. P), and 2.9 billion kg (6.45 billion lbs.) sediment per year (EPA, 2010b; Chesapeake Bay Program, 2017). The TMDL watershed thresholds were

designed to reduce N, P, and sediment by 25%, 24%, and 20% to restore the Bay by 2025 (EPA, 2010b). Virginia is allocated 24,230,904 kg N per year⁻¹, 2,431,255 kg P per year⁻¹, and 417,409,306 kg sediment per year⁻¹ (EPA, 2010b). Currently, the Chesapeake Bay TMDL 2017 Midpoint Assessment reports Virginia's contribution as total N 26,005,811 kg per year⁻¹ (57,333,000 lbs.), total P per year, 2,831,323 kg (6,242,000 lbs.) and total sediment per year⁻¹ 1,498,983,529 kg (3,304,693,000 lbs.) (Chesapeake Bay Program, 2017).

While legislation provided regulation, guidance and thresholds to reduce nutrient and sediment loading into the Bay; alternative options are needed to recycle and evenly redistribute PL nutrients. Research examining PL economic feasibility, agronomic applications, and environmental implications concluded a solution for heightened PL volumes involves alternative uses (Sharpley, 1994; Pelletier et al., 2001; Bock, 2004a; Middleton, 2015). Solution characteristics require an alternative product which recycles PL nutrients and is proven as a comparable fertilizer source, balances agronomic needs and environmental standards, as well as improves transportation logistics.

Manure-to-Energy Systems

Manure-to-energy systems originated in response to increased manure volumes generated by concentrated poultry production regions within the mid-Atlantic posing a threat to the Chesapeake Bay and surrounding ecosystems. Manure-to-energy systems were identified as a method to condense increased PL volumes into a densified PLA fertilizer product allowing nutrients to be economically shipped beyond poultry production regions (Crozier et al., 2009; Pagliari et al., 2009; Codling, 2013; Middleton, 2015). Numerous manure-to-energy techniques have been reviewed including: anaerobic digestion, pyrolysis, and direct combustion (Kelleher et al., 2002; Middleton, 2015). Each system varies in temperature, anaerobic or aerobic conditions, energy type, equipment cost, and manure co-product type produced (ie. ash, biochar, sludge).

Aerobic PL digestion is an effective process producing 60% methane from collectable biogas mixture (Kelleher et al., 2002). However, sludge produced disqualifies the system due to moisture and high sludge viscosity reducing transportation distances as well as ease for land application (Kelleher et al., 2002). Direct combustion technologies on average produce 13.5 GJ ton⁻¹, which is largely dependent upon combustion system type, temperature, and PL moisture (Kelleher et al., 2002). Co-product produced from this system is an ash material which can be easily transported beyond poultry production regions due to increased bulk density and nutrient densification as well as potential for PLA to be further manufactured into a granulized form for easier land application (Bock, 2004b; Crozier et al., 2009). Poultry litter ash has an increased bulk density 1.5 to 2.5 times greater than PL improving transportation logistics by increased bulk density per nutrient value (Bock, 2004a; Reiter and Middleton, 2016). Densifying PL into PLA allows nutrients to be economically shipped beyond poultry production regions in effort to redistribute nutrients. Utilizing PL as a fuel source in manure-to-energy systems serves a dual purpose, creating a renewable P PLA fertilizer as well as a green energy source in the form of steam or syngas. Nutrients in PLA are four to ten times more concentrated than the original PL source with P analysis suitable as an alternative industry fertilizer (Codling, 2006; Pagliari et al., 2010; Reiter and Middleton, 2016).

Finite Mineral Fertilizer Resources

Unlike N which can be replenished by N fixation or synthetically derived, P once removed from the soil can only be replenished by external P sources. Rock phosphate (RP) ores are the primary parent material for current P fertilizer production. However, RP is a non-renewable mineral in finite supply mined from phosphate deposits across the world. Estimates suggested global P production of environmentally and financially feasible RP will peak in 2033 and known P reserves will be depleted in the next 50 to 100 years with no current identification

of alternative P sources (Cordell et al., 2009). Quantifying RP supply is complicated due to variations in estimating supply (i.e. reserves vs resources), geopolitical constraints as developing countries begin to enter P production, and mined RP quality below heavy metal thresholds (Ayding et al., 2010; Van Kauwenbergh et al., 2013; Scholz et al., 2013). Van Kauwenbergh et al. (2013) extrapolated current P reserve estimates with current P consumption to predict the world has over 300 years of reserve and over 1,400 years of RP available. Despite discrepancies involved in predicting RP supply, it is indisputable RP is a non-renewable resource that will need to be provided by new deposits or alternative P sources to maintain sufficient crop production. If PLA is adopted by grain, oilseed, and vegetable producers, PLA will reduce reliance on finite nonrenewable mineral resources by transferring P resources to where they are most needed versus where they are produced within animal rich production areas. Current manure-to-energy technologies are efficient in converting PL into energy; however, the economic feasibility is contingent upon PLA effectiveness and subsequent adoption as a sustainable P fertilizer source (Bock, 2004).

Economic and technical analysis completed by Bock (2004) elaborated upon PL dual purpose as an electricity and fertilizer source creating a “net zero fuel equation”. In this review, Bock (2004) estimated the equation with projected values of PLA fertilizer between \$25 and \$75 per ton, energy value projected at \$50 per ton of ash, transportation cost \$7.50 per ton of PL, 1.0¢ per kWh, and \$1.00 per 1000 lb. of steam (Bock, 2004a). Poultry litter ash wholesale price was estimated for P with 25% P_2O_5 at \$4.00 per 20 lb of nutrient totaling \$96.00 per ton and K price with 15% K_2O at \$2.00 per 20lb of nutrient totaling \$32.00 per ton (Bock, 2005). Co-product equivalent values were estimated at \$50 per ton for PLA and \$7.50 per ton for PL (Bock, 2005). Estimated transportation cost accounts for PL cleanout and transport to an energy plant

but does not reference a specified distance (Bock, 2004a). Middleton (2015) evaluated PLA as a fertilizer source worth \$384.98 Mg⁻¹ compared to PL valued at \$58.46 Mg⁻¹. Currently, Virginia's Poultry Litter Transport Incentive Program, will subsidize \$15 per ton of PL originating from Page or Rockingham counties (DCR, 2017). Recently, VA Department of Conservation and Recreation in partnership with VA Poultry Federation established a subsidy program to transport PL from Accomack county to crop producing areas of the state (DCR, 2017). Therefore, alternative PL uses such as manure-to-energy could provide an additional method to redistribute nutrients beyond subsidy programs. Bock (2004) predicts transportation cost (cost/ton) will increase with plant size favoring industrial rather than utility energy production. Dual value of PL as energy and fertilizer source will offset PL transportation cost from concentrated areas, however the "net zero equation" relies on marketability and effectiveness of PLA as a fertilizer (Bock, 2004a).

Poultry Litter Ash Fertilizer Characteristics

Poultry litter ash recycles PL as dual purpose energy and fertilizer source, densifying P nutrients 4 to 10 times, and subsequently increases transportation logistics (Middleton, 2015). Research initially investigated PLA as an energy source with ash co-product tested as a dietary feed supplement for poultry production (Akpe et al., 1984). The poultry nutrition bioassay reported ash samples containing 72% P availability (Akpe et al., 1984). Recycling PL nutrients into poultry feedstock's was not readily adapted; however, nutrient concentrations in ash indicated that ash co-products could potentially be utilized as a fertilizer source for crop production (Codling et al., 2002). Nutrient composition in PLA varies depending on litter source, bedding type, poultry feed nutrient concentrations, bird age, and thermo-combustion system (Kunkle et al., 1981; Codling et al., 2002; Coufal et al., 2006; Middleton, 2015). Poultry litter ash nutrient composition is dependent upon thermo-conversion system type. There are several

systems utilized for PL conversion including: direct combustion systems, pyrolysis, fluidized combustion beds, and gasification (Middleton, 2015). A technical challenge associated with PL used as fuel is the moisture content as well as N and S concentrations ten times higher than wood; thereby increasing nitrogen oxide and sulfur oxide emissions (Bock, 2004a). Each manure-to-energy system approaches litter conversion with different tactics addressing challenges associated with converting PL by lowering temperatures, injecting lime, and staggering combustion (Bock, 2004a; Middleton, 2015). The PLA (FB Fly and FB Bulk) utilized in the current study was converted using a fluidized bed combustion (FBC) developed by BHSL <http://www.bhsl.com/> in Limerick, Ireland (BHSL, 2017). The FBC systems were specifically developed for variable moisture content fuels (BHSL, 2017). A fluidized bed of sand is suspended via combustion air $> 593^{\circ}\text{C}$ injected into the bottom of the furnace to stabilize and store heat without constantly relying on outside fuel sources (BHSL, 2017). Depending on site specific needs FBC systems can be configured as combined-heat-and-power (CHP) systems for thermal and electrical generation (BHSL, 2017). Other thermo-conversion systems can convert PL into combustible gas through a two-step process resulting in “syn gas” (carbon monoxide and hydrogen) that can be converted into high quality energy (Buckley and Schwarz, 2003). Thermal gasification relies on chemical processes at temperatures >700 degrees $^{\circ}\text{C}$ with temperature range depending upon material heating value (Buckley and Schwarz, 2003). A report from the Thermal Gasification of Manure located in the Baltic Sea region, cited dry matter of PL is 65 to 80% requiring a heating value of 15.3 Gg t^{-1} (Buckley and Schwarz, 2003; Kuligowski and Luostarinen, 2011).

The main influence hindering widespread adoption of litter-to-energy systems is new technology novelty, awareness, cost, and associated markets developed for PLA use (Buckley

and Schwarz, 2003; Bock, 2004a; Kuligowski and Luostarinen, 2011). Higher bulk density and increased PLA nutrient concentrations resulted in nutrient densities of material ten to seventeen times greater than PL (Bock, 2004a). There are numerous studies reporting PLA nutrient concentration ranges. In a study comparing eleven methods of thermo-conversion systems, Middleton (2015) found P concentrations were 4 to 7 times concentrated, K 2.5 to 5.0 times concentrated, and S 2 to 3 times concentrated. Total elemental concentrations varied between 9.4 to 104.9 g P kg⁻¹, 32.03 to 42.49 g K kg⁻¹, and 9.06 to 162.58 g S kg⁻¹ (Middleton, 2015). Total P concentrations in Codling et al. (2002) found that extractable P were two to three times concentrated and ranged from 76 to 114 g P kg⁻¹ compared to PL concentrations 22.0 to 27 g P kg⁻¹. Nutrient analysis of turkey manure ash (TMA) resulted in citrate soluble P 43 g P kg⁻¹, water soluble K 117 g K kg⁻¹, and S 17 g S kg⁻¹ (Pagliari et al., 2010). The trace elements found in PL include Cu, As, Se, Pb, Hg, and Cd with average concentrations 319, 35, 3.4, 0.31, 0.55 mg kg⁻¹, respectively (Kunkle et al., 1981). Trace elements in PL fluctuate due to components in poultry nutrition, poultry production type, and PL management (Kunkle et al., 1981; Gupta and Charles, 1999). Variation in PLA nutrient solubility concentrations can be explained by differences in ash particle sizes, Adams (2005) notes that as particle size decreased elemental concentrations for P, K, Ca, Mg, Cu, Mn, and Zn increased. Phosphorus nutrient concentrations in PLA increased from 79 g P kg⁻¹ (<2 mm) to 104 g P kg⁻¹ (< 0.25 mm), respectively (Adams, 2005).

Recent PLA studies confirm nutrients within litter co-products are more concentrated than original PL source and further testing is needed to determine optimum application for crop growth (Codling, 2006; Pagliari et al., 2010; Middleton, 2015). In a greenhouse study comparing PLA effectiveness to industry standard potassium phosphate (KP), wheat dry matter yields

harvested at boot stage where equal for both soils amended with PLA and KP (Codling et al., 2002). Two fertilizers sources, PLA and KP, were applied at three rates 0, 39, and 78 kg KP ha⁻¹ resulting in similar P plant tissue concentrations in soils amended with PLA 1.02 to 1.12 g P kg⁻¹ as soils amended with KP 0.90 and 0.89 g P kg⁻¹ (Codling et al., 2002). Alfalfa production in Minnesota sandy and silt loam soils found TMA was an effective source of nutrients in the second year of production with yields similar to fertilizer and greater than control (Pagliari et al., 2009). Reiter et al. (2004) found that soybean and wheat had equal yields and plant tissue concentrations for crops grown on silt loam soils amended with PLA and PL in Arkansas production systems.

Although recent PLA studies consistently confirm PL co-products are more concentrated than original PL source, the same studies conclude a potential agronomic obstacle is lower PLA nutrient solubility (Codling et al., 2002; Codling, 2006; Pagliari et al., 2010; Wells, 2013; Middleton, 2015). Thermo-conversion systems high temperatures decrease PLA nutrient solubility. Lower water solubility translates into slower release of plant available nutrients over longer periods of time. A greenhouse experiment to reduce nutrient leaching was conducted comparing PLA and triple super phosphate (TSP) as a fertilizer source, specifically testing lower PLA solubility to reduce P losses (Wells, 2013). Poultry litter ash applications reduced dissolved reactive phosphorus (DRP) and effluent-total phosphorus (TP) losses by 92% and 69% when compared to TSP, respectively (Wells, 2013). Codling (2006) utilized a modified Hedley fractionation technique to compare extractable fractions of PLA with PL. Effectiveness of modified sequential extraction produced inorganic P (ranked highest to lowest) from PLA in the following order HCl > NaHCO₃ > NaOH = H₂O. Inorganic P from PL was extracted (ranked highest to lowest) in the following order H₂O > HCl > NaHCO₃ > NaOH (Codling, 2006). Inorganic

PLA P extracted by H₂O accounted for 1.45% of total inorganic P, whereas 82% of total inorganic P was removed with HCl extraction (Codling, 2006). Various extractions represent portions of inorganic P. Water and sodium bicarbonate soluble P represented labile inorganic P fractions (Codling, 2006). Sodium hydroxide extractable P is considered moderately labile and HCl extraction is considered moderately stable (Dou et al., 2000; Zhang et al., 2004; Codling, 2006; Negassa and Leinweber, 2009). High solubility is a positive attribute for crop uptake but a negative characteristic as a dissolved pollutant. Comparatively water extractions for inorganic P for PL was 55% and 1.45% for PLA, highlighting lower solubility of inorganic P from PLA (Codling, 2006). An early corn response study referenced slower P dissolution rates from TMA as the cause for decreased corn growth at 24 days after emergence when compared to TSP (Pagliari et al., 2010). However, 38 to 52 days after emergence there was no significant difference in stalk height or diameter (Pagliari et al., 2010). Turkey manure ash and TSP supplied similar quantities of plant available P with similar net P uptake 52 days after emergence (Pagliari et al., 2010). Interpretation of results concluded that lower P solubility in TMA caused slower plant development that did not compensate for the 7 to 8-week interval of reduced P availability when compared to increases in dry matter accumulated by industry fertilizer treatments (Pagliari et al., 2010). Granulated animal waste by-product (AWP) efficacy was tested across three experimental systems including: a greenhouse study with low P soil, a long-term research site with preexisting soil P gradients, and agricultural fields with prior P fertilization (Crozier et al., 2009). Across P gradients results illustrated lower P solubility in AWP, but Crozier et al. (2009) stated that lower solubility may not be an agronomic constraint with repeated application of AWP increasing residual P levels and lower dissolution rates reducing environmental concerns.

Recent studies confirmed PLA co-products have higher P concentrations than PL, the same studies identified two major barriers associated with PLA adoption including application logistics due to fine ash particulate matter and decreased nutrient solubility (Codling, 2006; Crozier et al., 2009; Pagliari et al., 2010; Wells, 2013). Manure-to-energy systems' high conversion temperatures effectively recycle PL, but reduce PLA nutrient solubility (Codling, 2006). Therefore, the project research objectives are to 1) Identify chemical, elemental, and physical characteristics effecting of PLA solubility; 2) To prepare and characterize physical parameters associated with granulated PLA (GPLA); 3) Define PLA solubility fractions and determine factors effecting P solubility; and 4) Compare PLA effects on corn productivity parameters compared to industry standard fertilizers.

References

- Adams, Z. 2005. Comparison of broiler litter, broiler litter ash with reagent grade materials as sources of plant nutrients. M.S. thesis, Auburn University, AL.
- Akpe, M.P., P.E. Waibel, and R.V. Morey. 1984. Bioavailability of phosphorus in poultry litter biomass ash residues for turkeys. *Poult. Sci.* 63(10): 2100–2102.
- Ayding, I., F. Aydin, A. Saydut, G.E. Bakirdere, and C. Hamamci. 2010. Hazardous metal geochemistry of sedimentary phosphate rock used for fertilizer (Mazıdag, SE Anatolia, Turkey). *Microchem. J.* 96: 247–251. doi: 10.1016/j.microc.2010.03.006.
- Bender, R.R., J.W. Haegele, and F.E. Below. 2015. Modern Soybean Varieties' Nutrient Uptake Patterns. *Agron. J.* 99(2): 7–10.
- Bender, R.R., J.W. Haegele, M.L. Ruffo, and F.E. Below. 2013. Modern Corn Hybrids' Nutrient Uptake Pattern. *Agron. J.* 97(1): 7–10.
- Bennett, E.M., S.R. Carpenter, and M.K. Clayton. 2005. Soil phosphorus variability: Scale-dependence in an urbanizing agricultural landscape. *Landsc. Ecol.* 20(4): 389–400. doi: 10.1007/s10980-004-3158-7.
- BHSL. 2017. BHSL Fluidized Bed Combustion. <http://www.bhsl.com/fluidised-bed-combustion-new/> (accessed 4 June 2017).
- Bock, B.R. 2004a. Poultry litter to energy: Technical and economic feasibility. TVA Public Power Institute, Muscle Shoals, AL.
- Bock, B.R. 2004b. Demonstrating optimum fertilizer value of ash from the biomass energy sustainable technology (BEST) demonstration project for swine and poultry manure management. TVA Public Power Institute, Muscle Shoals, AL.
- Bock, B. 2005. Potential for ash value to make or break a poultry litter energy project. http://www.brbock.com/RefFiles/SouthernBioproducts3_23_05.pdf (accessed 29 July 2017).
- Bricker, S.B., C.G. Clement, D.E. Pirhalla, S.P. Orlando, and D.R.G. Farrow. 1999. National estuarine eutrophication assessment: Effects of nutrient enrichment in the nation's estuaries. U.S. Department of Commerce, National Oceanic and Atmospheric Administration, and National Ocean Service.
- Buckley, J.C., and P.M. Schwarz. 2003. Thermal Gasification of Manure: An innovative technology in search of fertile policy. *Environ. Monit. Assess.* 84(1–2): 111–127.
- Chesapeake Bay Program. 2017. Chesapeake progress - 2017 and 2025 Watershed implementation plans (WIPs). <http://www.chesapeakeprogress.com/clean-water/watershed-implementation-plans> (accessed 25 July 2017).

- Codling, E.E. 2006. Laboratory characterization of extractable phosphorus in poultry litter and poultry litter ash. *Soil Sci.* 171(11): 858–864. doi: 10.1097/01.ss.0000228059.38581.97.
- Codling, E.E. 2013. Phosphorus and arsenic uptake by corn, wheat, and soybean from broiler litter ash and egg layer manure ash. *J. Plant Nutr.* 36(7): 1083–1101. doi: 10.1080/01904167.2013.776079.
- Codling, E.E., R.L. Chaney, and J. Sherwell. 2002. Poultry litter ash as a potential phosphorus source for agricultural crops. *J. Environ. Qual.* 31(3): 954–61.
- Cordell, D., J.-O. Drangert, and S. White. 2009. The story of phosphorus: Global food security and food for thought. *Tradit. Peoples Clim. Change* 19(2): 292–305. doi: 10.1016/j.gloenvcha.2008.10.009.
- Coufal, C.D., C. Chavez, P.R. Niemeyer, and J.B. Carey. 2006. Measurement of broiler litter production rates and nutrient content using recycled litter. *Poult. Sci.* 85(3): 398–403. doi: 10.1093/ps/85.3.398.
- Crozier, C.R., J.L. Havlin, G.D. Hoyt, J.W. Rideout, and R. McDaniel. 2009. Three Experimental Systems to Evaluate Phosphorus Supply from Enhanced Granulated Manure Ash. *Agron. J.* 101(4): 880–888. doi: 10.2134/agronj2008.0187x.
- DCR. 2017. Virginia poultry litter transport incentive program. <http://www.dcr.virginia.gov/soil-and-water/nmlitter> (accessed 26 July 2017).
- Delmarva Poultry Industry. 2017. Delmarva meat chickens, soybeans, and corn production and use. <http://www.dpichicken.org/facts/facts-figures.cfm> (accessed 30 August 2018).
- Dou, Z., J.D. Toth, D.T. Galligan, C.F. Ramberg, and J.D. Ferguson. 2000. Laboratory procedures for characterizing manure phosphorus. *J. Environ. Qual.* 29(2): 508–514. doi: 10.2134/jeq2000.00472425002900020019x.
- EPA. 2010a. Section 4: Sources of nitrogen, phosphorus and sediment to the Chesapeake Bay.
- EPA. 2010b. Chesapeake Bay total maximum daily load executive Summary. EPA.
- Fleming-Wimer, C., M.S. Reiter, R.O. Maguire, and S. Phillips. 2018. Long-Term Impacts of Poultry Litter on Soil pH and Phosphorus in No-Till. *Better Crops* 102(2): 21–221. doi: <https://doi.org/10.24047/BC102221>.
- Gellis, A.C., C.R. Hupp, M.J. Pavich, J.M. Landwehr, W.S. Banks, et al. 2009. Sources, transport, and storage of sediment at selected sites in the Chesapeake Bay watershed. U. S. Geological Survey and U.S. Department of the Interior.
- Gupta, G., and S. Charles. 1999. Trace elements in soils fertilized with poultry litter. *Poult. Sci.* 78(12): 1695–1698. doi: 10.1093/ps/78.12.1695.

- Havlin, J., S. Tisdale, W. Nelson, and J. Beaton. 2014. *Soil Fertility and Fertilizers: An Introduction to Nutrient Management*. 8th ed. Pearson, New Jersey.
- Howarth, R.W., A. Sharpley, and D. Walker. 2002. Sources of nutrient pollution to coastal waters in the United States: Implications for achieving coastal water quality goals. *Estuaries Res. Found.* 25(4b): 565–676. doi: <https://doi.org/10.1007/BF02804898>.
- Kelleher, B.P., J.J. Leahy, A.M. Henihan, T.F. Dwyer, D. Sutton, et al. 2002. Advances in poultry litter disposal technology- a review. *Bioresour. Technol.* 83: 27–36. doi: [https://doi.org/10.1016/S0960-8524\(01\)00133-X](https://doi.org/10.1016/S0960-8524(01)00133-X).
- Kuligowski, K., and S. Luostarinen. 2011. *Thermal gasification of manure*. University of Gdansk–POMCERT, Poland.
- Kunkle, W.E., L.E. Carr, T.A. Carter, and E.H. Bossard. 1981. Effect of flock and floor type on the levels of nutrients and heavy metals in broiler litter. *Poult. Sci.* 60(6): 1160–1164. doi: <https://doi.org/10.3382/ps.0601160>.
- Maguire, R.O., D.A. Crouse, and S.C. Hodges. 2007. Diet modification to reduce phosphorus surpluses: A mass balance approach. *J Environ. Qual.* 36: 1235–1240. doi: 10.2134/jeq2006.0551.
- Metson, G.S., J. Lin, J.A. Harrison, and J.E. Compton. 2017. Linking terrestrial phosphorus inputs to riverine export across the United States. *Water Res.* doi: 10.1016/j.watres.2017.07.037.
- Middleton, A.J. 2015. *Nutrient availability from poultry litter co-products*. M.S. thesis, Virginia Polytechnic and State University, Blacksburg, VA.
- Mueller, D.K., and D.R. Helsel. 2016. *Nutrients in the Nation’s Waters--To Much of a Good Thing?* *Natl. Water Quality Assess.* <https://pubs.usgs.gov/circ/circ1136/circ1136.html> (accessed 28 December 2016).
- Negassa, W., and P. Leinweber. 2009. How does the Hedley sequential phosphorus fractionation reflect impacts of land use and management on soil phosphorus: A review. *J. Plant Nutr. Soil Sci.* 172(3): 305–325. doi: 10.1002/jpln.200800223.
- Pagliari, P.H., C.J. Rosen, and J.S. Strock. 2009. Turkey manure ash effects on alfalfa yield, tissue elemental composition, and chemical soil properties. *Commun. Soil Sci. Plant Anal.* 40(17–18): 2874–2897. doi: 10.1080/00103620903173863.
- Pagliari, P., C. Rosen, J. Strock, and M. Russelle. 2010. Phosphorus availability and early corn growth response in soil amended with turkey manure ash. *Commun. Soil Sci. Plant Anal.* 41(11): 1369–1382. doi: 10.1080/00103621003759379.
- Pelletier, B.A., J. Pease, and D. Kenyon. 2001. *Economic Analysis of Virginia Poultry Litter Transportation*. Va. Tech. <https://scholar.lib.vt.edu/ejournals/vaes/01-1.pdf> (accessed 22 December 2016).

- Phillips, S.W., and B.D. Lindsey. 2012. The influence of groundwater on nitrogen delivery to the Chesapeake Bay. U. S. Geol. Surv. <http://md.water.usgs.gov/publications/fs-091-03/html/> (accessed 28 December 2016).
- Reiter, M.S., T.S. Daniel, N.A. Slaton, C.E. Wilson, C.H. Tingle, et al. 2004. Poultry litter ash and raw litter residual effects on wheat and soybeans in an Eastern Arkansas rice, wheat, and soybean rotation. *Wayne E Sabbe Ark. Soil Fertil. Stud.* 2004: 72–77.
- Reiter, M.S., and A. Middleton. 2016. Nutrient availability from poultry litter co-products. Virginia Tech University, Painter, VA.
- Scholz, R.W., A.E. Ulrich, M. Eilitta, and A. Roy. 2013. Sustainable use of phosphorus: A finite resource. *Sci. Total Environ.* 461: 799–803. doi: <https://doi.org/10.1016/j.scitotenv.2013.05.043>.
- Sharpley, A., S.C. Chapra, J.T. Sims, J.T. Wedepohl, T.C. Daniel, et al. 1994. Managing agricultural phosphorus for protection of surface waters: Issues and options. *J. Environ. Qual.*: 437–451. doi: [doi:10.2134/jeq1994.00472425002300030006x](https://doi.org/10.2134/jeq1994.00472425002300030006x).
- Sims, J.T., R.R. Simard, and B.C. Joern. 1998. Phosphorus loss in agricultural drainage: Historical perspective and current research. *J. Environ. Qual.* 27(2): 277–293. doi: [doi:10.2134/jeq1998.00472425002700020006x](https://doi.org/10.2134/jeq1998.00472425002700020006x).
- Slaton, N.A., K.R. Byre, M.B. Daniels, T.C. Daniel, R.J. Norman, et al. 2004. Nutrient input and removal trends for agricultural soils in nine geographic regions in Arkansas. *J. Environ. Qual.* 33(5): 1606–1615. doi: [DOI: 10.2134/jeq2004.16](https://doi.org/10.2134/jeq2004.16).
- The Fertilizer Institute. 2015. Soil test levels in North America. <http://soiltest.ipni.net/charts/distribution> (accessed 24 July 2017).
- USDA. 2012. Census of Agriculture - 2012 Census Publications - State and County Profiles - Virginia. https://www.agcensus.usda.gov/Publications/2012/Online_Resources/County_Profiles/Virginia/ (accessed 30 May 2017).
- Van Kauwenbergh, S.J., M. Stewart, and R. Mikkelsen. 2013. World reserves of phosphate rock... a dynamic and unfolding story. *Better Crops* 97(3): 18–20.
- Virginia Department of Environmental Quality. Chesapeake Bay preservation act. <http://www.deq.virginia.gov/Programs/Water/ChesapeakeBay/ChesapeakeBayPreservationAct.aspx> (accessed 31 May 2017).
- Wells, D. 2013. Poultry litter ash as a phosphorus source for greenhouse crop production. Ph.D. dissertation, Louisiana State University, Baton Rouge, LA.
- Zhang, T.Q., A.F. MacKenzie, B.C. Liang, and C.F. Drury. 2004. Soil Test Phosphorus and Phosphorus Fractions with Long-Term Phosphorus Addition and Depletion. *Soil Sci Soc Am J* 68(2): 519–528. doi: [doi:10.2136/sssaj2004.5190](https://doi.org/10.2136/sssaj2004.5190).

Chapter 2: Poultry Litter Ash and Co-Products Elemental and Chemical Composition

Abstract

Manure-to-energy systems were identified as a method to condense poultry litter (PL) volumes into a densified poultry litter ash (PLA) fertilizer product. Densifying PL into PLA allows nutrients to be economically shipped beyond poultry production regions. The objective of this study was to characterize PLA and co-products' chemical and elemental composition for phosphorus (P) and potassium (K) nutrient availability. Three PLA products [(fluidized bed bulk (FB Bulk), fluidized bed fly (FB Fly), and combustion Mix (CMix)], three manufactured co-products [(granulated poultry litter ash-bulk (GPLA-B), and GPLA-Acd2, and ash coated urea (ACU)] were evaluated by total elemental analysis, backscatter-electron dispersive (BSED) microscopy, and X-ray absorption near edge structure (XANES) spectroscopy. Poultry litter ash elemental concentrations are highly variable ranging from 50.60 to 101.97 g P kg⁻¹ and 62.57 to 119.95 g K kg⁻¹ and are comparatively higher than PL concentrations. Phosphorus structures that provided and controlled P solubility were Ca and Ca-Mg-phosphate compounds. Spectroscopy, confirmed Ca structures as predominately monetite (dicalcium phosphate anhydrous; CaHPO₄; log K[°] 0.30) and brushite (dicalcium phosphate dehydrate; CaHPO₄·2H₂O; 0.63 log K[°]) species which were supported by BSED and elemental ratios (Ca:P; 1.12 to 1.71:1). Additionally, GPLA acidified from FB Fly had higher brushite and monetite weight percentage describing spectra models, translating into a more soluble Ca-phosphate species when compared to FB Fly original P species. Stoichiometric ratios failed to support varscite (AlPO₄·2H₂O; log K[°] -2.50) and bobierrite (Mg₃(PO₄)₂·8 H₂O; log K[°] 14.10) XANES detection. Findings support Ca as the dominate cation influencing P structural formation, species, and solubility. Potassium BSED analysis revealed KCl and KCl-Na structures providing readily soluble K. In conclusion PLA elemental concentrations are suitable as an alternative fertilizer source, however Ca-phosphate

species control of P solubility will need to be taken into consideration as a slowly available fertilizer source.

Introduction

Poultry litter ash (PLA) originated in response to increased manure volumes generated by concentrated poultry production regions within the mid-Atlantic. As poultry production increases to meet world consumption demands, poultry litter (PL) nutrient amounts will reflect increased production. Subsequently, increased PL nutrients and resulting land application that may inflate soil test phosphorus (STP) concentrations prompted research to balance practical and environmentally sound alternative P solutions (Sharpley, 1994; Howarth et al., 2002). Issues surrounding increased PL production and associated nutrients are conversely aligned with issues surrounding decreases in total world rock phosphate supply due to geopolitical and quality threats (Sharpley, 1994, 1995; Cordell et al., 2009; Ayding et al., 2010; Van Kauwenbergh et al., 2013; Scholz et al., 2013).

Recognizing complex P dynamics, researchers collaborated to identify seven major future research opportunities to improve and regulate P nutrient cycling with collaborated priorities published by George et al. (2017) to direct prospective research. Priorities included renewable resources specifically “using wastes containing organic P as fertilizer to close the loop” and environmental pollution detailing “needing to manage the balance of food security vs environmental pollution” (George et al., 2018). Aligning under these global P priorities, manure-to-energy systems have been identified as a method to condense increased PL volumes into a densified PLA fertilizer product while providing green energy and a renewable P fertilizer source (Crozier et al., 2009; Pagliari et al., 2009; Codling, 2013; Middleton, 2015). Densifying PL into PLA allows nutrients to be economically shipped beyond poultry production regions around the world. Aiding in redistributing PL nutrients to crop deficit regions and reducing environmental P loading in concentrated poultry production areas allows most efficient nutrient use.

Poultry litter ash nutrient concentrations vary depending upon PL type (broiler vs. layer), bird age, feed concentrations, time between house cleanout, and thermo-conversion systems (Kunkle et al., 1981; Codling et al., 2002; Coufal et al., 2006; Middleton, 2015). Numerous studies reported ranges in PLA nutrient concentrations. Middleton (2015) found P concentrations were 4 to 7, K 2.5 to 5.0, and S 2 to 3 times more concentrated than original PL sources. Total elemental concentrations varied between 9.4 to 104.9 g P kg⁻¹, 32.03 to 42.49 g K kg⁻¹, and 9.06 to 162.58 g S kg⁻¹ (Middleton, 2015). Poultry litter ash analysis by Bock (2004a) found P, K, and S nutrient concentrations six to seven times more concentrated with a bulk density 1.5 to 2.5 times greater than PL. Total P concentrations by Codling et al. (2002) found extractable P two to three times more concentrated and ranged from 76 to 114 g P kg⁻¹ compared to PL concentrations 22.0 to 27.0 g P kg⁻¹ (Kunkle et al., 1981). Turkey manure ash (TMA) nutrient analysis resulted in citrate soluble P 43 g P kg⁻¹, water soluble K 117 g K kg⁻¹, and 17 g S kg⁻¹ (Pagliari et al., 2010). Trace elements in PL fluctuate due to components in poultry nutrition (feeding supplements and grains in feed), production type, and PL management (Kunkle et al., 1981; Gupta and Charles, 1999; Leeson and Caston, 2008). Variation in PLA nutrient concentrations can also be explained by differences in ash particle sizes. Adams (2005) noted that as particle size decreased, elemental concentrations for P, K, Ca, Mg, Cu, Mn, and Zn increased. Phosphorus nutrient concentrations in PLA increased from 79 g P kg⁻¹ (< 2mm) to 104 g P kg⁻¹ (< 0.25 mm), respectively (Adams, 2005).

Unlike N, which can be replenished by N fixation or synthetically derived, P and K once removed from soil can only be replenished by external sources. Potassium fertilizer is mined from non-renewable potash salt deposits across the world (Yager, 2016). Currently, Canadian potash resources are largest known in the world and is a major U.S. K supplier (Yager, 2016).

Global estimates forecast that there will be no foreseeable potash shortage and denote largest challenges associated with potash supply is cost and distribution (Yager, 2016). Rock phosphate (RP) ores are primary parent material for current P fertilizer production. However, RP is a non-renewable mineral in finite supply mined from phosphate deposits across the world. Estimates suggest global P production of environmentally and financially feasible RP will peak in 2033 and known P reserves will be depleted in the next 50 to 100 years with no current identification of alternative P sources (Cordell et al., 2009). Quantifying RP supply is complicated due to variations in estimating supply (i.e. reserves vs. resources), geopolitical constraints as developing countries begin to enter P production, and mined RP quality below heavy metal thresholds (Ayding et al., 2010; Van Kauwenbergh et al., 2013; Scholz et al., 2013). Van Kauwenbergh et al. (2013) extrapolates current P reserves and consumption to predict the world has over 300 years of reserve and over 1,400 years of RP available. Despite discrepancies involved in predicting RP supply, it is indisputable RP is a non-renewable resource that will need to be provided by new deposits or replaced with alternative P sources to maintain sufficient crop production.

Poultry litter ash nutrient concentrations are foundational to disprove, validate, or improve PLA fertilizers as an alternative P and K source. Several PLA studies confirmed nutrients were more concentrated than original PL sources with nutrient analysis suitable as an alternative industry fertilizer (Codling, 2006; Pagliari et al., 2010; Reiter and Middleton, 2016). However, further testing is needed to determine optimum application for crop growth, particularly addressing variations in PLA nutrient concentrations and solubility as an alternative fertilizer source (Codling et al., 2002). Nutrient concentrations across numerous studies revealed variations in elemental analysis as well as decreased P solubility from PLA (Codling et al., 2002;

Codling, 2006; Pagliari et al., 2010; Reiter and Middleton, 2016). However, insight beyond elemental concentrations is needed to understand P and K chemistry altered by manure-to-energy technology temperatures (171- 593 °C) (Middleton, 2015).

Electron scanning microscopy (ESM) and X-ray absorption near edge structure (XANES) spectroscopy are methods providing semi-quantitative elemental composition, identifying physical structures providing P and K, as well as P speciation. Specifically, electron microscopy provides two imaging views, secondary electron microscopy (SEM) and backscattered-electron dispersive (BSED) microscopy. Secondary electron imaging provides material surface topography allowing analysis of submicron and crystalline structure in three-dimensional orientation (Sparks et al., 1996; Virginia Tech Institute for Critical Technology and Applied Science, 2018). Back-scattered electron imaging provides semi-quantitative elemental analysis based upon sample composition atomic number (protons or nucleus charge). When an electron beam is emitted from ESM to sample surface, emitted electrons are repulsed by protons, subsequently changing trajectory. Change in electron trajectory or proton repulsive force is unique to each atomic element based upon elements' atomic number. Dependent upon sample element nucleus charge, the emitted electron will change trajectory due to magnitude of nucleus. This change in trajectory produces a characteristic signal recorded in electron volts (keV) a unit of momentum and counts per second of eV (cps/eV). Ultimately, ESM provides a visual structure identification as well as semi-quantitative elemental analysis. Electron microscopy with granulated swine and PLA revealed particles were coated with an amorphous Si gel (Bock, 2004b). High concentrations in TMA of 473,000 mg SiO₂ kg⁻¹ (221,000 mg Si kg⁻¹) compared to averages of 265,000 mg SiO₂ kg⁻¹ (123,900 mg Si kg⁻¹) and 239,000 mg SiO₂ kg⁻¹ (111,700 mg Si kg⁻¹) from other turkey litter surveys and 81,000 mg SiO₂ kg⁻¹ (37,900 mg Si kg⁻¹) from broiler

litter ash were identified as a major obstacle for ash granulation. Bock (2004b) hypothesized Si was a soil artifact from PL cleanout. Due to high conversion temperatures, Si formed an amorphous coating around TMA particles creating a barrier preventing reaction with phosphoric acid. Addressing amorphous silica coating, Bock (2004b) consulted with a former engineer at the Tennessee Valley Authority National Fertilizer Development Center to determine methods to penetrate Si gel coated on P compounds in manure ash products. Recommendations were made to substitute sulfuric acid for phosphoric acid (H_3PO_4) as a granulation binder, drastically improving P availabilities of 384 g P kg^{-1} ($880 \text{ g P}_2\text{O}_5 \text{ kg}^{-1}$) compared to 184 g P kg^{-1} ($420 \text{ g P}_2\text{O}_5 \text{ kg}^{-1}$), respectively (Bock, 2004b). Furthermore, Bock (2004b) cited Si's negative two-fold effect decreasing P and K concentrations via nutrient dilution as an additional detrimental impact to manure-to-energy nutrient densification efforts.

As noted by Sparks et al. (1996), although a single technique was not a solution for understanding complex soil chemistries, employing XANES in combination with analytical techniques has the potential to reveal PLA complex P speciation. Sequential extraction techniques as well as field studies noted reduced P PLA solubility and speciation exploration has occurred on manures and biosolids to explain P speciation in correlation with availability (Codling, 2006; Pagliari et al., 2010; Reiter and Middleton, 2016). Studies examining P speciation in manures and biosolids revealed recalcitrant inorganic calcium phosphate minerals in lime stabilized manures and biosolids that reduced P solubility (Shober et al., 2006). Toor et al. (2005) examined modified poultry diets on P total, solubility, and manure speciation. The study found a positive linear correlation between water soluble P (WSP) and increasing dicalcium phosphate, suggesting available PL P originates from dicalcium phosphate (Toor et al., 2005). X-ray absorption near edge structure spectroscopy provided elemental speciation through

atomic geometrical arrangement around absorbing atoms (Franke and Hormes, 1995). Energy ranges and electron volts (eV) are specific to each element and are equal to electron binding energy (BE) needed to eject an electron from an inner K orbital (Sparks et al., 1996). When BE is applied, x-rays are absorbed by sample element and a core K electron is ejected into continuum, leaving a vacancy in inner most orbital (core K). Speciation spectra produced by x-ray absorption results in quantum state change as an electron from an outside orbitals fills the unoccupied orbital creating a white line peak (absorption edge) and subsequently qualitative spectra utilized to determine elemental speciation (Sparks et al., 1996). Spectra results are then compared to library of reference compounds to identify similarities comprising species describing XANES spectral results (Sparks et al., 1996; Peak et al., 2002). Identifying P species comprising PLA can improve understanding of P availability. Shober et al. (2006) utilized biosolid and manure speciation to predict lime stabilized manure availability, identifying hydroxyapatite ($\text{Ca}_5(\text{PO}_4)_3\text{OH}$) and tricalcium phosphate ($\beta\text{-Ca}_3(\text{PO}_4)_2$) as slowly soluble P sources on mid-Atlantic acidic soils. Peak et al. (2002) stated the distinctive and most important calcium phosphate feature is the presence of a shoulder past 2160 to 2165 eV. Sequential extractions, field and greenhouse trials, and granulation experiments have provided useful information on PLA potential as a P fertilizer source; however, these methods cannot provide specific information identifying chemical species influencing and providing P (Bock, 2004b; Codling, 2006; Pagliari et al., 2010; Middleton, 2015). Consequently, interpreting PLA effects as a fertilizer source is limited until foundational aspects identifying PLA P species is understood to shed light on short and long-term P plant availability.

Spectroscopy provided insight into both organic and inorganic compounds, solids, or amorphous structures controlling P solubility (Shober et al., 2006). Results from unamended PL

spectroscopy identified P is predominantly in variations of calcium phosphate forms with similar absorption edge (white line energy) at 4.05 keV as dicalcium phosphate (Peak et al., 2002). Calcium-phosphate is a nutrient supplement provided due to insufficient poultry digestive systems ability to extract P from phytic acid (Peak et al., 2002). Once calcium phosphate is digested, it dissociates due to acidic nature of gastrointestinal tract and is further excreted with high Ca content and organic and inorganic P fractions (Peak et al., 2002). Peak et al. (2002) speculated that inorganic PL P remained mainly as dicalcium phosphate due to organic material and associated organic acids preventing further crystallization and transformation to stable hydroxyapatite. However, when PL is utilized as a fuel source in manure-to-energy systems with temperatures ranging from 171 to 593 °C, organic PL components dissipate leaving inorganic P and Ca compounds (Reiter and Middleton, 2016). High thermal conversion temperatures, may alter Ca to P stoichiometric ratios and remove any organic or water components ultimately causing calcium phosphate structures to reorganize (Tonsuaadu et al., 2012). Similarly, rock phosphate is thermally processed at temperatures above 1200 °C to defluorinate apatite in fertilizer production (Marshall et al., 1937; Tonsuaadu et al., 2012). Tonsuaadu et al. (2012) states apatite thermal stability is influenced by Ca:P stoichiometric ratios and degree of structural substitution. Increased Ca structural substitution (greater Ca:P ratios) increases thermal stability and stability decreases as other metal ions or P substitution increases (lower Ca:P ratios). Brushite ($\text{CaHPO}_4 \cdot 2 \text{H}_2\text{O}$) originating from guano was subjected to thermal decomposition ultimately dehydrating and collapsing the structure (Frost and Palmer, 2011). At 105 °C two moles of calcium phosphate dihydrate combined and eliminated one mole of water, and as temperature increased to 165 °C three moles of water were lost forming more stable monetite (CaHPO_4) (Duff, 1971; Frost and Palmer, 2011). One can infer as PL is thermally converted into

PLA, original P species are continually changing until a stable species forms. Therefore, identifying PLA P species will aid in explaining P solubility and elucidate methods to resolve reduced P nutrient availability.

Determining PLA fertilizer elemental composition is a foundational component validating PLA as an alternative fertilizer source and subsequently promoting surplus nutrient redistribution from concentrated poultry production regions to nutrient deficit areas within the Commonwealth. The following research objectives addressed include: 1) Determine PLA fertilizers (FB Bulk, FB Fly, CMix and GPLA) total measurable USEPA 3050B elemental analysis; 2) Determine physical structures providing P and K via electron microscopy; 3) Identify within P and K structures elemental compounds influencing P or K availability; and 4) Classify P PLA speciation through X-ray absorption near edge spectroscopy.

Materials and Methods

Poultry Litter Ash Sources

Poultry litter ash sources were obtained from two separate manure-to-energy systems. Fluidized bed fly (FB Fly), fluidized bed bulk (FB Bulk), granulated poultry litter ash (GPLA), and ash coated urea (ACU) originate from broiler litter thermally converted at temperatures of 593 °C via fluidized bed combustion system located in Rhodesdale, MD. Granulated poultry litter ash is created from FB Fly, through mixing with a weight percentage of phosphoric acid. Ash coated urea was created by coating FB Fly onto a urea granule by a binder developed by Whitehurst Associates, which will not be disclosed due to proprietary materials utilized. Combustion mix (CMix) originated from broiler litter thermally converted at temperatures of 171 °C via a combustion system located in Lancaster county, PA. Further PLA source and thermo-conversion system information is outlined by Middleton (2015).

Elemental and Chemical Composition Analysis

All fertilizer samples (1.0 gram) were acid digested according to USEPA method 3050B using nitric acid and hydrogen peroxide followed by analysis via inductively coupled plasma spectroscopy (ICP-AES) (ICP-AES; CirOS Vision Model, Spectro Analytical) for total digestible elemental analysis (United States Environmental Protection Agency, 1996). Total C, N, and S was analyzed via combustion procedure using the Dumas method with a Vario EL Cube (Elementar Americas, Mt. Laurel, NJ, USA) (Bremner, 1996).

Electron Microscopy Elemental Analysis and Physical Structure Identification

Poultry litter ash fertilizers (CMix, FB Bulk FB Fly, and Granulated Poultry Litter Ash) and commercial fertilizers (TSP, KCl, and Urea) were examined via a field emission scanning electron microscope (SEM) (Leo 1500 model, Zeiss). Leo (Zeiss) 1500 is a high performance Schottky field-emission SEM capable of resolution in 2 to 5 nm size range (Virginia Tech Institute for Critical Technology and Applied Science, 2018). Poultry litter ash fertilizers, due to fine particulate matter, were attached to a sample mount by a C coated conductive tape and then coated with 20 nm gold palladium (AuPd). Granulated fertilizer (TSP, KCL, Urea and GPLA) products, due to larger sizes, were attached to a sample mount by a water based C conductive adhesive and allowed to harden overnight and then coated with 30 nm AuPd. Preliminary work with fertilizer products was conducted under both SED (secondary electron) and BSED (backscattered-electron dispersive) at 50, 200, 500, 2000, 5000, and 10,000x magnification to identify best methodology for a creating a protocol. Initial sample viewing began with SED imaging to identify material topography as well as analyze submicron structure and crystalline structure three-dimensional orientation (Virginia Tech Institute for Critical Technology and Applied Science, 2018).

From preliminary trials, the following protocol was designed to employ consistent examination across variability in PLA structures and composition in efforts to balance data sets for statistical analysis in a completely randomized design (CRD). Poultry litter ash sources (CMix, FB Bulk FB Fly, and Granulated Poultry Litter Ash) had three replications by fertilizer source ($4 \times 3 = 12$ samples) to be analyzed. Samples were analyzed via BSED to provide qualitative elemental composition in atomic percent for each element present (%). Two analysis for each sample replication occurred including: 1) overview region and 2) multipoint structure identification (Figure 2.1). Utilizing BSED imaging, an overview elemental analysis of two regions at 200x from each sample was conducted focusing on the following elements: O, P, Ca, K, Cl, S, Si, C, Fe, Mg, Cu, Al. Additionally, within each overview analysis, several structures were selected for multipoint analysis. Poultry litter ash samples had variations in physical structures (i.e. square crystal, amorphous, circular, spiral) within fertilizer composition. Common physical structures identified for each fertilizer source included: KCl cubes, variations of P crystalline structures, and undercoating (defined as unorganized material behind aggregated structures) that were identified via multipoint BSED. Each analysis resulted in two categories including an elemental overview region and identified multipoint structure elemental analysis. The BSED data is semi-quantitative analysis and only relative concentrations can be interpreted from characteristic element peaks (Shepard et al., 1998; Spokas et al., 2014). Due to inconsistency across PLA structures and inherently different elemental composition, multipoint elemental results are presented as an average.

Poultry Litter Ash Phosphorus Speciation via XANES Spectroscopy

All XANES spectroscopic work was graciously conducted at beam line 9-BM of the Argonne National Laboratory Advanced Photon Source in Lemont, IL with colleagues from the University of Delaware, Maryland, and U.S.-EPA. All sample spectra photon energy was used at

approximately 2150 eV in a double crystal monochromator in helium (He) atmosphere. Sample preparation included grinding fertilizers into fine powder via agate mortar and pestle mixed with PVP (polyvinylpyrrolidone) followed by pellet pressing (7-mm diameter). Pellets were attached to an eight-carousel sample holder by double-sided C tape before spectra collection. Poultry litter ash samples were collected in K-edge XANES spectra using fluorescence mode with multiple scans (3-8) per sample and then averaged to improve signal-to-noise ratio. Phosphorus reference standards were collected with similar protocols as described by Qin et al., (2018) in total electron yield (TEY) mode using an electron yield detector to minimize sample adsorption. Multiple scans per sample were collected (2-5) for each sample and averaged. Standard spectra were normalized with a two normalization order from a pre-edge of -50 to -10 eV and normalization range of 15 to 115 eV. Additional standards' spectra that were collected in previous studies were included in linear combination fitting (Shober et al., 2006; Qin et al., 2018). Poultry litter ash K-edge spectra were compared to 15 standards in our spectra library (Table 2.1).

Spectra data processing was conducted using Athena software (Ravel and Newville, 2005). Raw PLA sample spectra were normalized with a normalization order of two from a pre-edge of -29 to -7 and -29.5 to -19.5 eV and normalization range of 15 to 110 and 15 to 120 eV corresponding to white line peak. All sample spectrums electron binding energy (E_0) were assigned to maximum peak of the first derivative. Linear combination fitting (LCF) was utilized to identify spectra standards comprising PLA P samples. Goodness of fit determined by residual factor (R-factor) and reduced chi-square produced by Athena LCF were utilized to evaluate model accuracy in describing sample spectra (Ravel and Newville, 2005). Residual factor (R-factor) generated by Athena LCF are utilized to determine goodness of fit, with smaller values indicating best spectral fitting of library standards (Qin et al., 2018). Initially, all standards were

selected for LCF and were sequentially eliminated based upon standard weight contributing to the model. Standard samples contributing < 10% of LCF spectra were removed until all remaining standards describing the model contributed at least 10% or greater. Reference standard spectra E_0 was allowed to shift up to + or – 1 eV during LCF.

Statistical and Data Analysis

Total elemental quantitative and ESM overview analysis were subjected to analysis of variance conducted with General Linear Model procedure (PROC GLM) in SAS Enterprise Guide 7.1 (SAS Institute Inc., 2017). Fishers protected least significant difference (LSD) test was used to separate statistically significant means at LSD of 0.05. Due to variability across PLA sample multipoint structures data will be presented as an average. X-ray absorption near edge structure spectroscopy spectra was analyzed via Athena XAS data linear combination fitting (LCF) software (Ravel and Newville, 2005).

Results and Discussion

Elemental and Chemical Composition Analysis

Total elemental analysis resulted in significant differences across all elements and PLA's tested (As, B, Be, Cd, Co, Cr, Cu, Mo, Ni, Pb, Se, Si, Zn, Al, Ca, Fe, K, Mg, Na, P, and S) (Table 2.2 a, b, and c). Additionally, FB Fly and FB Bulk, both PLA's originating from the same thermo-conversion system, revealed nineteen of the twenty-one elements analyzed were significantly different. Potassium concentrations ranged from 128.59 (CMix) to 0.69 (ACU) g K kg⁻¹. Unexpectedly FB Fly, which is granulated into GPLA-B and GPLA-Adc2, revealed significant decreases in K concentrations from 119.15 to 102.20 and 93.91 g K kg⁻¹, respectively; this can be potentially explained by H₃PO₄ weight dilution effect. Granulated PLA products had significantly higher P (GPLA-B 90.47 and GPLA-Adc2 101.97 g P kg⁻¹) than other PLA

products followed by CMix, FB Fly, FB Bulk and ACU ($LSD_{0.05} = 4.34 \text{ g P kg}^{-1}$). Across PLA sources tested, elemental concentrations were similar to a study previously completed by Middleton (2015) and Codling (2006). Calcium to phosphorus ratios (Ca:P) revealed differences between all PLA products with CMix (Ca:P; 1.77:1) having significantly higher ratios that translated into increased Ca and P bonds and subsequent increased stability (Tonsuaadu et al., 2012). Granulation processes utilizing H_3PO_4 to granulate FB Fly into GPLA altered Ca to P stoichiometric ratios and increased overall total P (TP) (Ca:P; FB Fly at 1.48:1 vs GPLA-B at 0.67:1 and GPLA-Acd2 at 0.55:1). We speculate that increased TP was a result of one known and one unexpected factor. As expected, GPLA-B TP should increase due to additions of H_3PO_4 . However, it is hypothesized that H_3PO_4 caused a pre-acidifying unexpected effect before USEPA 3050B digest, ultimately increasing P digested from recalcitrant calcium compounds (United States Environmental Protection Agency, 1996). Maguire et al. (2001), in determining relationships between biosolids treatments and soil P availability, found that USEPA 3050B digested P was ~80% of TP and oxalate extractable P. The authors further explained that TP and oxalate extractable P commonly exceed USEPA 3050B digest results; however, biosolids that are treated with lime and contain high Ca concentrations, like PLA, are not as effectively extracted by oxalate extraction (Maguire et al., 2001). Therefore, we cautiously assume that increased GPLA-B TP is due to H_3PO_4 's twofold effect on USEPA 3050B TP digestion including: 1) H_3PO_4 contributed P as well as reacted and solubilized Ca-phosphate forms and 2) however unexpectedly, H_3PO_4 pre-acidified PLA; therefore, increasing EPA 3050B efficacy of extracting more total P. Margins that H_3PO_4 increased USEPA 3050B TP results are unknown; therefore, we have collectively decided to label USEPA 3050B as total measurable P.

Subsequently, TP results throughout the experiments should be interpreted with H_3PO_4 's and EPA 3050B's TP two-fold effect in mind.

Examining significant differences in Si concentrations identified highest concentrations in ACU ($203.82 \text{ mg Si kg}^{-1}$) followed by FB Bulk, GPLA-Acd2, FB Fly, CMix, and GPLA-B. Although Bock (2004b) found significant Si concentrations in turkey manure ash, all current projects PLA sources are below average Si concentrations of $37,900 \text{ mg Si kg}^{-1}$ found in Bock's broiler litter ash survey. Therefore, Si is not thought to effect current PLA nutrient solubility and dilution. Codling's (2013) egg layer manure ash and broiler litter ash elemental analysis found As concentrations of 10.9 and $12.9 \text{ mg As kg}^{-1}$, respectively. Poultry litter ash products examined in the current study had concentrations below these thresholds ranging from 0.44 to $11.11 \text{ mg As kg}^{-1}$. Arsenic is supplied to poultry as roxarsone (ROX) in ranges of 21.3 to $43.7 \text{ } \mu\text{g As g}^{-1}$ to promote growth, feed conversion efficiency, and disease control (Kazi et al., 2013). Differences between Codling's (2013) As levels and the current study can be explained by differences in nutrition provided between laying and broiler production.

When comparing triple superphosphate (TSP) P concentration ($201.81 \text{ g P kg}^{-1}$) recorded by Middleton (2015), PLA concentrations are approximately 3 times less than TSP and 4 times more concentrated than PL ($12.51 \text{ g P kg}^{-1}$). Average GPLA total P concentrations (96.2 g P kg^{-1}) were approximately 7.7 times and 1.7 times more concentrated than PL and PLA as well as 2.1 times less than TSP. Poultry litter ash and granulated sources contain valuable nutrient concentrations that could be adapted as an alternative lower analysis P fertilizer.

Electron Microscopy Elemental Analysis and Physical Structure Identification

The goal of examining P and K structures through BSED was to identify structures providing P or K and further analyze elemental compounds within structures influencing

solubility. Overview BSED semi-quantitative analysis identified significant elemental composition differences for P, Ca, Cl, Na, and Al atomic percent across fertilizers analyzed (Table 2.3). Granulated poultry litter ash-Acd2 (17.93 P%) resulted in significantly higher atomic percent P than other PLA sources and significantly less Ca (1.65%). Amongst raw unmanufactured PLA, FB Bulk and CMix resulted in significantly higher Ca% than FB Fly. Comparatively, Ca:P ratios detected were slightly lower than results in total digest elemental analysis; however, ratios followed similar trends with increasing ratios (decreasing solubility) in the order of: CMix > FB Bulk > FB Fly > GPLA-Acd2 or GPLA-B. Although K analysis did not produce significant differences, manufactured GPLA had higher K% than original FB Fly sources; which is in contrast to elemental quantitative analysis findings. Although Si significant differences (*p-value* 0.13) were not detected across PLA, FB Bulk had numerically larger Si atomic percent in accord with elemental analysis, denoting its origin from a fluidized sand bed. In support of our findings, chicken manure biochar cross-sectional TEM line scans found high Al:Si ratios at interface between biochar and mineral phases in work by Lin et al., (2012). Due to variations in thermal conversion processes, submicron visual differences between PL biochar were observed by Lin et al. (2012) and Spokas et al. (2014) were less crystalline than results from PLA surface morphology (Figures 2.2, 2.3, 2.4, 2.5). Porous and hollow channels comprised Lin et al. (2012) biochar submicron structure, whereas PLA structures were more uniform ordered crystalline structures implying greater stability and subsequent decreased solubility. Supporting elements identified in PLA BSED imaging (Table 2.3), Lin et al. (2012) EDS analysis also identified Al, Si, O, and Ca presence in biochar phases and mineral forms that were due to original artifacts in PL prior to pyrolysis.

Fluidized bed bulk exhibited fairly consistent physical structures including: bright cubes, undercoating, and defined crystals. Predominate structures that provided plant available K include bright cubes (Figure 2.2 pt. 1.1; Table 2.4) averaging 43.06% K, 49.42% Cl, and 2.96% Na as an additional impurity. Sodium found in K cubes are not thought to negatively impact K solubility; however, Na detection does suggest potential for K nutrient dilution. The undercoating (Figure 2.2 pt. 1.2; Table 2.4) consisted of 49.85% O, 14.38% Si, 13.0% Mg, 5.03% P, 4.79% Ca, 4.66% K, 2.71% Na, and 0.56 % Cl. Lastly, defined crystals (Figure 2.1 pt. 1.3) were predominantly Ca-phosphate structures averaging 55.66% O, 22.83% Ca, 14.40% P, and 3.59% Mg with minor detection of trace elements. Due to FB Bulk alkalinity (pH 10.21) and Ca-phosphate structure identified, it was hypothesized that Ca compounds provided as well as reduced P solubility.

Fluidized bed fly revealed two Cl crystalline cubes differing by color brightness delineating KCl (Figure 2.3a pt. 2.1) or NaCl (Figure 2.3b pt. 2.3). Brighter KCl (Figure 2.3a pt. 2.1) cubes averaged 46.16% K and 53.84% Cl. Sodium chloride structure (Figure 2.3b pt. 2.3; Table 2.5) averaged 44.91% Cl, 37.66% Na, and 15.08% K with additional elements (O, P, Ca, and Si). Potassium-Cl cubes identified in FB Fly were similar to FB Bulk structures that provided plant available K unhindered by additional elements. Separate NaCl structures will not affect K availability; however as mentioned, increased NaCl compounds can cause K nutrient dilution and may unnecessarily raise salt concentrations that could impede crop growth (Intani et al., 2018). Two P crystals were identified as structures providing P. Structures included P compounds as Ca (Figure 2.3a pt. 2.2; Table 2.5) and Ca-Mg-phosphate (Figure 2.2c pt. 2.4) minerals averaging 36.60% P and 63.40% Ca and 21.44% P, 21.51% Ca and 12.69% Mg, respectively. Surprisingly, Ca-phosphate mineral (Figure 2.2a pt. 2.2) elemental analysis

detected 7.03% K with all other elements below detection limit. Calcium-Mg-phosphate structures on average contained 7.04% K, 5.76% Na, 0.67% Cl, 57.87% O, 21.51% Ca, 0.73% Si, and 1.63% S; which appeared to have structural layers composed of elongated crystalline structures. Calcium-Mg and Ca-phosphate structures were visually very different. Calcium-phosphate structures appeared rectangular in comparison to Ca-Mg-phosphate compounds. Structural variability is due to elemental compounds altering stoichiometric ratios and subsequent structure formation. Based upon Ca:P elemental ratios of 1.73:1 (pt 2.2) versus 1:1 (pt 2.4) and noted effect of Mg substitution for Ca, the Ca-Mg-phosphate structure will be more soluble than the Ca-phosphate structure (Tonsuaadu et al., 2012). Calcium and Ca-Mg-phosphate structures are main structures providing and controlling P solubility. Magnesium identification is noteworthy as it suggested cationic substitution for Ca; subsequently decreasing Ca and P bonding strength resulting in a more soluble P structure (Tonsuaadu et al., 2012).

Combustion mix PLA structural composition was by far the least consistent. Various structures were identified including a cubed KCl crystal (Figure 2.4a pt. 3.1) and amorphous structures (Figure 2.4b pt. 3.2, 3.3, 3.4). Potassium chloride cubes commonly found in FB Bulk and Fly were also found in CMix. The cubed structure in figure 2.3 was rare resulting in only 48.12%K and 51.88% Cl detected with zero detection of other elements (Table 2.6). Elemental compounds in KCl structure is conducive to high K solubility. Although amorphous structures (Figure 2.4b pt. 3.2; Table 2.6) lacked structural consistency, O, Ca, Mg, and P elemental composition was a main commonality averaging 64.25% O, 12.42% Ca, 5.60% P, and 7.69% Mg with additional elements. Additionally, figure 2.4b pt. 3.3 was largely C (75.16% C, 18.39% O, 1.02% S, 1.54% K, and 1.29 Ca) and pt. 3.4 predominately Al and Si (59.65% O, 12.50% Al, 11.30% Si, 4.41% K and 2.0% Ti) illustrating CMix structural and elemental variation. Although

Ti is a surprising element to find in PLA, Lin et al. (2012) also identified Ti phases in chicken manure biochar. Unlike previous PLA structures analyzed, a dominant P structure were not identified in CMix preventing interpretation of structural compounds controlling P solubility. Lack of P structures can be explained by CMix lower thermo-conversion temperatures of 171 °C compared to FB Fly and Bulk conversion temperatures (593 °C) creating amorphous structures with lower P concentrations.

Granulated poultry litter ash (GPLA-Acd2) multipoint analysis structural identification was easily grouped into two categories; crystalline structure (Figure 2.5pt. 4.1) and undercoating (Figure 2.5 pt. 4.2). Phosphorus crystalline structure (Figure 2.5 pt. 4.1; Table 2.7) contained 70.45% O, 16.28% P, 0.88% Ca, and 12.38% K. The undercoating analysis (Figure 2.5 pt. 4.2; Table 2.7) averaged 55.63% O, 20.70% P, 6.96% K, 3.74% Ca, 3.36% Mg, 3.13% S, 2.28% Si, 0.56% Fe, and 0.26% Mn. Examining differences between FB Fly and GPLA-Acd2, revealed visual changes to P crystals likely caused by H₃PO₄ granulation (Al-Fariss et al., 1993). Drastic decreases in GPLA-Acd2 crystals Ca:P ratio (0.05:1) when compared to FB Fly P crystal ratio of 1.73:1 support not only visual but elemental changes to original FB Fly P compounds. Calcium to P ratios are correlated to P solubility due to ratios effect on structure bonding strength and stability (Tonsuaadu et al., 2012). Through H₃PO₄ granulation several simultaneous reactions alter original FB Fly Ca:P ratios into more soluble GPLA-Acd2. Acidifying FB Fly is similar to phosphate rock acidulation as described by Al-Fariss et al. (1993). Phosphoric acid acidulation causes an exothermic reaction, where H⁺ ions decompose and dissolve FB Fly P compounds that recrystallize into a more soluble P form (Al-Fariss et al., 1993). A more soluble P crystal reforms due to decreased pH and higher P concentrations from H₃PO₄ in proportion to Ca. Examining

GPLA-Acd2 structural composition confirmed changes in P compounds and improvements in Ca:P ratios translating into a more soluble and plant available version.

Overall, multipoint analysis identified structural elemental differences between sources and revealed compounds providing as well as influencing P and K availability. Potassium cubes examined identified Na as an additional element found in KCl cubes or separately as NaCl, which is also commonly found in muriate of potash. Predominate P crystals identified included Ca and Ca-Mg-phosphate with K, and traces of micronutrients that may influence P solubility in PLA. Supporting crystalline structures found in PLA, Lin et al. (2012) attributed aggregate accumulation of Ca, K, P, and Mg elements to chicken manure feedstock source. Additionally, alkaline PLA pH (>9.0), high elemental Ca concentrations, and Ca:P ratios provided parameters which should result in precipitation of insoluble Ca-phosphate minerals (Lindsay, 1979; Shober et al., 2006). However, additional elements like Mg, identified in Ca-phosphate compounds is thought to reduce structure stability and subsequently increase P availability. Phosphorus and K structures identified allowed insight into elemental compounds or structures that provide soluble K and aid in explaining decreased P plant availability.

Poultry Litter Ash Phosphorus Speciation via XANES Spectroscopy

The goal of XANES analysis and linear combination fitting (LCF) were to identify dominant P species in PLA sources that would control P solubility. Determining P species allows reference to formation constants ($\log K^\circ$) and insight into solubility (Table 2.1) (Lindsay, 1979; Chow and Eanes, 2001). Linear combination fitting (LCF) indicated presences of Al and Ca-phosphate species in FB Fly, FB Bulk, and CMix (Table 2.8, Figures 2.6, 2.7, 2.8). Whereas GPLA spectra LCF predominately contained Ca-phosphates (monetite; dicalcium phosphate; CaHPO_4 ; $\log K^\circ 0.30$) and brushite; $\text{CaHPO}_4 \cdot 2\text{H}_2\text{O}$; $0.63 \log K^\circ$) and Mg-phosphate (bobierrite; $(\text{Mg}_3(\text{PO}_4)_2 \cdot 8 \text{H}_2\text{O})$; $\log K^\circ 14.10$) as P species describing sample spectra (Figure 2.9).

Linear combination fitting identified bobierrite in FB Fly, FB Bulk, and GPLA. Molar Mg to P stoichiometric ratios failed to support evidence of bobierrite detected in PLA samples (Table 2.9). Bobierrite's Mg:P ratio of 1.5:1 was not supported by PLA total elemental stoichiometric ratios that ranged from 0.27 to 0.86 (Mg:P). Elemental ratios are utilized to support or disqualify species detected based upon stoichiometrically possible ratios due to total elemental analysis results (Shober et al., 2006).

Specifically, varscite ($\text{AlPO}_4 \cdot 2\text{H}_2\text{O}$; $\log K^\circ -2.50$) was identified in all three PLAs, with FB Fly LCF model containing greatest varscite weight percent 55.9%, compared to brushite 25.7% and bobierrite 18.4% (Figure 2.6; $R=0.002614$). Additionally, CMix LCF detected 10.3% non-crystalline (amorphous) Fe-phosphate describing spectra ($R=0.004215$). Varscite and amorphous Fe-phosphate detection was surprising due to PLA alkalinity. Aluminum to P (Table 2.9) molar ratios calculated from USEPA 3050B elemental digest failed to support varscite Al to P ratio (1:1). Shober et al. (2006) also found contradictory results between XANES Al species detection and Al:P stoichiometric ratios of PL samples and biosolids. Aligning with Shober et al.'s (2006) explanation, we hypothesized that soil artifacts from PL cleanout may introduce more Al and Fe than expected, thus resulting in minor species detected in PLA sources. Aluminum and Fe species are not thought to be the main species or cations controlling P solubility in PLA.

Calcium phosphate species differed amongst PLA generally with one or more Ca-phosphate species identified in each model fit. Calcium phosphate species' solubility decreased in the order of monocalcium phosphate $\text{Ca}(\text{H}_2\text{PO}_4)_2$ > brushite > monetite > octacalcium phosphate ($\text{Ca}_4\text{H}(\text{PO}_4)_3 \cdot 2.5 \text{H}_2\text{O}$) > beta-tricalcium phosphate ($\beta\text{-Ca}_3(\text{PO}_4)_2$) > hydroxyapatite ($\text{Ca}_5(\text{PO}_4)_3\text{OH}$) > fluorapatite ($\text{Ca}_5(\text{PO}_4)_3\text{F}$) (Table 2.1) (Lindsay, 1979; Chow and Eanes, 2001).

It is theorized that insoluble Ca-phosphate minerals composed PLA P species based upon alkaline PLA pH (>9.0), high elemental Ca concentrations, increased Ca:P ratios, and Ca-phosphate structures identified in BSED (Lindsay, 1979; Shober et al., 2006). The basis for this hypothesis was due to numerous studies reporting drastically lower P solubility and conditions (high pH and Ca:P ratios) conducive for insoluble Ca-phosphate precipitation (Lindsay, 1979; Codling et al., 2002; Codling, 2006; Pagliari et al., 2010; Middleton, 2015). Contrary to our hypothesis and findings from Shober et al. (2006) and Toor et al. (2005), LCF indicated absences of highly insoluble octacalcium phosphate, beta-tricalcium phosphate, hydroxyapatite, and fluorapatite species. Spectral features of FB Fly, FB Bulk, and GPLA (Figure 2.6, 2.7, and 2.9) displayed Ca-phosphate characteristic shoulder past absorption edge (white line energy) at 2160 to 2165 eV, denoting dicalcium phosphate presences (Peak et al., 2002). Specifically, soluble monetite was detected in FB Bulk (34.4%), CMix (76.8%), and GPLA (50.0%). Supporting monetite findings, Toor et al. (2005) XANES analysis detected monetite presences in broiler litter reporting Ca:P ratios ranging from 1.12 to 1.71, respectively. Our current PLA Ca:P ratios (1.15 to 1.37) fall within those reported by Toor et al. (2005) broiler litter XANES analysis and contradict initial theory that manure-to-energy temperatures alter P species from original PL. Brushite was detected in FB Fly (25.7%) and GPLA (33.2%) LCF and is supported by elemental ratios. Additionally, GPLA acidified from FB Fly had higher brushite and monetite weight percentage describing spectra models, translating into a more soluble Ca-phosphate species when compared to FB Fly original P species (Lindsay, 1979; Chow and Eanes, 2001). Unexpectedly, highly soluble monocalcium phosphate was detected in FB Bulk describing 10.6% of total P; however, elemental ratios failed to support monocalcium detection (Ca:P; 0.5:1) (Chow and Eanes, 2001). Stoichiometric Ca:P ratios supported monetite and brushite identification in

sample spectra LCF. In general, Ca appears to be dominate cation influencing PLA P species formation and solubility.

Unexamined in the current study is surface chemistry and PLA species potential to sequester or adsorb P from the soil. Higher pH values, larger surface area, smaller and more numerous pore sizes, and decreased carboxyl functional groups are characteristics conducive for P sorption according to Yingxue et al. (2019). These characteristics could aid in explaining decreased solubility from soluble monetite and brushite species identified in PLA spectra. Further examination beyond PLA P species, into noted sorption characteristics is needed to define P sorption effect on solubility beyond current species findings.

Conclusion

In agreement with numerous studies, PLA nutrient concentrations are highly variable as illustrated by significant differences detected across all twenty-one elements analyzed. Phosphorus concentrations ranged from 50.60 to 101.97 g P kg⁻¹. In comparison to triple superphosphate or ammoniated phosphorus fertilizers, all PLA P concentrations were considerably lower analysis fertilizer products than commercially available sources. However, PLA P nutrient concentrations on average are drastically higher than common PL analysis. Poultry litter ash K concentrations ranged from 62.57 to 119.15 g K kg⁻¹ following a similar comparison trend as P when compared to commercially sold muriate of potash and PL K analysis. Potassium structures identified via electron microscopy did not identify additional elements in compounds potentially influencing K availability. Sodium chloride identification as well as Na detected in predominately KCl crystals did suggest potential for K nutrient dilution in PLA products. Predominate P crystals identified included Ca, Ca-Mg-phosphate with K, and traces of micronutrients that control P solubility in PLA. Although BSED and XANES identified

Mg concentrations and bobierite ($\text{Mg}_3(\text{PO}_4)_2 \cdot 8 \text{H}_2\text{O}$), total elemental ratios failed to support stoichiometric possibilities. Conflicting results between quantitative elemental results and semi-quantitative advanced analysis highlighted complex P PLA chemistry. Interpretation of additional elements (Mg and K) in P structures and species (varscite, bobierite, and amorphous Fe) detected suggested that these are minor elements that influenced P solubility. The degree to which these additional elements (Mg, K, Fe, and Al) positively or negatively influenced P solubility unfortunately was not addressed in this work. However, results and literature support Ca as the dominate cation influencing P structural formation, P species, and P solubility (Lindsay, 1979; Toor et al., 2005; Shober et al., 2006). Results characterizing PLA elemental and chemical composition validated PLA use as a lower analysis P and K fertilizer source to commercial standards. When calibrating PLA sources as a fertilizer, elemental variability and P solubility controlled by Ca-phosphate species (monetite and brushite) will need to be taken into consideration as a slow release P source to adequately provide sufficient nutrients to maintain crop growth.

Acknowledgements

This research used resources of the Advanced Photon Source, a U.S. Department of Energy (DOE) Office of Science User Facility operated for the DOE Office of Science by Argonne National Laboratory under Contract No. DE-AC02-06CH11357. Funding for this work was provided in part by the Virginia Agricultural Experiment Station and the Hatch program of the National Institute of Food and Agriculture, US Department of Agriculture, and National Fish and Wildlife Foundation project number 0602.16.053565.

References

- Adams, Z. 2005. Comparison of broiler litter, broiler litter ash with reagent grade materials as sources of plant nutrients. M.S. thesis, Auburn University, AL.
- Al-Fariss, T.F., H.O. Ozbelge, and H.S. El-Shall. 1993. On the modeling of phosphate rock acidulation process. *J. Kind Saud University-Eng. Sci.* 5(2): 243–255. doi: [https://doi.org/10.1016/S1018-3639\(18\)30583-X](https://doi.org/10.1016/S1018-3639(18)30583-X).
- Ayding, I., F. Aydin, A. Saydut, G.E. Bakirdere, and C. Hamamci. 2010. Hazardous metal geochemistry of sedimentary phosphate rock used for fertilizer (Mazıdag, SE Anatolia, Turkey). *Microchem. J.* 96: 247–251. doi: 10.1016/j.microc.2010.03.006.
- Bock, B.R. 2004a. Poultry litter to energy: Technical and economic feasibility. TVA Public Power Institute, Muscle Shoals, AL.
- Bock, B.R. 2004b. Demonstrating optimum fertilizer value of ash from the biomass energy sustainable technology (BEST) demonstration project for swine and poultry manure management. TVA Public Power Institute, Muscle Shoals, AL.
- Bremner, J.M. 1996. Nitrogen-total. *Methods of Soil Analysis Part 3- Chemical Methods*. SSSA, Madison, WI.
- Chow, L.C., and E.D. Eanes, editors. 2001. *Octacalcium Phosphate*. Karger Medical and Scientific Publishers, Giathersburg, MD.
- Codling, E.E. 2006. Laboratory characterization of extractable phosphorus in poultry litter and poultry litter ash. *Soil Sci.* 171(11): 858–864. doi: 10.1097/01.ss.0000228059.38581.97.
- Codling, E.E. 2013. Phosphorus and arsenic uptake by corn, wheat, and soybean from broiler litter ash and egg layer manure ash. *J. Plant Nutr.* 36(7): 1083–1101. doi: 10.1080/01904167.2013.776079.
- Codling, E.E., R.L. Chaney, and J. Sherwell. 2002. Poultry litter ash as a potential phosphorus source for agricultural crops. *J. Environ. Qual.* 31(3): 954–61.
- Cordell, D., J.-O. Drangert, and S. White. 2009. The story of phosphorus: Global food security and food for thought. *Tradit. Peoples Clim. Change* 19(2): 292–305. doi: 10.1016/j.gloenvcha.2008.10.009.
- Coufal, C.D., C. Chavez, P.R. Niemeyer, and J.B. Carey. 2006. Measurement of broiler litter production rates and nutrient content using recycled litter. *Poult. Sci.* 85(3): 398–403. doi: 10.1093/ps/85.3.398.
- Crozier, C.R., J.L. Havlin, G.D. Hoyt, J.W. Rideout, and R. McDaniel. 2009. Three experimental systems to evaluate phosphorus supply from enhanced granulated manure ash. *Agron. J.* 101(4): 880–888. doi: 10.2134/agronj2008.0187x.

- Ervin, C.R. 2019 Poultry litter ash as an alternative fertilizer for corn. Ph.D. dissertation, Virginia Polytechnic and State University, Painter, VA.
- Duff, E.J. 1971. Orthophosphates XIII: Thermal decomposition of secondary calcium orthophosphate (CaHP04) and secondary calcium orthophosphate dihydrate (CaHP04 2H2O). *J. Appl. Chem. Biotechnol.* 21(8): 233–235. doi: <https://doi.org/10.1002/jctb.5020210804>.
- Franke, R., and J. Hormes. 1995. The P K-near edge absorption spectra of phosphates. *Phys. B* (216): 85–95. doi: [https://doi.org/10.1016/0921-4526\(95\)00446-7](https://doi.org/10.1016/0921-4526(95)00446-7).
- Frost, L.R., and S.J. Palmer. 2011. Thermal stability of the ‘cave’ mineral brushite CaHPO4·2H2O—Mechanism of formation and decomposition. *Thermochim. Acta* 521(1–2): 14–17. doi: [https://doi.org/10.1016/0921-4526\(95\)00446-7](https://doi.org/10.1016/0921-4526(95)00446-7).
- George, T.S., C.D. Giles, and D. Menezes-Blackburn. 2018. Organic phosphorus in the terrestrial environment: a perspective on the state of the art and future priorities. *Plant Soil* 427(1–2): 191–208. doi: <https://doi-org.ezproxy.lib.vt.edu/10.1007/s11104-017-3391-x>.
- Gupta, G., and S. Charles. 1999. Trace elements in soils fertilized with poultry litter. *Poult. Sci.* 78(12): 1695–1698. doi: 10.1093/ps/78.12.1695.
- Howarth, R.W., A. Sharpley, and D. Walker. 2002. Sources of nutrient pollution to coastal waters in the United States: Implications for achieving coastal water quality goals. *Estuaries Res. Found.* 25(4b): 565–676. doi: <https://doi.org/10.1007/BF02804898>.
- Kazi, T.G., A.Q. Shah, H.I. Afridi, N.A. Shah, and M.B. Arain. 2013. Hazardous impact of organic arsenical compounds in chicken feed on different tissues of broiler chicken and manure. *Ecotoxicol. Environ. Safety* 87: 12–123. doi: <https://doi-org.ezproxy.lib.vt.edu/10.1016/j.ecoenv.2012.10.012>.
- Kunkle, W.E., L.E. Carr, T.A. Carter, and E.H. Bossard. 1981. Effect of flock and floor type on the levels of nutrients and heavy metals in broiler litter. *Poult. Sci.* 60(6): 1160–1164. doi: <https://doi.org/10.3382/ps.0601160>.
- Leeson, S., and L. Caston. 2008. Using minimal supplements of trace minerals as a method of reducing trace mineral content of poultry manure. *Anim. Feed Sci. Technol.* 142: 339–347. doi: <https://doi.org/10.1016/j.anifeedsci.2007.08.004>.
- Lin, Y., P. Munroe, S. Joseph, S. Kimber, and L.V. Zwieten. 2012. Nanoscale organo-mineral reactions of biochars in ferrosol: An investigation using microscopy. *Plant Soil* 357(1–2): 369–380. doi: 10.1007/s11104-012-1169-8.
- Lindsay, W.L. 1979. *Chemical Equilibria in Soils*. The Blackburn Press, Caldwell, NJ.
- Maguire, R.O., J.T. Sims, S.K. Dentel, F.J. Coale, and J.T. Mah. 2001. Relationships between biosolids treatment process and soil phosphorus availability. *J. Environ. Qual.* 30(3): 1023–1033. doi: 10.2134/jeq2001.3031023x.

- Marshall, H.L., D.S. Reynolds, K.D. Jacob, and T.H. Tremearne. 1937. Phosphate fertilizers by calcination process. *Industrial Eng. Chem. Chem. Eng. Data Ser.* 29(11): 1294–1298. doi: DOI: 10.1021/ie50335a022.
- Middleton, A.J. 2015. Nutrient availability from poultry litter co-products. M.S. thesis, Virginia Polytechnic and State University, Blacksburg, VA.
- Pagliari, P.H., C.J. Rosen, and J.S. Strock. 2009. Turkey manure ash effects on alfalfa yield, tissue elemental composition, and chemical soil properties. *Commun. Soil Sci. Plant Anal.* 40(17–18): 2874–2897. doi: 10.1080/00103620903173863.
- Pagliari, P., C. Rosen, J. Strock, and M. Russelle. 2010. Phosphorus availability and early corn growth response in soil amended with turkey manure ash. *Commun. Soil Sci. Plant Anal.* 41(11): 1369–1382. doi: 10.1080/00103621003759379.
- Peak, D., J.T. Sims, and D.L. Sparks. 2002. Solid-state speciation of natural and alum-amended poultry litter using XANES spectroscopy. *Environ. Sci. Technol.* 36(20): 4253–4261. doi: 10.1021/es025660d.
- Qin, Z., A.L. Shober, K.G. Scheckel, C.J. Penn, and K.C. Turner. 2018. Mechanisms of phosphorus removal by phosphorus sorbing materials. *J. Environ. Qual.* 47(5): 1232–1241. doi: 10.2134/jeq2018.02.0064.
- Ravel, B., and M. Newville. 2005. ATHENA, ARTEMIS, HEPHAESTUS: Data analysis for X-ray absorption spectroscopy using IFEFFIT. *J. Synchrotron Radiat.* 12(4): 537–541. doi: doi.org/10.1107/S0909049505012719.
- Reiter, M.S., and A. Middleton. 2016. Nutrient availability from poultry litter co-products. Virginia Tech University, Painter, VA.
- SAS Institute Inc. 2017. SAS Institute. SAS Institute Inc., Cary, NC.
- Scholz, R.W., A.E. Ulrich, M. Eilitta, and A. Roy. 2013. Sustainable use of phosphorus: A finite resource. *Sci. Total Environ.* 461: 799–803. doi: https://doi.org/10.1016/j.scitotenv.2013.05.043.
- Sharpley, A. 1994. Managing agricultural phosphorus for protection of surface Waters: Issues and options. <https://dl-sciencesocieties-org.ezproxy.lib.vt.edu/publications/jeq/pdfs/23/3/JEQ0230030437> (accessed 19 December 2016).
- Sharpley, A.N. 1995. Soil phosphorus dynamics: agronomic and environmental impacts. *Ecol. Eng.* 5: 261–279. doi: https://doi.org/10.1016/0925-8574(95)00027-5.
- Shepard, T.J., C. Ayora, D.L. Cendon, S.R. Chenery, and A. Moissette. 1998. Quantitative solute analysis of single fluid inclusions in halite by LA-ICP-MS and cryo-SEM-EDS: complementary microbeam techniques. *Eur. Journal Mineral.* 10(6): 1097–1108. doi: 10.1127/ejm/10/6/1097.

- Shober, A.L., D.L. Hesterberg, J.T. Sims, and S. Gardner. 2006. Characterization of phosphorus species in biosolids and manures using XANES spectroscopy. *J. Environ. Qual.* 35(6): 1983–1993. doi: 10.2134/jeq2006.0100.
- Sparks, D.L., A.L. Page, P.A. Helmke, R.H. Loeppert, P.N. Soltanpour, et al., editors. 1996. *Methods of Soil Analysis*. Soil Science Society of America, Inc. American Society of Agronomy, Inc., Madison, WI.
- Spokas, K.A., J.M. Novak, C.A. Masiello, M.G. Johnson, E.C. Colosky, et al. 2014. Physical disintegration of biochar: An overlooked process. *Environ. Sci. Technol. Lett.* 1: 326–332. doi: dx.doi.org/10.1021/ez500199t.
- Tonsuaadu, K., K. Gross, L. Pluduma, and M. Veiderma. 2012. A review on the thermal stability of calcium apatites. *J. Therm Anal Calorm* (110): 647–659. doi: DOI 10.1007/s10973-011-1877-y.
- Toor, G., D.J. Peak, and T.J. Sims. 2005. Phosphorus speciation in broiler litter and turkey manure produced from modified diets. *J. Environ. Qual.* 34(2): 687–97. doi: doi:10.2134/jeq2005.0687.
- United States Environmental Protection Agency. 1996. Method 3050B: Acid digestion of sediments, sludges, and soils, Revision 2. U.S. EPA, Washington, DC.
- Van Kauwenbergh, S.J., M. Stewart, and R. Mikkelsen. 2013. World reserves of phosphate rock... a dynamic and unfolding story. *Better Crops* 97(3): 18–20.
- Virginia Tech Institute for Critical Technology and Applied Science. 2018. Leo (Zeiss) 1500. NCFL. https://www.ncfl.ictas.vt.edu/?page_id=57.
- Yager, D.B. 2016. Potash—A vital agricultural nutrient sourced from geologic deposits. U.S. Geological Survey Open File Report 2016-1167, Reston, VA.
- Yingxue, L., D. Xu, Y. Guan, K. Yu, and W. Wang. 2019. Phosphorus sorption capacity of biochars from different waste woods and bamboo. *Int. J. Phytoremediation* 21(2): 145–151. doi: 10.1080/15226514.2018.1488806.

Table 2.1 Phosphorus K-XANES spectra phosphate standards used in linear combination fitting.

Standard	Formula	Formation Constant $\log K^\circ$ †
Aluminum Phosphate Species		
Phosphate sorbed to Alumina hydroxide‡	$\text{Al}(\text{OH}_3)\text{PO}_4$	-\$
Wavelite	$\text{Al}_3(\text{PO}_4)_2(\text{OH},\text{F})_3 \cdot 5 \text{H}_2\text{O}$	
Varscite	$\text{AlPO}_4 \cdot 2 \text{H}_2\text{O}$	-2.50
Calcium Phosphate Species		
Monocalcium phosphate	$\text{Ca}(\text{H}_2\text{PO}_4)_2$	-1.15
Brushite (Dicalcium phosphate dihydrate)	$\text{CaHPO}_4 \cdot 2 \text{H}_2\text{O}$	0.63
Monetite (Dicalcium phosphate anhydrous)	CaHPO_4	0.30
Octacalcium phosphate	$\text{Ca}_4\text{H}(\text{PO}_4)_3 \cdot 2.5 \text{H}_2\text{O}$	11.76
Beta-tricalcium phosphate	$\beta\text{-Ca}_3(\text{PO}_4)_2$	10.18
Hydroxyapatite	$\text{Ca}_5(\text{PO}_4)_3\text{OH}$	14.46
Fluorapatite	$\text{Ca}_5(\text{PO}_4)_3\text{F}$	-0.21
Iron Phosphate Species		
Non-crystalline iron phosphate (FePAmp)	-	-
Strengtite	$\text{FePO}_4 \cdot 2 \text{H}_2\text{O}$	-6.85
MnFeP	-	-
Magnesium and Phosphate Species		
Bobierite	$\text{Mg}_3(\text{PO}_4)_2 \cdot 8 \text{H}_2\text{O}$	14.10
Newberryite	$\text{MgHPO}_4 \cdot 3 \text{H}_2\text{O}$	1.38

† Formation constant ($\log K^\circ$) relating two species is numerically equal to the pH at which the reacting species have equal activities for various phosphate reactions at 25 °C. Solubility constant adapted from Chemical Equilibria in Soils by Lindsay (1979).

‡ Phosphorus standard preparation, synthesis, and spectra utilized for LCF are described in supplemental information by Qin et al. (2018).

§ Unknown equilibrium constant.

Table 2.2a Total elemental analysis of broiler litter converted into poultry litter ash (PLA) via fluidized bed combustion system in Rhodesdale, MD producing fluidized bed fly (FB Fly), fluidized bed bulk (FB Bulk), granulated poultry litter ash (GPLA), and ash coated urea (ACU) and from combustion thermo-conversion system in Lancaster county, PA producing combustion mix (CMix).

Source	As	B	Be	Cd	Co	Cr	Cu	Mo
	mg kg⁻¹							
FB Fly	3.05 b†	155.24 c	0.33 c	1.21 c	2.57 b	15.35 c	1413.5 b†	28.72 b
FB Bulk	2.33 c	114.5 d	0.24 d	0.43 e	2.33 b	11.55 d	636.2 d	21.10 d
CMix	11.11 a	349.60 b	0.94 b	1.77 b	8.00 a	25.17 b	4028.5 a	43.12 a
GPLA-B	2.34 c	121.25 d	1.0 a	6.58 a	2.10 b	56.1 a	1090.6 c	23.65 c
GPLA-Acd2	2.22 c	118.71 d	0.25 d	0.97 d	2.08 b	14.83 cd	1064.7 c	24.34 c
ACU	0.22 d	1106.69a	0.03 e	0.18 f	0.34 c	3.15 e	171.7 e	8.25 e
LSD_{0.05}	0.65	23.47	0.03	0.18	0.54	3.35	117.1	2.13
p-value	<0.0001	<0.0001	<0.0001	<0.0001	<0.0001	<0.0001	<0.0001	<0.0001

† Within columns, means followed by the same letter are not significantly different according to LSD (0.05).

Table 2.2b Total elemental analysis of broiler litter converted into poultry litter ash (PLA) via fluidized bed combustion system in Rhodesdale, MD producing fluidized bed fly (FB Fly), fluidized bed bulk (FB Bulk), granulated poultry litter ash (GPLA), and ash coated urea (ACU) and from combustion thermo-conversion system in Lancaster county, PA producing combustion mix (CMix).

Source	Ni	Pb	Se	Si	Zn	Al	Ca	Fe
	mg kg ⁻¹					g kg ⁻¹		
FB Fly	19.92 b†	11.55 a	9.93 a	45.38 bc	2066.8 a	7.65 b†	75.01 b	5.49 b
FB Bulk	16.35 c	2.12 c	5.94 d	56.72 b	1665.2 b	5.79 c	72.89 b	4.32 c
CMix	40.15 a	2.0 c	6.29 d	42.12 bc	1639.8 b	17.72 a	123.73 a	13.22 a
GPLA-B	15.18 c	9.0 b	7.77 c	32.92 c	1562.0 bc	7.25 b c	60.06 c	5.98 b
GPLA-Acd2	14.56 c	9.81 b	8.82 b	47.66 bc	1469.6 c	5.78 c	55.85 c	4.20 c
ACU	2.96 d	2.45 c	2.45 e	203.82 a	220.8 d	0.81 d	8.07 d	0.69 d
LSD 0.05	1.87	1.01	0.85	15.31	116.0	1.49	4.70	0.55
p-value	<0.0001	<0.0001	<0.0001	<0.0001	<0.0001	<0.0001	<0.0001	<0.0001

† Within columns, means followed by the same letter are not significantly different according to LSD (0.05).

Table 2.2c Total elemental analysis of broiler litter converted into poultry litter ash (PLA) via fluidized bed combustion system in Rhodesdale, MD producing fluidized bed fly (FB Fly), fluidized bed bulk (FB Bulk), granulated poultry litter ash (GPLA), and ash coated urea (ACU) and from combustion thermo-conversion system in Lancaster county, PA producing combustion mix (CMix).

	K	Mg	Na	P	S	Ca:P	C	N	pH
Source	g kg⁻¹								
FB Fly	119.15 b†	20.76 b	40.65 a	50.60 d†	30.50 a	1.48 c	15.85 c	2.58 b	9.16 c
FB Bulk	62.57 e	19.11 c	25.62 d	44.95 e	22.00 c	1.62 b	1.50 d	0.55 b	10.21 b
CMix	128.59 a	47.18 a	31.87 c	69.89 c	24.27 b	1.77 a	33.78 b	2.38 b	10.50 a
GPLA-B	102.20 c	19.16 c	34.76 b	90.47 b	25.91 b	0.67 d	12.13 c	2.70 b	5.53 d
GPLA-Acd2	93.91 d	16.34 d	32.17 c	101.97 a	22.16 c	0.55 e	12.63 c	2.28 b	4.85 e
ACU	13.98 f	2.14 e	4.71 e	5.38 f	1.69 d	1.50 c	204.80 a	456.38 a	9.07 c
LSD_{0.05}	6.26	1.25	1.55	4.34	2.05	0.03	5.48	3.59	0.13
p-value	<0.0001	<0.0001	<0.0001	<0.0001	<0.0001	<0.0001	<0.0001	<0.0001	<0.0001

† Within columns, means followed by the same letter are not significantly different according to LSD (0.05).

Table 2.3 Electron scanning microscopy back scatter overview elemental analysis of broiler litter converted into poultry litter ash (PLA) via fluidized bed combustion system in Rhodesdale, MD producing fluidized bed fly (FB Fly), fluidized bed bulk (FB Bulk), granulated poultry litter ash (GPLA), and ash coated urea (ACU) and from combustion thermo-conversion system in Lancaster county, PA producing combustion mix (CMix).

	O	P	Ca	Ca:P	K	Al	Cl	Na	Si
Source	Element Atomic %								
FB Fly	58.9	3.57 b†	4.27 b	1.20 b	10.5	0.67 b	8.09 a	6.02 a	2.23
FB Bulk	55.62	4.93 b	6.73 a	1.37 b	6.48	1.12 a	5.33 ab	7.97 a	8.43
CMix	60.81	4.07 b	6.45 a	1.62 a	9.78	1.05 ab	4.04 b	2.89 b	2.22
GPLA-Acd2	57.04	17.93 a	1.65 c	0.09 c	12.08	0.17 c	0.76 c	1.01 b	0.53
LSD 0.05	ns‡	2.11	1.15	0.25	ns	0.41	3.15	2.42	ns
p-value	0.64	<0.0001	<0.0001	<0.0001	0.28	0.01	0.01	0.02	0.15

† Within columns, means followed by the same letter are not significantly different according to LSD (0.05)

‡ ns, nonsignificant.

Table 2.4 Electron scanning microscopy back scatter electron dispersive physical structure identification providing average elemental analysis of fluidized bed bulk (FB Bulk) selected structures.

	K†	Na	Cl	O	P	Ca	Si	S	Mg	Fe	Mn
Identified Structure	Element Atomic %										
Figure 2.2 Pt. 1.1	43.06	2.96	49.42	-‡	-‡	-‡	-‡	-‡	-‡	-‡	-‡
Figure 2.2 Pt 1.2	4.66	2.71	0.56	49.85	5.03	4.79	14.38	-‡	13.0	-‡	1.48
Figure 2.2 Pt. 1.3	1.04	1.90	0.58	55.66	14.40	22.83	0.67	-‡	3.59	0.54	-‡

† Average of element atomic % across structure point identified.

‡ Element below detection limit.

Table 2.5 Electron scanning microscopy back scatter electron dispersive physical structure identification providing average elemental analysis of fluidized bed fly (FB Fly) selected structures.

	K†	Na	Cl	O	P	Ca	Si	S	Mg
Identified Structure	Element Atomic %								
Figure 2.3a Pt. 2.1	46.16	-‡	53.84	-‡	-‡	-‡	-‡	-‡	-‡
Figure 2.3a Pt. 2.2	7.03	-‡	-‡	-‡	36.60	63.40	-‡	-‡	-‡
Figure 2.3b Pt. 2.3	15.08	37.66	44.91	31.49	1.43	1.63	0.73	-‡	-‡
Figure 2.3c Pt. 2.4	7.04	5.76	0.67	57.87	21.44	21.51	0.73	1.63	12.69

† Average of element atomic % across structure point identified.

‡ Element below detection limit.

Table 2.6 Electron scanning microscopy back scatter electron dispersive physical structure identification providing average elemental analysis of combustion mix (CMix) selected structures.

Identified Structure	K†	Na	Cl	O	P	Ca	Si	S	Mg	Fe	Mn	Al	C	Ti
	Element Atomic %													
Figure 2.4a Pt. 3.1	48.1 2	-‡	51.88	-‡	-‡	-‡	-‡	-‡	-‡	-‡	-‡	3.11	-‡	-‡
Figure 2.4b Pt. 3.2	2.95	0.94	-‡	64.2 5	5.60	12.4 2	2.45	-‡	7.69	0.66	0.54	2.27	-‡	-‡
Figure 2.4b Pt. 3.3	1.54	0.41	0.51	18.3 9	0.90	1.29	-‡	1.02	0.78	-‡	-‡	-‡	75.1 6	-‡
Figure 2.4b Pt. 3.4	4.41	2.23	0.50	59.6 5	0.92	0.29	11.30	0.59	1.86	3.74	-‡	12.50	-‡	2.00

† Average of element atomic % across structure point identified.

‡ Element below detection limit.

Table 2.7 Electron scanning microscopy back scatter electron dispersive physical structure identification providing average elemental analysis of granulated poultry litter ash (GPLA) selected structures.

	K†	Na	Cl	O	P	Ca	Si	S	Mg	Fe	Mn	Al
Identified Structure	Element Atomic %											
Figure 2.5 Pt. 4.1	12.38	-‡	-‡	70.45	16.28	0.88	-‡	-‡	-‡	-‡	-‡	-‡
Figure 2.5 Pt. 4.2	6.96	2.14	-‡	55.63	20.70	3.74	2.28	3.13	3.36	0.56	0.26	-‡

† Average of element atomic % across structure point identified.

‡ Element below detection limit.

Table 2.8 Linear combination fitting weight percentage of standards describing spectra poultry litter ash P spectra fitting.

Standard Species	Monetite (CaHPO₄)	Bobierite (Mg₃(PO₄)₂ · 8 H₂O)	Brushite (CaHPO₄·2H₂O)	Monocalcium P Ca(H₂PO₄)₂ · H₂O	Varscite (AlPO₄ · 2H₂O)	FeAmorP	Residual Factor (R)	Chi- Square
Source†	% of total P							
FB Fly	-‡	18.4	25.7	-‡	55.9	-‡	0.002614	0.25
FB Bulk	34.4	39.5	-‡	10.6	15.5	-‡	0.003873	0.32
CMix	76.8	-‡	-‡	-‡	12.9	10.3	0.004215	0.05
GPLA	50.0	16.8	33.2	-‡	-‡	-‡	0.01	0.75

† Fluidized bed fly (FB Fly), fluidized bed bulk (FB Bulk), and granulated poultry litter ash (GPLA) originate from thermally converted broiler litter via fluidized combustion system in Rhodesdale, MD. Combustion Mix (CMix) originates from broiler litter thermally converted via a combustion system in Lancaster county, PA.

‡ Species was not detected in Athena linear combination fitting (LCF). Standards were sequentially eliminated when standard described < 10% of LCF spectra.

Table 2.9 Selected poultry litter ash elemental properties that were used for XANES analysis.

Source	Total					Molar Ratio			
	P	Al	Ca	Mg	Fe	Al:P	Ca:P	Mg:P	Fe:P
	g kg ⁻¹					mol mol			
FB Fly	50.60	7.65	75.01	20.76	5.49	0.17	1.15	0.52	0.06
FB Bulk	44.95	5.79	72.89	19.11	4.32	0.15	1.25	0.54	0.05
CMix	69.89	17.72	123.73	47.18	13.22	0.29	1.37	0.86	0.10
GPLA-B	90.47	7.25	60.6	19.16	5.98	0.09	0.52	0.27	0.04

† Fluidized bed fly (FB Fly), fluidized bed bulk (FB Bulk), and granulated poultry litter ash (GPLA) originate from thermally converted broiler litter via fluidized combustion system in Rhodesdale, MD. Combustion Mix (CMix) originates from broiler litter thermally converted via a combustion system in Lancaster county, PA.

Figure 2.1 Diagram illustrating protocol implemented to examine poultry litter ash (PLA) samples via electron microscopy (ESM) backscatter electron dispersive (BSED) analysis. First, two regions (a) were chosen for overview elemental analysis of each sample. Then specific structures (b) within each region were identified for multipoint structural analysis.

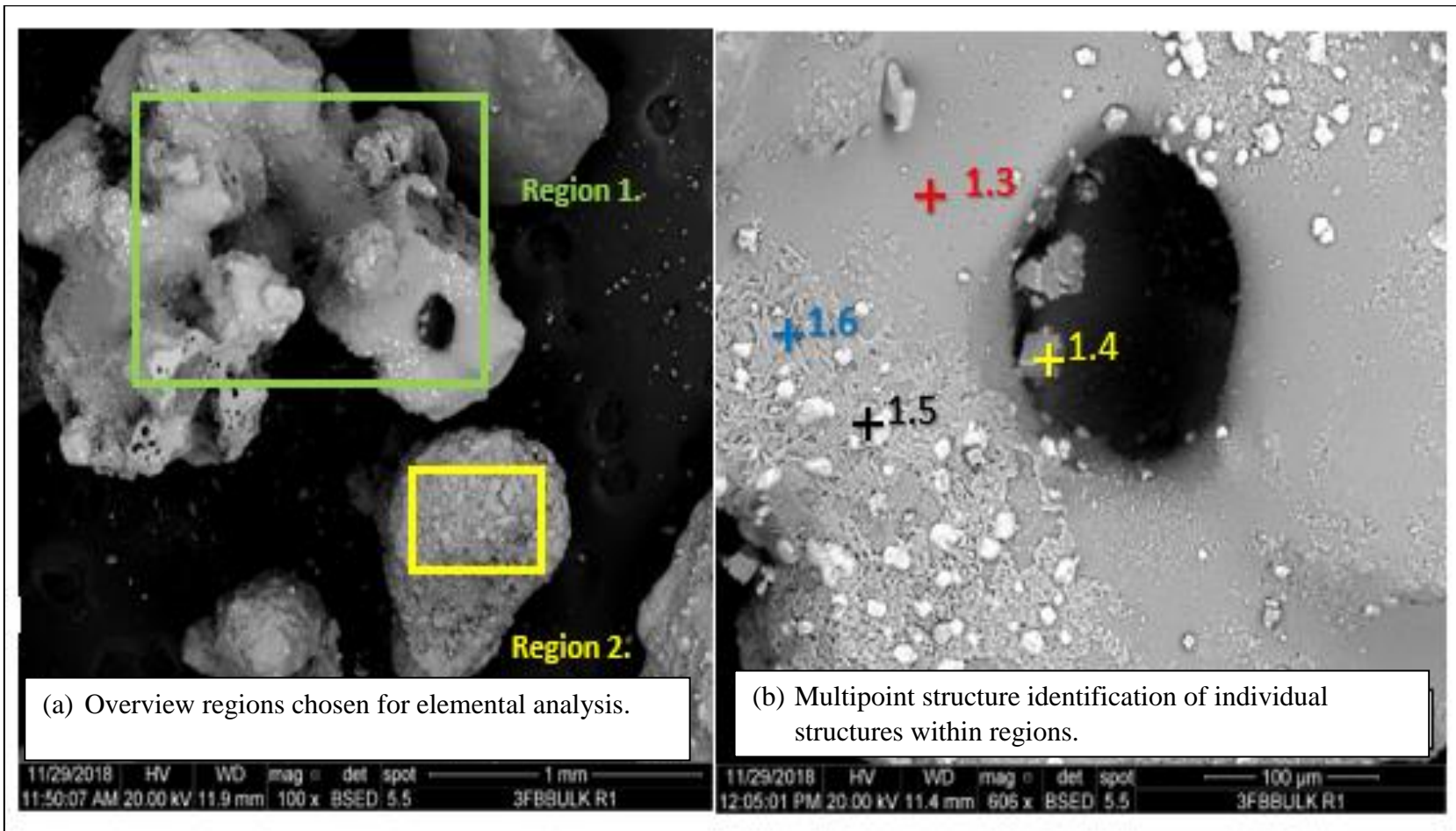


Figure 2.2 Fluidized bed bulk (FB Bulk) backscatter electron dispersive (BSED) elemental analysis of multipoint identified structures (Pts. 1.1, 1.2, and 1.3).

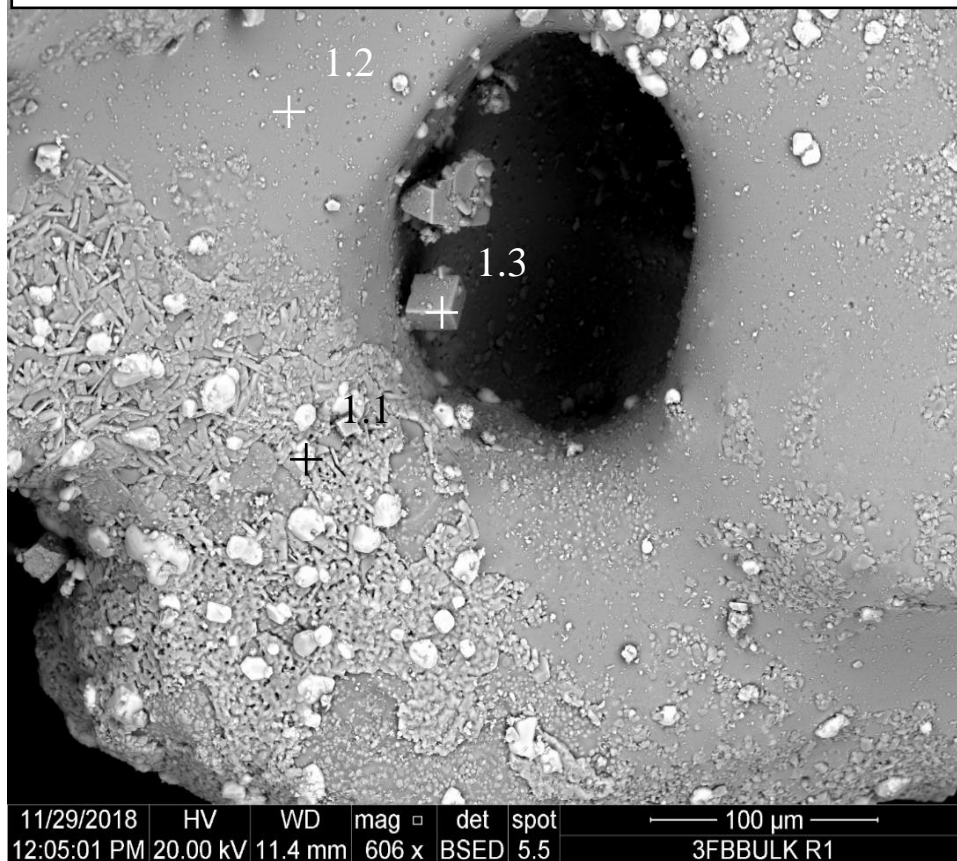


Figure 2.3a Fluidized bed fly (FB Fly) backscatter electron dispersive (BSED) elemental analysis of multipoint identified structures (Pts. 2.1 and 2.2).

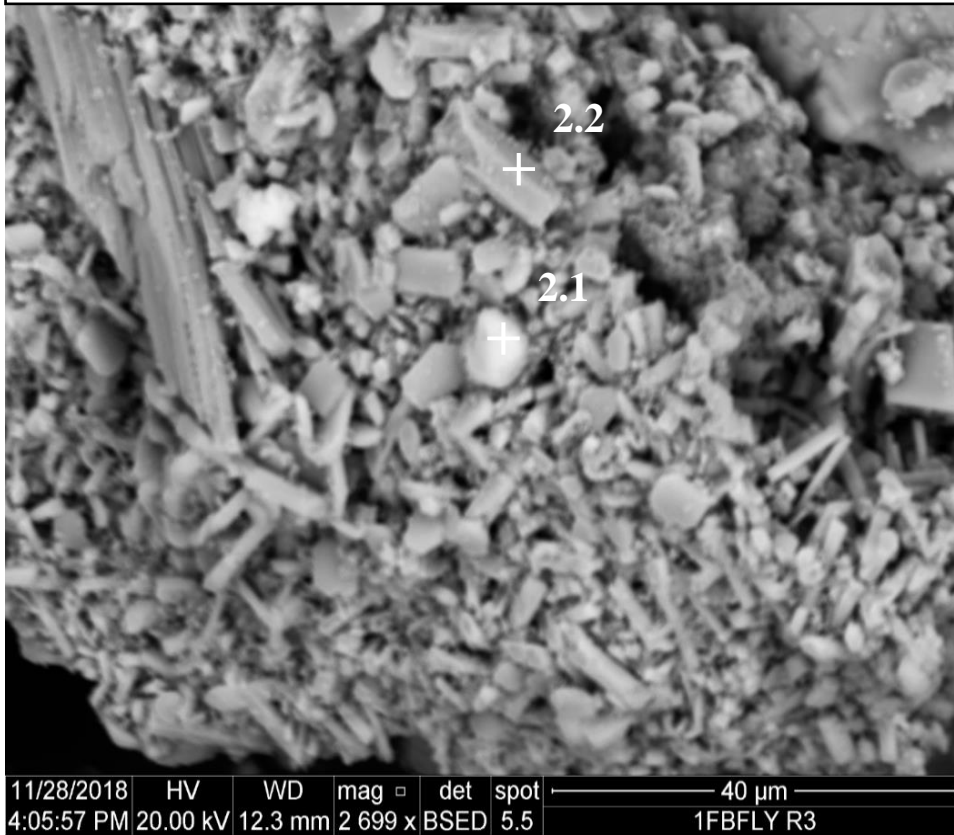


Figure 2.3b Fluidized bed fly (FB Fly) backscatter electron dispersive (BSED) elemental analysis of multipoint identified structures (Pt 2.3).

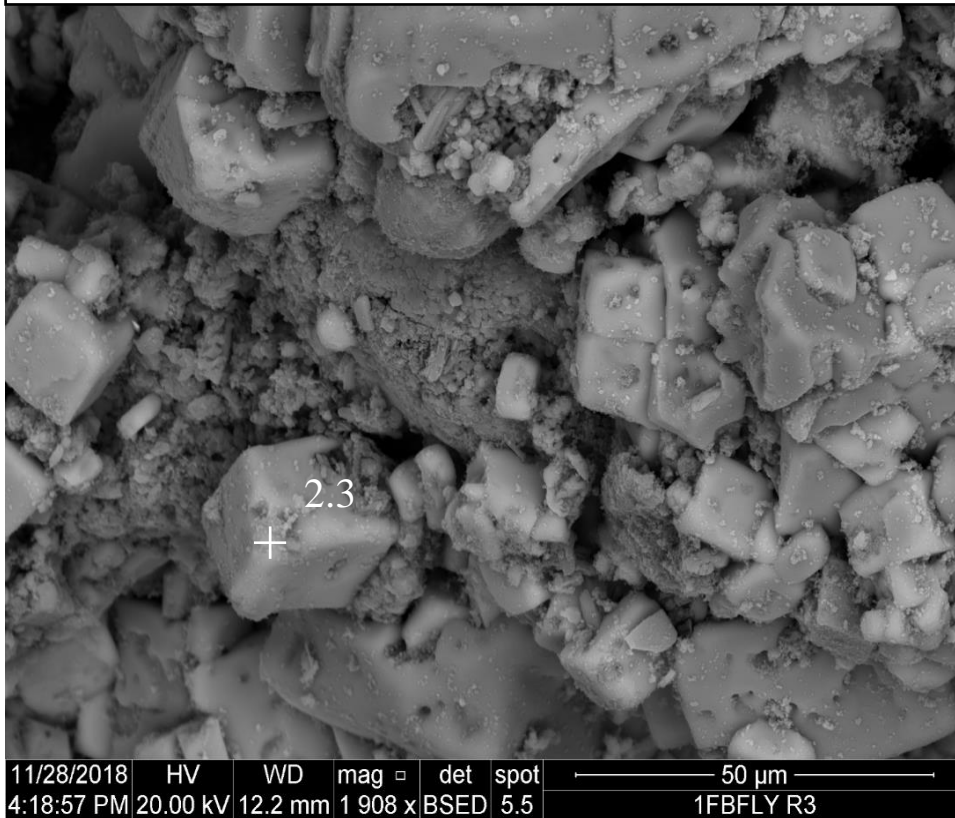


Figure 2.3c Fluidized bed fly (FB Fly) backscatter electron dispersive (BSED) elemental analysis of multipoint identified structures (Pt 2.4).

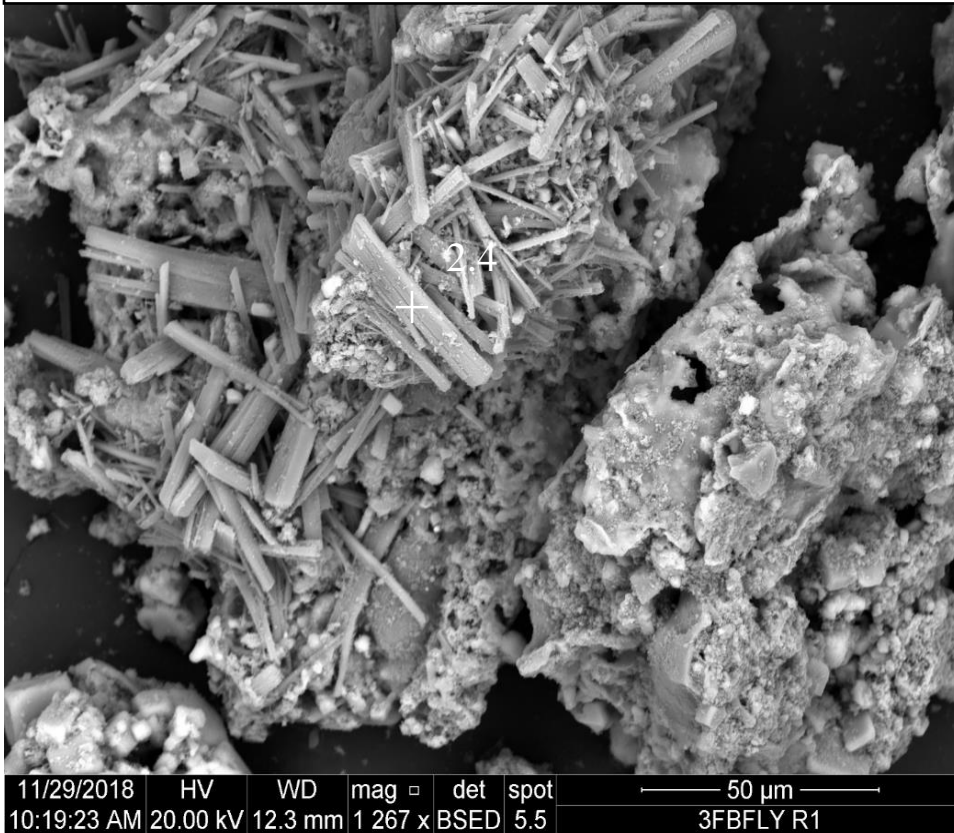


Figure 2.4a Combustion mix (CMix) backscatter electron dispersive (BSED) elemental analysis of multipoint identified structures (Pt 3.1).

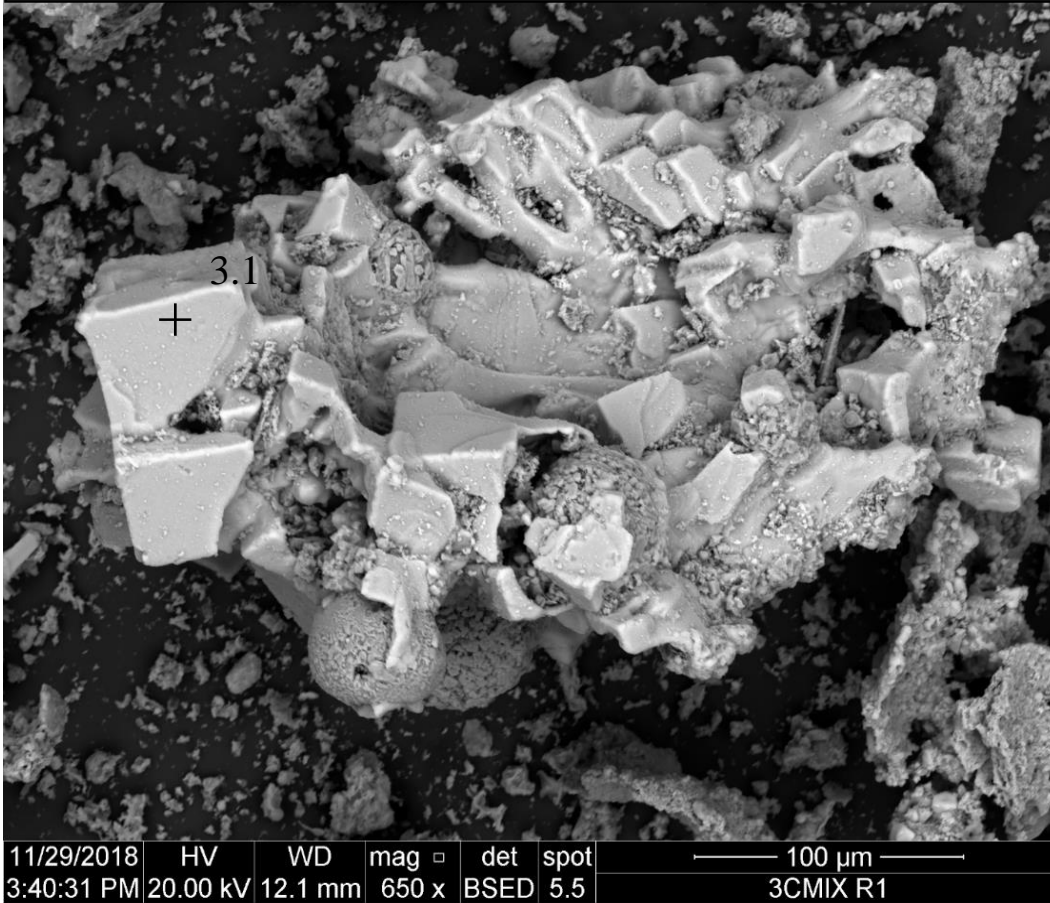


Figure 2.4b Combustion mix (CMix) backscatter electron dispersive (BSED) elemental analysis of multipoint identified structures (Pts. 3.2, 3.3, and 3.4).

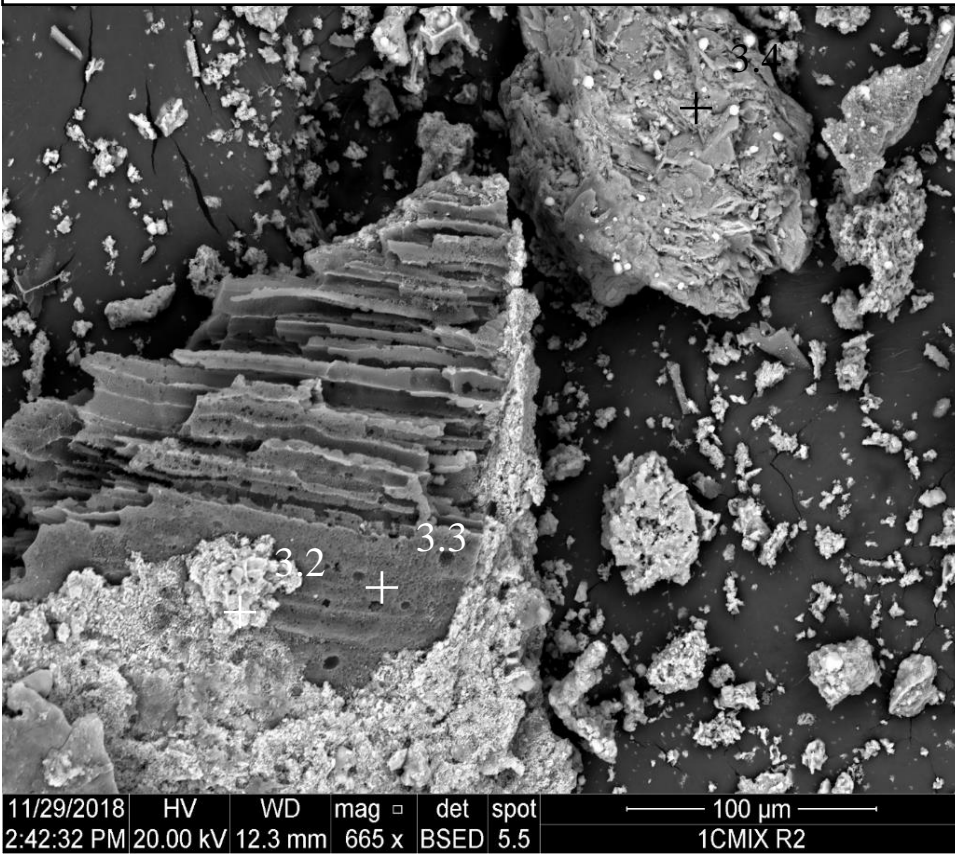


Figure 2.5 Granulated poultry litter ash (GPLA) backscatter electron dispersive (BSED) elemental analysis of multipoint identified structures (Pts. 4.1 and 4.2).



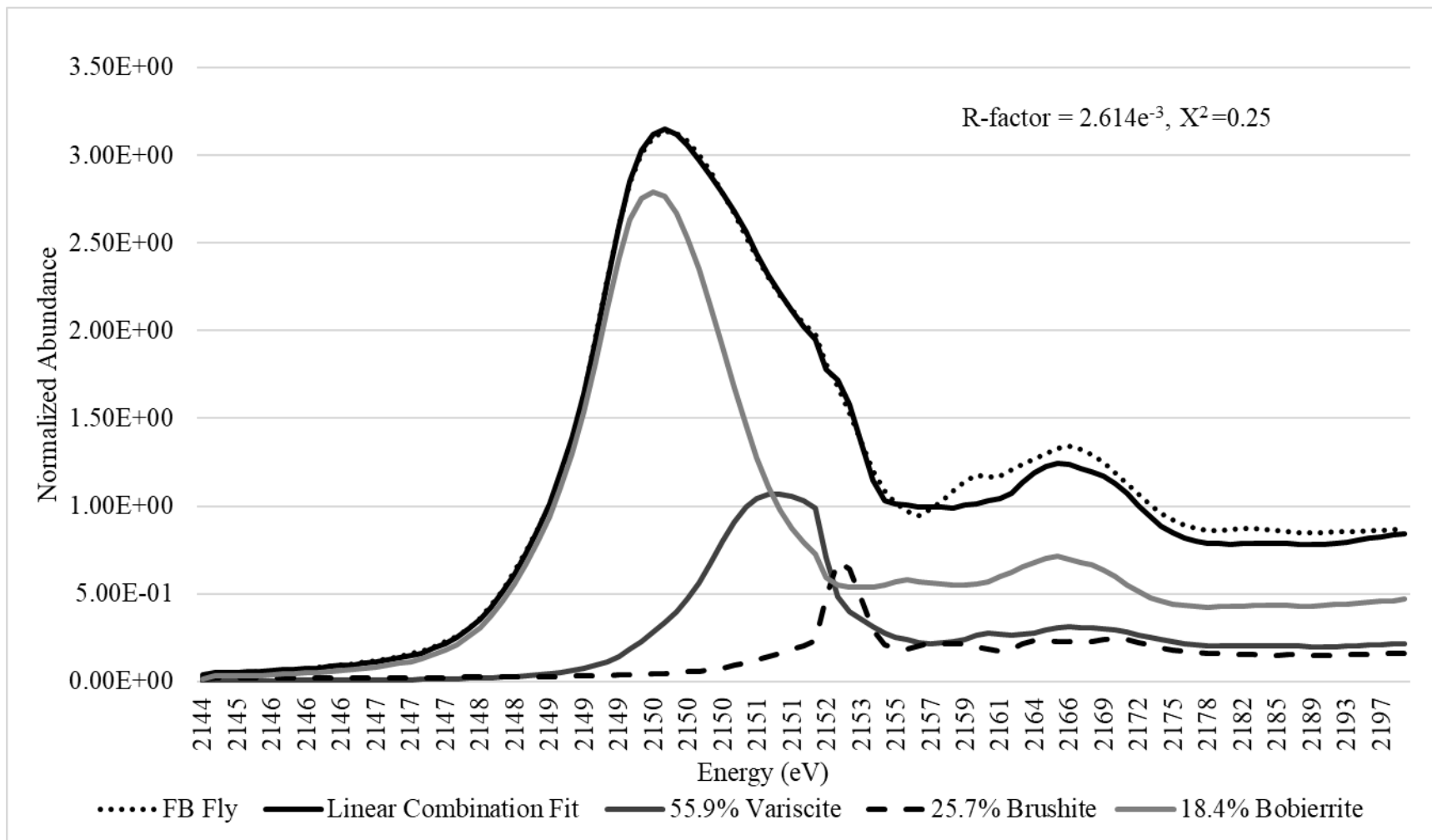


Figure 2.6 Linear combination fitting (LCF) results of P K-edge X-ray absorption near-edge structure (XANES) spectra of fluidized bed fly (FB Fly) poultry litter ash. The spectra of the reference standards represent the relative proportion of each standard describing sample spectra species.

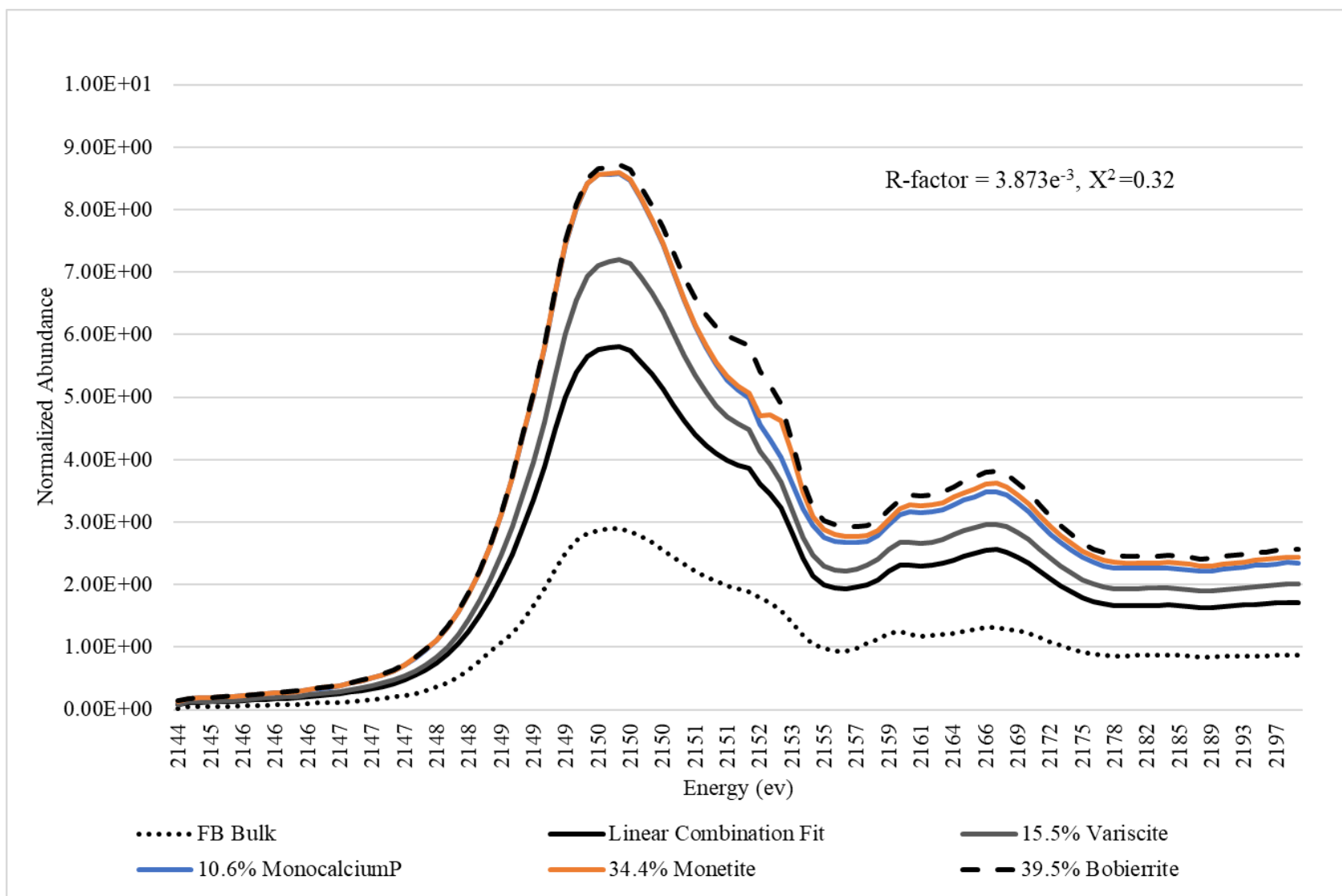


Figure 2.7 Linear combination fitting (LCF) results of P K-edge X-ray absorption near-edge structure (XANES) spectra of fluidized bed bulk (FB Bulk) poultry litter ash. The spectra of the reference standards represent the relative proportion of each standard describing sample spectra species.

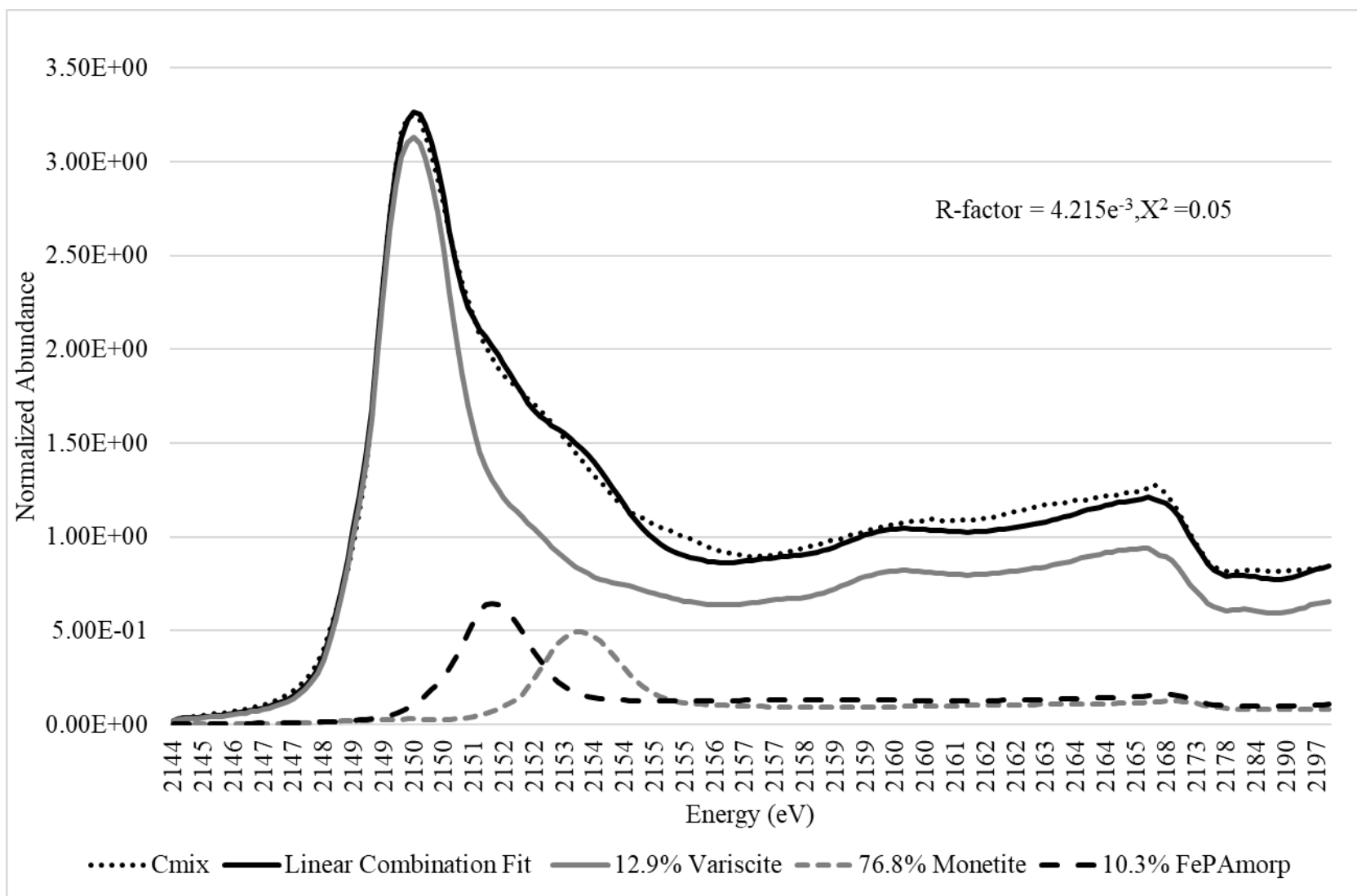


Figure 2.8 Linear combination fitting (LCF) results of P K-edge X-ray absorption near-edge structure (XANES) spectra of combustion mix (CMix) poultry litter ash. The spectra of the reference standards represent the relative proportion of each standard describing sample spectra species.

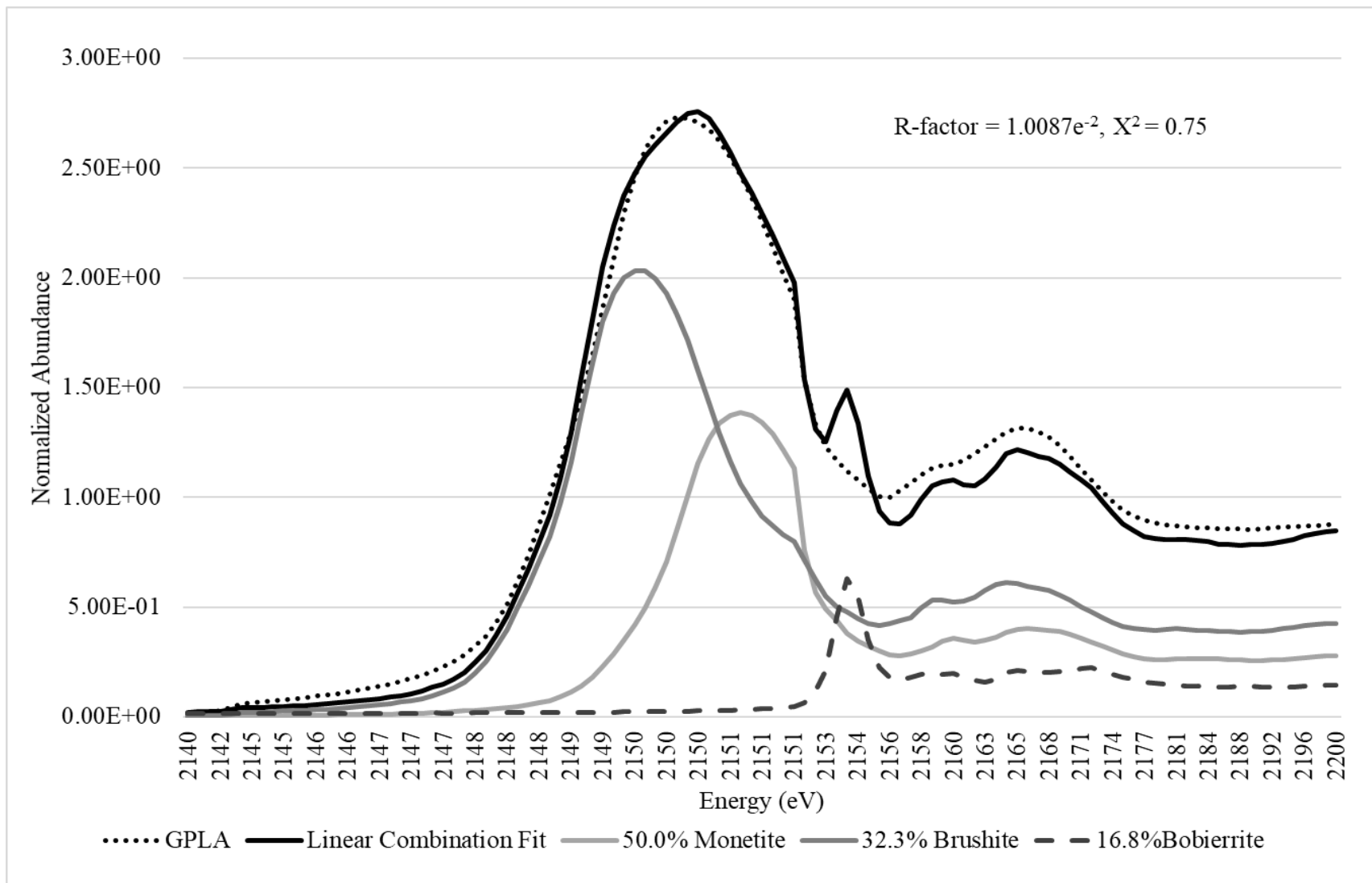


Figure 2.9 Linear combination fitting (LCF) results of P K-edge X-ray absorption near-edge structure (XANES) spectra of granulated poultry litter ash (GPLA) poultry litter ash. The spectra of the reference standards represent the relative proportion of each standard describing sample spectra species.

Chapter 3: Granulated Poultry Litter Ash Acidulation and Physical Characteristics

Abstract

Poultry litter ash (PLA) originated in response to increased manure volumes generated by concentrated poultry production regions within the mid-Atlantic, USA. Manure-to-energy systems effectively recycle poultry litter (PL) into PLA that densifies and concentrates original P nutrients 4 to 10 times. However, high conversion temperatures reduce nutrient solubility as well as produce small particulate materials. In effort to redistribute manure nutrients by improving PLA physical and chemical characteristics, the following objectives included: 1) Determine phosphoric acid (H_3PO_4) acidifying effect on water soluble P (WSP), measurable total P (TP), granulation point, and fertilizer granule size and 2) Conduct large scale GPLA-Bulk (GPLA-B) granulation to determine larger scale formulations and granule physical characteristics produced. We measured bulk density, force and friction resistance, and granule size as compared to industry standard triple superphosphate (TSP). Acidulation experiments were arranged in a completely randomized design with four replications per H_3PO_4 acidulation percentage treatment. Increasing acidulation percentages from 0 to 50% H_3PO_4 (laboratory grade white phosphoric acid) increased extractable TP from 50.63 to 116.9 g kg^{-1} and WSP from 0.31 to 47.4 g P kg^{-1} ($\text{LSD}_{0.05}$ 10.13 and 2.65 g P kg^{-1} , respectively). Acidulation dose response relationships created simple linear regression equations to predict changes in measurable TP and WSP, pH, and exothermic reaction temperatures that increased with acidulation. Bulk GPLA-B loose (1.01 g cm^{-3}) and packed (1.03 g cm^{-3}) bulk density was significantly less than TSP (1.3 and 1.14 g cm^{-3} , respectively) ($\text{LSD}_{0.05} = 0.03$ and 0.02 g cm^{-3}). Compared to TSP (2.86 mm), GPLA (3.73

mm) diameter was significantly larger ($LSD_{0.05} = 0.61$ mm); however, GPLA (4.53 kgf) force resistance was significantly less than TSP (5.95 kgf) ($LSD_{0.05} = 0.61$ kgf).

Introduction

As the expanding world population places pressure on poultry production to meet consumption demands, increased poultry litter (PL) volumes present environmental concerns. Poultry operations in the mid-Atlantic are unequally distributed throughout the region and are concentrated in the Shenandoah Valley and Delmarva peninsula. In high density poultry production regions, high soil test phosphorus (STP) and environmental concerns within the Chesapeake Bay watershed prompted research investigating methods to redistribute PL nutrients outside of concentrated poultry production regions (Sharpley, 1994; Maguire and Sims, 2002; Codling, 2006; Kleinman et al., 2012; Middleton, 2015). Nutrients within PL are valuable for crop production; however, as with any fertilizer, PL has potential to negatively affect environmental resources if nutrients reach surface or ground-water. When manure is continually applied over long periods of time based on crop N needs, soil P concentrations will increase as PL provides more P than removed by crops (Sharpley, 1994; Howarth et al., 2002; Sharpley et al., 2007). High STP concentrations combined with conservation tillage that reduces nutrient incorporation leads to more surface STP possibly increasing non-point source pollution (Sharpley and Smith, 1994).

Examining agricultural systems' effect on regional nutrient cycling and subsequent nutrient distribution resulted in disproportional nutrient concentrations across agricultural areas, namely P (Slaton et al., 2004). Major crop production regions remain nutrient deficit as surplus nutrients build in livestock production regions due to manure transportation difficulties. Maguire et al. (2007) conducted a mass balance estimate of P generated from livestock manures, and identified that 78% of US counties fall into lowest manure P production of less 0 to 15 kg P ha⁻¹ while 22% of counties produced greater than 15 kg manure P ha⁻¹. The authors concluded that

mass balance calculations demonstrated that animal production and subsequent manure P generated is concentrated in a small percentage of counties across the US (Maguire et al. 2007).

Disrupted nutrient distribution within the USA is caused by large spatial distribution between crop and livestock production areas. Unlike grain or commercial fertilizers, PL is rarely shipped 80 to 160 km beyond original source due to low bulk density per nutrient value. For example, PL is commonly around 0.37 g cm^3 and ~ 9 to 22.0 g P kg^{-1} vs. triple superphosphate fertilizer (TSP) that averages 1.09 g cm^3 and approximately $201.0 \text{ g P kg}^{-1}$ (Pelletier et al., 2001; Reiter and Daniel, 2013; Havlin et al., 2014). Due to PL low bulk and nutrient density, PL nutrients are rarely redistributed to crop production regions where soils are left in a deficit relying on mined and synthetic fertilizers sources. In effort to redistribute PL nutrients, manure-to-energy systems were investigated as a method to convert PL into poultry litter ash (PLA) for condensing P nutrients 4 to 10 times while creating green energy (Reiter and Middleton, 2016). Densifying nutrients into PLA increased shipping potential; however, PLA fine particulate physical characteristics compounded with confirmed decreased nutrient solubility were major agronomic obstacles for PLA adoption as a viable P fertilizer (Codling, 2006; Reiter and Middleton, 2016). Studies testing turkey manure ash (TMA) on early corn (*Zea Mays L.*) growth identified slow initial plant development caused by decreased TMA P solubility (Pagliari et al., 2010). In a separate study, Pagliari et al. (2009) tested TMA effects on alfalfa (*Medicago sativa*) yield and tissue concentrations and found that second year alfalfa yield was similar to those with industry fertilizer; however, tissue P concentrations were greater in inorganic fertilized plots. Reiter et al. (2004) found that soybean (*Glycine max*) and wheat (*Triticum aestivum L.*) had equal yields and plant tissue concentrations for crops grown on silt loam soils in Arkansas production systems when PLA was used. Whereas Codling et al. (2002) noted wheat tissue P

concentration increased with PLA applications when compared to potassium phosphate and control treatments. Codling et al. (2002) continued to explain only significant tissue P differences were detected at the 78 kg ha⁻¹ rate, but ultimately concluded that sources tested were not significantly different. The study further concludes PLA is a potential P source, however further research is needed to determine optimum application rates (Codling et al., 2002).

Mixed PLA agronomic responses compounded with reduced P water solubility led researchers to investigate methods to address decreased nutrient solubility (Codling et al., 2002; Reiter et al., 2004; Bock, 2004; Codling, 2006; Crozier et al., 2009; Pagliari et al., 2009, 2010). A sequential extraction technique identified PLA P predominately in bound plant unavailable P fractions with only 1.45% total P extracted by deionized H₂O in soluble forms (Codling, 2006). In collaboration with a manure-to-energy pilot study and Tennessee Valley Authority personal, Bock (2004) refined granulation trials initiated by the International Fertilizer Development Center. A granulated animal waste product (AWP) was produced by reacting animal waste ash and phosphoric acid (H₃PO₄), subsequently chemically and physically altering animal waste ash into granulated AWP. Bock's (2004) granulated AWP was then tested in a study by Crozier et al. (2009) that examined the product in three different experimental approaches to discern agronomic AWP evaluation to industry standard TSP in corn, wheat, and soybean production. An initial wheat and corn greenhouse study found only a P response plateau with corn receiving TSP; however, comparing response curves of P source by rate revealed only subtle differences between sources with increasing P rate (Crozier et al., 2009). Long-term low P (min 8, 1, 18 and max 57, 9, 56 mg P kg⁻¹; Mehlich-3) research sites found that both TSP and AWP improved crop growth and were effective P sources; however, in a few experiments decreased AWP solubility compared to TSP was noticeable (Crozier et al., 2009). Crozier et al. (2009) suggested slightly

lower AWP availability was due to reduced P water solubility and further cited that water soluble differences would have minimal impacts, being that 90% of maximum yields have been recorded with < 50% water soluble P (WSP) fertilizers (Prochnow et al., 2008). In conclusion, Crozier et al. (2009) stated that lower AWP availability compared to TSP is not an agronomic obstacle since repeated applications will lead to higher residual P levels.

Mechanisms involved in fertilizer granule growth or granulation, as cited by Walker et al. (2000) in reference to an original study by Sastry and Fuerstenau (1973), include agglomerate formation by nucleation, coalescence, abrasion transfer, breakage, and snowballing. Acidulation with H_3PO_4 acting as a liquid binder as implemented in Bock's (2004) AWP granulation trial and tested under agronomic conditions by Crozier et al. (2009) and in this current study are largely formed by coalescence. Coalescence is described as large sized granule production by colliding two or more granules resulting in varied granule size distribution (Sastry and Fuerstenau, 1973). Granulation via coalescences is illustrated by colliding masses of granules, p_1 and p_2 , by the following equation: $(p_1 + p_2 = p_{1+2})$ and further illustrated in figure 3.1 adapted from Sastry and Fuerstenau (1972). Initially, granules are formed in the rotating drum by nucleation process as capillary action from H_3PO_4 binder attracts particles together forming primary nuclei, which later form into larger granules via coalescences (Figure 3.2) (Sastry and Fuerstenau, 1973).

In effort to redistribute PL nutrients, the overarching goal is to enhance PLA by addressing unsuitable PLA characteristics by changing physical form into granulated poultry litter ash (GPLA) products and subsequently increasing P nutrient solubility. Mimicking rock phosphate experiments used to create single super and TSP fertilizers, an acidulation experiment was designed to measure H_3PO_4 acidifying effect on WSP and TP as conducted by other researchers (Hardesty et al., 1942; Havlin et al., 2014; Mizane et al., 2016). Additionally, large

scale GPLA-Bulk (GPLA-B) manufacturing was conducted to validate large scale formulations and determine physical characteristics including bulk density, force and friction resistance, and granule size compared to TSP. Specific objectives included: 1) determine H₃PO₄ acidifying effect on WSP, TP, granulation point, and fertilizer granule size and 2) conduct large scale GPLA-Bulk granulation to determine larger scale formulations and granule physical characteristics produced (bulk density, force and friction resistance, and granule size) compared to industry standard TSP.

Materials and Methods

Poultry Litter Ash Acidulation

Poultry litter ash, labeled as fluidized bed fly (FB Fly), was collected from a fluidized bed combustion system in Rhodesdale, MD (BHSL, 2017). Original PLA, FB Fly, elemental analysis before granulation was 2.58 g N kg⁻¹, 15.85 g C Kg⁻¹, 50.60 g P kg⁻¹, 119.15 g K kg⁻¹, and 75.01 g Ca kg⁻¹ and water pH (1:1; w/w) of 9.16. Poultry litter ash was acidified with increasing H₃P0₄% (laboratory grade white phosphoric acid) on a weight by weight (w/w) basis to determine minimum and maximum acidulation effects on granulation point, WSP, total measurable P (TP), and pH of granules dissolve in water. Two acidulation trials (GPLA-Acd1 and GPLA-Acd2) were conducted (Table 3.1 and 3.2). Granulated PLA-Acd2 was implemented to identify or granulation point for desired granule size. Each acidulation trial was conducted with 50 g PLA reacted with a weight percentage of 75% H₃P0₄ (236 g P kg⁻¹; 23.6% P; 54% P₂O₅) creating an acid to PLA ratio (H₃P0₄ g : PLA g). Utilizing a handheld mixer to simulate fertilizer mixing and to expedite exothermic reactions, 50 g of PLA was reacted with each acidulation percentage weight (g/g) in a 200 mL Pyrex glass container. Mixing occurred at a medium speed for two minutes total with temperature recorded at one minute and again at

mixing termination. Acidified samples were allowed to cool and harden prior to transferring into storage containers.

Acidulated samples were adjusted for moisture to determine sample size needed per elemental analysis (Peters et al., 2003). A representative one-gram sample (dry weight basis) was acid digested according to USEPA 3050B method using nitric acid and hydrogen peroxide followed by analysis for TP via inductively coupled plasma spectroscopy (ICP-AES) (ICP-AES; CirOS Vision Model, Spectro Analytical) (United States Environmental Protection Agency, 1996). Water soluble P from acidulated samples were extracted in a 100:1 (50 ml water: 0.5 g granules) ratio with deionized water shaken for an hour and filtered through 2.5 μm quantitative filter paper (Whatman 42) with filtrate acidified with HCl followed by analysis via ICP-AES (Kleinman et al., 2007; Revell et al., 2012). Lastly, pH determination was taken from each acidified sample in a 1:1 (10 g granule: 10 ml water) ratio (Sparks et al., 1996).

Bulk Granular Manufacturing

Larger scale GPLA-Bulk (GPLA-B) production in 45.36 kg batches were conducted in a concrete barrel mixer simulating commercial fertilizer blending via rotating drum. Granulated PLA formulation was calculated based on PLA P_2O_5 to CaO ratio. To determine the 75% H_3PO_4 (fertilizer grade phosphoric acid) weight needed to convert PLA Ca-phosphate compounds into soluble forms, the following calculation was formulated by Whitehurst (personnel communication, 2018). The intent of the calculation was designed to alter PLA P_2O_5 to CaO ratios to those similar to TSP of 2.536:1. In accordance with GPLA-B granulation calculations, 45.36 kg of PLA was added to the concrete barrel mixer and allowed to mix while pouring in 14.56 kg of 75% H_3PO_4 (32% acidulation) and allowed to blend until granules began to form and harden over 15 minutes. Granulated PLA granules were dumped and allowed to cool and cure before transferring to storage container to prevent clumping.

Physical Characteristic Analysis

Two bulk density measurements were taken from the GPLA-B fertilizer manufacturing experiment. Fertilizer bulk density measurements were completed as described by Reiter and Daniel (2013) according to ASABE Standards (2006) to measure loose and packed bulk density (g cm^{-3}). Due to mass dependent nature of exothermic reactions, bulk manufactured GPLA was chosen for physical characteristic measurements due to stronger granules created by higher reaction temperatures. Before measuring bulk density, GPLA-B granules were sieved to granule sizes smaller than 6.35 mm and larger than 2.2 mm. Triple superphosphate and FB Fly were also tested for comparison purposes and were not sieved prior to measurement and left “as is”. Loose bulk density was measured according to ASABE Standards (2006) by pouring fertilizer granules through a funnel from 610 mm height into a 1000 mL graduated cylinder until reaching 1000 mL final volume with weight recorded upon completion. Packed bulk density was taken after tapping the graduated cylinder and adding additional fertilizer granules until a constant 1000 mL volume was obtained and weighed upon completion (ASABE Standards, 2006). Both loose and packed bulk density were replicated four times. Loose and packed density were utilized to calculate fertilizer settling rate. Average GPLA and TSP diameter was recorded by randomly choosing 5 granules in 4 replicates totaling 20 fertilizer granules and measured using calipers. Resistance to force was measured by using a New Leader Crush Strength Tester (New Leader, 2016). Fertilizers were subjected to crush strength test by randomly choosing 10 granules in 5 replications totaling 50 GPLA-B and TSP granules to determine force resistance. Simulating friction encountered during manufacturing, transportation, and land application, GPLA-B and TSP were subjected to an attrition test to measure friction resistance. As detailed by Reiter and Daniel (2013) in accordance to ASABE Standards (2006), 100 g of fertilizer granules were placed on a 0.85 mm screen and were shaken at 200 rpm for 10 min on an oscillating shaker.

Weakly attached particulates from fertilizer granules were collected below the 0.85 mm sieve and weighed to determine loss due to friction. Attrition percentage was determined from total test weight.

Statistical Analysis

Acidulation experiments were conducted in a completely randomized design. Four replications were used on all procedures, except in force crush and granule size where 5 reps of 10 and 4 reps of 5 granules were used. Physical analysis measurements were subjected to analysis of variance conducted with the General Linear Model procedure (PROC GLM) in SAS Enterprise Guide 7.1 (SAS Institute Inc., 2017). Additionally, Fishers protected least significant difference (LSD) mean separation procedure was used to separate statistically significant means at significance level of 0.05. Simple linear regression was conducted using SAS procedure (Proc Reg) Enterprise Guide 7.1 (SAS Institute Inc., 2017).

Results and Discussion

Poultry Litter Ash Acidulation

In the GPLA-Acd1 trial, temperature increased with increasing H₃PO₄ acidulation percentage (Figure 3.3). One-minute mixing interval produced a positive simple linear regression equation of temperature °C = 24.5 + 0.49 × Acidulation % (R²=0.96) with highest recorded temperature reached of 46.1 °C. Mixing termination at two minutes resulted in lower temperatures with temperature reaching at 45 °C at 50% acidulation. The exothermic reaction observed increased in a mass dependent nature as H₃PO₄ acidulation percentage increased. Increasing acidulation and subsequent temperature effects are thought to aid in fertilizer granule strength and force resistance to a certain granulation point (Holm et al., 1985). In this study, beyond 30% acidulation the material became vicious and eventually hardened into a solid mass. Holm et al. (1985) tested temperature changes during granulation and revealed a relationship

between heat development and granule growth due to increased plasticity and friction resistances. Authors suggested stress-strain relationships of moistened samples during granulation developed frictional heat (Holm et al., 1985). As liquid was added, material further compacted forming plastic agglomerates that increased granule strength and force resistance (Holm et al., 1985). Likewise, increasing compaction through frictional heat ultimately shrunk granule pore size; which is cited as a dominant factor governing granule strength (Kasai et al., 1991).

Acidulation's impact on WSP increased in a positive linear relationship with an R^2 value of 0.96 describing equation $\text{g WSP kg}^{-1} = 3.63 + 1.85 \times \text{Acidulation \%}$ (Figure 3.4). Total P followed a similar linear trend with $R^2 = 0.85$ with regression equation $\text{g TP kg}^{-1} = 57.84 + 1.20 \times \text{Acidulation \%}$. Contrary to P concentrations, pH decreased with increasing acidulation from 9.34 at 0% to 3.51 at 50% H_3PO_4 acidulation as expected. Total measurable and WSP solubilized by acidulation intervals produced positive simple linear regression models with goodness of fit $R^2 = 0.82$ and 0.96 , respectively (Figure 3.5). Solubilized P in this calculation is defined as P amount previously unavailable that was increased by H_3PO_4 additions. The calculation subtracts original P amount from original FB Fly of WSP 0.62 g P kg^{-1} and TP $50.63 \text{ g P kg}^{-1}$ as well as subtracts P amounts added from each H_3PO_4 acidulation percentage. Increased solubilized P is hypothesized to occur due to H_3PO_4 increasing dissolution of FB Fly species monetite (CaHPO_4) and brushite ($\text{CaHPO}_4 \cdot 2 \text{ H}_2\text{O}$) (Ervin, 2019). It is believed H_3PO_4 caused similar reaction to FB Fly as acidulation to rock phosphate (RP), where H^+ ions decompose and dissolve RP apatite particles (Al-Fariss et al., 1993). Rock phosphate reaction occurs as follows: $2\text{Ca}_3(\text{PO}_4)_2 + 5\text{H}_3\text{PO}_4 + 9 \text{ H}_2\text{O} \rightarrow 3\text{Ca}(\text{H}_2\text{PO}_4)_2 \cdot \text{H}_2\text{O} + 3\text{Ca}(\text{HPO}_4) \cdot 2\text{H}_2\text{O}$ (Chaouqi et al., 2017). The reaction objective, as was the goal of acidifying GPLA, was to alter original Ca-phosphate structures into

more soluble forms (Chaouqi et al., 2017). Withholding unprocessed P amounts extracted from original FB Fly and amounts added by H_3PO_4 , solubilized P averaged 92% from total WSP and 26.1 to 51.6% of TP. Admittedly, amounts of P solubilized was surprising and called for further investigation specifically into solubilized TP and USEPA 3050B acid digest efficacy (United States Environmental Protection Agency, 1996). Maguire et al. (2001), in determining relationships between biosolid treatment and soil P availability, found that USEPA 3050B digested P was ~80% of the TP and oxalate extractable P. The authors further explained that TP and oxalate extractable P commonly exceed USEPA 3050B digest; however, biosolids that are treated with lime and have high Ca concentrations, like PLA, are not as effectively extracted by oxalate extraction (Maguire et al., 2001). Therefore, we cautiously assume that H_3PO_4 has a twofold effect on USEPA 3050B TP extraction including: 1) H_3PO_4 reacts and solubilizes Ca-phosphate forms and 2) however unexpectedly, increasing H_3PO_4 pre-acidified PLA and increased USEPA 3050B efficacy of extracting more total P. Ultimately, it is hypothesized that increased acidulation increased USEPA 3050B digest total P due to pre-acidifying effect of H_3PO_4 upon granulation of PLA. However, margins that H_3PO_4 increased USEPA 3050B TP results are unknown, therefore; we have collectively decided to label USEPA 3050B as total measurable P. Subsequently, TP results throughout the experiments were interpreted with H_3PO_4 and EPA 3050B TP two-fold effects in mind.

Although small scale acidulation (GPLA-Acd2) resulted in visual and statistical differences in granule size (Figure 3.6 and Figure 3.7), WSP and TP simple linear regression equations resulted in low R^2 values, 0.07 and 0.23, respectively (Figure 3.8). Small scale acidulation trials produced a simple linear regression describing acidulation's effect on granule size with $R^2 = 0.61$ mm. Ideal granule size was identified at 29% acidulation (14.5 g acid to 50g

PLA) with granules averaging 3.14 mm. Granules formed at 26% acidulation resulted in smaller particles (≤ 1 mm) and 30% acidulation resulted in larger granules (≥ 5 mm); which remained viscous after ambient temperature dry down time. Significant differences in granule size can be explained namely by solution to solid phase ratio and binder viscosity; which govern granule formation via coalescences (Walker et al., 2000). Phosphoric acid (75% by weight) has a viscosity at 25 ° C is approximately 19.08 centipoises (cP) and can vary depending on temperature (Edwards and Huffman, 1958). At room temperature, approximately 20 ° C during GPLA-Acd2 trials, H₃PO₄ viscosity is cited to be 24 cP (Potash Corporation, 2012). Phosphoric acid viscosity during acidulation is not thought to have been a major influence in granule size variation; however, differences in granulation ratio between GPLA-Acd2 and GPLA-B trials could be explained by temperature differences effecting H₃PO₄ viscosity.

Granulated Poultry Litter Ash-Bulk Granular Manufacturing

Granular manufacturing validated formulation calculations, expected granule size, and physical properties when producing GPLA-B. The concrete mixing drum with fixed blades rotating around the drum's axis simulated commonly used fertilizer blenders (Ferraris, 2001). The blending cycle lifts PLA material and then drops material back into the drum allowing cascading and rolling motions to form granules (Ferraris, 2001). Variations in Ca-phosphate species influenced P solubility. As Ca to P ratios increase, bonding strength and stability increases as solubility decreases in the order of: fluorapatite (Ca₅(PO₄)₃F) < hydroxyapatite (Ca₅(PO₄)₃OH) < beta-tricalcium phosphate (β -Ca₃(PO₄)₂) < octacalcium phosphate (Ca₈H(PO₄)₃ · 2.5 H₂O) < monetite < brushite < monocalcium phosphate (Lindsay, 1979; Chow and Eanes, 2001). Phosphorus speciation identified moderately soluble CaHPO₄ and CaHPO₄ · 2 H₂O comprising GPLA spectra (Ervin, 2019). Original FB Fly, prior to granulation, Ca:P ratio of 1.48:1 was decreased in GPLA-B manufacturing to 0.67 creating a more soluble P fertilizer

source (Table 3.3). Phosphorus in TSP is largely $\text{Ca}(\text{H}_2\text{PO}_4)_2$ in ratio of 0.5:1 and is considered to be highly water soluble (Chow and Eanes, 2001; Havlin et al., 2014). Comparatively based on species and Ca:P ratios, TSP is a slightly more soluble P fertilizer source than GPLA. Lower solubility between granulated AWP when compared to TSP were also reported by Crozier et al. (2009), that concluded small differences in solubility should have minimal impact on yield (Prochnow et al., 2008). This conclusion is based upon a P fertilizer study examining plant availability due to variations in insoluble P compounds that reported 90% of maximum yields was achieved with < 50% WSP fertilizers (Prochnow et al., 2008; Crozier et al., 2009).

Additionally, GPLA manufacturing enhanced adaptability by granulating fine particulate PLA into fertilizer granules; that could be land applied by common commercial methods. Due to numerous manure-to-energy variables and PLA characteristics, calculations based on PLA P:CaO ratios are fundamental in defining formulations to create desired granules as well as increased measurable TP and WSP. Total P in bulk granulation resulted in significantly lower measurable P ($90.47 \text{ g P kg}^{-1}$) compared to TP from 29% granules (GPLA-Acd2) of $101.97 \text{ g P kg}^{-1}$. Measurable TP was significantly increased in GPLA-B and GPLA-Acd2 from original PLA (FB Fly) source from 50.6 to 90.47 and $101.97 \text{ g P kg}^{-1}$, respectively. Adapting TSP manufacturing from RP, similar principles were applied successfully to PLA producing a granulated product with increased measurable TP (Hardesty et al., 1942). When comparing bulk production formulation ($14.56 \text{ kg H}_3\text{PO}_4$ to $45.36 \text{ kg PLA} = 32\%$) to acidulation trial results ($14.5 \text{ g H}_3\text{PO}_4$ to $50 \text{ g PLA} = 29\%$), the desired granulation point differed by 3% suggesting that increasing total GPLA amount produced will require increased ratio margins by ~3%. Although GPLA-Acd2 granulation contained 3% less H_3PO_4 , measurable TP and Ca:P ratios were significantly improved when compared to GPLA-B. This leads to the interpretation that GPLA-B

processing efficiency could be improved by better mechanical blending equipment. Differences in granulation point between trials could be explained by higher mass dependent exothermic reaction temperatures, solution to solid phase ratio, and binder viscosity (Walker et al., 2000). Overall, GPLA-B granulation validates manufacturing feasibility that is adaptable across various manure-to-energy and PLA characteristics.

Physical Evaluation of Granulated Poultry Litter Ash

Bulk density measurements were made to determine storage and container size for transporting GPLA-B compared to commercial TSP. Both TSP loose (1.13 g cm^{-3}) and packed (1.14 g cm^{-3}) density measurements were statistically denser than loose and packed GPLA-B densities of 1.01 and 1.03 g cm^{-3} , respectively ($\text{LSD}_{0.05} = 0.03$ and 0.02 g cm^{-3} ; Table 3.4). Although statistically significant, this small difference in density will not alter commonly used transportation methods, containers, and packaging for shipments across the US. Common fertilizer loose bulk densities range from lower density urea 0.72 to 0.82 g cm^{-3} to higher density muriate of potash 1.03 to 1.2 g cm^{-3} (Fulton and Port, 2016). Average TSP loose density ranged from 0.95 to 1.2 g cm^{-3} , falling within ranges recorded in the experiment by both TSP and GPLA-B at 1.3 and 1.01 g cm^{-3} , respectively (Fulton and Port, 2016). Granulated poultry litter ash significantly improved loose and bulk densities when compared to raw PLA with loose and bulk densities of 0.94 and 0.96 g cm^{-3} . Attrition test measuring friction resistance between TSP and GPLA-B was not statistically significant ($p\text{-value} = 0.62$). Triple superphosphate was significantly more resistant to force (kgf) averaging 5.95 kgf^{-1} than GPLA-B 4.53 kgf^{-1} ($\text{LSD}_{0.05} = 0.61 \text{ kgf}^{-1}$). Crushing strength is minimum pressure required to crush individual granules. Fertilizer granules with crush rating under 3 kgf^{-1} should not be broadcast at normal speeds and spinner speeds should be adjusted below 700 rpm (New Leader, 2016). Therefore, granule

strength is an important characteristic influencing storage, transportation, and ease of land application. Granulated poultry litter ash bulk is significantly less resistant to force than TSP; however, GPLA-B (4.53 kgf) crush resistance will not alter common fertilizer land application methods and would be suitable for average rpm spinner speeds.

Average fertilizer diameter (mm) was significantly larger for GPLA-B (3.73 mm) granules than TSP (2.86 mm). Hofstee and Huisman (1990) placed particle size as one of the largest influences on particle size motion when spreading fertilizers. Particle size directly impacted air motion movement and subsequent fertilizer spread distribution with common upper fertilizer diameter limits between 4.0 to 4.75 mm (Hofstee and Huisman, 1990). To prevent fertilizer granule segregation in blend mixes, particles must have similar size distribution by weight; which is equally important when determining GPLA-B particle size suitability for bulk blending (Hoffmesiter et al., 1964). Particle size influence on aerial spreading distribution (spread width and consistency) can be described by regression equation of $Y = 18.9 + 0.952X$, where Y is spreader width (m) and X represented percentage of particles > 2.0 mm (Heyman et al., 1964; Hofstee and Huisman, 1990). The experiment found that spread width increased by 1 m for every increase in granule fraction greater than 2.0 mm (Heyman et al., 1964; Hofstee and Huisman, 1990). The regression equation was based on aircraft fertilizer application; however, similar results have been reported with ground application (Davies, 1972; Heyman et al., 1964; Hofstee and Huisman, 1990). Average GPLA diameters of 3.73 mm occurred within recommend diameter ranges; however, compared to commercial fertilizer products GPLA is 0.53 mm larger than diammonium phosphate (DAP) which is the largest fertilizer commonly sold (Hofstee and Huisman, 1990; Fulton and Port, 2016). Granulated poultry litter ash granule size can be addressed, similar to granule size separation via sieves in TSP processes where granules under or

over desired granule size (<2 mm or > 4 mm) are then crushed and recycled back into the initial granulation process (Chaouqi et al., 2017). Addressing significantly larger GPLA granule size, a sieve step can be added after granulation to segregate granules into needed fertilizer diameters. Estimating spreader width according to Heyman et al. (1964) regression equation for application via aircraft, using average GPLA granule size of 3.73 mm predicts a 19.8 m spread width. It can be expected since GPLA falls within common fertilizer sizes, that ground spread width by common application methods will be within commonly cited spinner widths of 18.28 m (60ft.) (Stewart and Bandel, 1997). Poultry litter ash, un-granulated, particle size is well below 2 mm (majority PLA particle size is < 0.25 mm; Ervin, 2019); therefore, spreading width would decrease and fertilizer distribution would be disproportionate. Speelman (1979) recommended that granules less than 1.6 mm should be eliminated because smaller particle sizes will drastically limit spreading width. Consequently, decreased PLA spreader width would require increased fertilizer application passes in the field, more time, and decreased fertilizer efficacy due to disproportionate spread patterns. Therefore, GPLA is an improved and superior alternative fertilizer source than PLA. Fortunately, GPLA aligned within commercial granule size and common spreader widths that are important characteristics from multiple standpoints, including: 1) due to similar spread widths, additional passes in the field from the applicator will not be needed, 2) current fertilizer blending and spreading equipment can be utilized, and 3) an equally distributed fertilizer spread pattern would be expected. Ultimately, GPLA granule physical characteristics were comparable to common fertilizers and more importantly legitimize the potential for GPLA fertilizer adoption.

Conclusions

Enhancing PLA into GPLA solves agronomic obstacles identified in previous studies including: 1) Increasing WSP and measurable TP and 2) Improving land application, transportation, and storage by granulizing PLA into a convenient fertilizer form. Acidulation experiments revealed linear relationships with increasing WSP, measurable TP, fertilizer granulation point and granule size, and pH decreases as acidulation increased. Regression models predicted exothermic reaction temperatures to be expected at different acidulation percentages. Granulated poultry litter ash physical characteristics were comparable to TSP and validated adaptability as an alternative P source. Furthermore, GPLA is a higher analysis, more soluble, and improved form when compared to un-granulated PLA. Within given parameters tested and prediction models, it should be noted that while GPLA is similar in physical characteristics to industry standard TSP (~200.87 g P kg⁻¹; 20.09% P; 46% P₂O₅), elemental analysis is approximately half (GPLA-B = 90.47 g P kg⁻¹; 9.47% P; 12.68% P₂O₅), subsequently doubling P application rates when compared to TSP. Large scale manufacturing verifies formulations based on P:CaO ratios and elucidates expected manufacturing and granule product results. Adaptable granulation formulations that address differences across PLA manure-to-energy variables is vital to repurpose co-products for viable agronomic uses and to aid in PL nutrient redistribution.

Acknowledgments

Funding for this work was provided in part by the Virginia Agricultural Experiment Station, the Hatch program of the National Institute for Food and Agriculture, US Department of Agriculture, and National Fish and Wildlife Foundation project number 0602.16.053565.

References

- Al-Fariss, T.F., H.O. Ozbelge, and H.S. El-Shall. 1993. On the modeling of phosphate rock acidulation process. *J. Kind Saud Univ.-Eng. Sci.* 5(2): 243–255. doi: [https://doi.org/10.1016/S1018-3639\(18\)30583-X](https://doi.org/10.1016/S1018-3639(18)30583-X).
- ASABE Standards. 2006. Cubes, pellets and crumbles--Definitions and methods for determining density, durability, and moisture content. ASABE S269.4.
- BHSL. 2017. BHSL Fluidized Bed Combustion. <http://www.bhsl.com/fluidised-bed-combustion-new/> (accessed 4 June 2017).
- Bock, B.R. 2004. Demonstrating optimum fertilizer value of ash from the biomass energy sustainable technology (BEST) demonstration project for swine and poultry manure management. TVA Public Power Institute, Muscle Shoals, AL.
- Chaouqi, N., M.E. Gharous, and M. Bouzziri. 2017. The improvement of TSP fertilizer production and quality. *bioRxiv*: 1–12. doi: <https://doi.org/10.1101/213223>.
- Chow, L.C., and E.D. Eanes, editors. 2001. Octacalcium Phosphate. Karger Medical and Scientific Publishers, Giathersburg, MD.
- Codling, E.E. 2006. Laboratory characterization of extractable phosphorus in poultry litter and poultry litter ash. *Soil Sci.* 171(11): 858–864. doi: [10.1097/01.ss.0000228059.38581.97](https://doi.org/10.1097/01.ss.0000228059.38581.97).
- Codling, E.E., R.L. Chaney, and J. Sherwell. 2002. Poultry litter ash as a potential phosphorus source for agricultural crops. *J. Environ. Qual.* 31(3): 954–61.
- Crozier, C.R., J.L. Havlin, G.D. Hoyt, J.W. Rideout, and R. McDaniel. 2009. Three experimental systems to evaluate phosphorus supply from enhanced granulated manure ash. *Agron. J.* 101(4): 880–888. doi: [10.2134/agronj2008.0187x](https://doi.org/10.2134/agronj2008.0187x).
- Edwards, O.W., and E.F. Huffman. 1958. Viscosity of aqueous solutions of phosphoric acid at 25C. *Ind. Eng. Chem. Chem. Eng. Data Ser.* 3(1): 145–146.
- Ervin, C.R. 2019. Poultry litter ash as an alternative fertilizer source for corn. Ph.D. dissertation, Virginia Polytechnic and State University, Painter, Va.
- Ferraris, C.F. 2001. Concrete Mixing Methods and Concrete Mixers: State of the Art. *J. Res. Natl. Inst. Stand. Technol.* 106(2): 391–399. doi: [10.6028/jres.106.016](https://doi.org/10.6028/jres.106.016).
- Fulton, J., and K. Port. 2016. Physical Properties of Granular Fertilizers and Impact on Spreading. *Ohioline Ohio State Univ. Ext.* <https://ohioline.osu.edu/factsheet/fabe-5501> (accessed 25 August 2018).
- Hardesty, John.O., W.H. Ross, and K.D. Jacob. 1942. Process for the Granulation of Fertilizers. 1–8.

- Havlin, J.L., S.L. Tisdale, W.L. Nelson, and J.D. Beaton. 2014. *Soil Fertility and Fertilizers: An Introduction to Nutrient Management*. 8th ed. Pearson, Inc., New Jersey.
- Heyman, W., E. Linke, and H. Zschuppe. 1964. Performance and capacity fertilizer distributors in relation to fertilizer quality [Arbeitsqualität und Streuleistung von Diinger streumaschinen in Abhängigkeit von der Diingerqualitlt]. *Dtsch. Agratechnik* 21(4): 187–191.
- Hoffmesiter, G., S.C. Watkins, and J. Silverburg. 1964. Bulk blending of fertilizer material: Effect of size, shape, and density on segregation. *J. Agric. Food Chem.* 12(1): 64–69.
- Hofstee, J.W., and W. Huisman. 1990. Handling and spreading of fertilizers part 1: Physical properties of fertilizer in relation to particle motion. *J. Agric. Eng. Res.* 47: 213–234. doi: [https://doi-org.ezproxy.lib.vt.edu/10.1016/0021-8634\(90\)80043-T](https://doi-org.ezproxy.lib.vt.edu/10.1016/0021-8634(90)80043-T).
- Holm, P., T. Schaefer, and H.G. Kristensen. 1985. Granulation in high-speed mixers part V. Power consumption and temperature changes during granulation. *Powder Technol.* 43(3): 213–223. doi: [https://doi.org/10.1016/0032-5910\(85\)80002-4](https://doi.org/10.1016/0032-5910(85)80002-4).
- Howarth, R.W., A. Sharpley, and D. Walker. 2002. Sources of nutrient pollution to coastal waters in the United States: Implications for achieving coastal water quality goals. *Estuaries Res. Found.* 25(4b): 565–676. doi: <https://doi.org/10.1007/BF02804898>.
- Intani, K., Latif, S., Islam, M.S., Muller, J. 2018. Phytotoxicity of corncob biochar before and after heat treatment and washing. *Sustainability.* 11 (1). 1-18.
- Kasai, E., W. Shengli, and Y. Omori. 1991. Factors governing the strength of agglomerated granules after sintering. *ISIJ Int.* 31(1): 17–23.
- Kleinman, P., K.S. Blunk, R. Bryant, L. Saportio, D. Beegle, et al. 2012. Managing manure for sustainable livestock production in the Chesapeake Bay Watershed. *J. Soil Water Conserv.* 67(2): 54–61. doi: [doi:10.2489/jswc.67.2.54A](https://doi.org/10.2489/jswc.67.2.54A).
- Kleinman, P., D.M. Sullivan, R.C. Brandt, Z. Dou, H. Elliot, et al. 2007. Selection of a water-extractable phosphorus test for manures and biosolids as an indicator of runoff loss potential. *J. Environ. Qual.* 36: 1357–1367. doi: [doi:10.2134/jeq2006.0450](https://doi.org/10.2134/jeq2006.0450).
- Lindsay, W.L. 1979. *Chemical Equilibria in Soils*. The Blackburn Press, Caldwell, NJ.
- Maguire, R.O., and J.T. Sims. 2002. Soil testing to predict phosphorus leaching. *J. Environ. Qual.* 31(5): 1601–1609. doi: [doi:10.2134/jeq2002.1601](https://doi.org/10.2134/jeq2002.1601).
- Maguire, R.O., J.T. Sims, S.K. Dentel, F.J. Coale, and J.T. Mah. 2001. Relationships between biosolids treatment process and soil phosphorus availability. *J. Environ. Qual.* 30(3): 1023–1033. doi: [doi:10.2134/jeq2001.3031023x](https://doi.org/10.2134/jeq2001.3031023x).

- Maguire, R.O., D.A. Crouse, and S.C. Hodges. 2007. Diet modification to reduce phosphorus surpluses: A mass balance approach. *J Environ. Qual.* 36: 1235–1240. doi: 10.2134/jeq2006.0551.
- Middleton, A.J. 2015. Nutrient availability from poultry litter co-products. M.S. thesis, Virginia Polytechnic and State University, Blacksburg, VA.
- Mizane, A., A. Boumerah, D. Noureddine, R. Rabah, and S. Belhait. 2016. Obtaining the partially acidulated phosphate rocks by means of intermediate-grade phosphate and diluted phosphoric acid: Influence of some parameters. *Pol. J. Chem. Technol.* 18(3): 39–43. doi: 10.1515/ptj-2016-01486,
- New Leader. 2016. SGN and crush strength test kit guideline and instructions.
- Pagliari, P.H., C.J. Rosen, and J.S. Strock. 2009. Turkey manure ash effects on alfalfa yield, tissue elemental composition, and chemical soil properties. *Commun. Soil Sci. Plant Anal.* 40(17–18): 2874–2897. doi: 10.1080/00103620903173863.
- Pagliari, P., C. Rosen, J. Strock, and M. Russelle. 2010. Phosphorus availability and early corn growth response in soil amended with turkey manure ash. *Commun. Soil Sci. Plant Anal.* 41(11): 1369–1382. doi: 10.1080/00103621003759379.
- Pelletier, B.A., J. Pease, and D. Kenyon. 2001. Economic analysis of Virginia poultry litter transportation. *Va. Tech.* <https://scholar.lib.vt.edu/ejournals/vaes/01-1.pdf> (accessed 22 December 2016).
- Potash Corporation. 2012. Purified phosphoric acid: Technical information bulletin. Potash Corporation, Northbrook, IL.
- Prochnow, L.I., S.H. Chien, G. Carmona, E.F. Dillard, and J. Henao. 2008. Plant availability of phosphorus in four superphosphate fertilizers varying in water-insoluble phosphate compounds. *Soil Sci. Soc. Am. J.* 72(2): 462–470. doi: 10.2136/sssaj2006.0421.
- Peters, J., Combs, S., Hoskins, B., Jarman, J., Kovar, J., Watson, M., Wolf, A., Wolf, N., 2003. Recommended methods of manure analysis. University of Wisconsin-Extension.
- Reiter, M.S., and T.C. Daniel. 2013. Binding agents effect on physical and chemical attributes of nitrogen-fortified poultry litter and biosolid granules. *Am. Soc. Agric. Biol. Eng.* 56(5): 1695–1702. doi: 10.12031/trans.56.9979.
- Reiter, M.S., T.S. Daniel, N.A. Slaton, C.E. Wilson, C.H. Tingle, et al. 2004. Poultry litter ash and raw litter residual effects on wheat and soybeans in an Eastern Arkansas rice, wheat, and soybean rotation. *Wayne E Sabbe Ark. Soil Fertil. Stud.* 2004: 72–77.
- Reiter, M.S., and A. Middleton. 2016. Nutrient availability from poultry litter co-products. Virginia Tech University, Painter, VA.

- Revell, K.T., R.O. Maguire, and F.A. Agblevor. 2012. Influence of poultry litter biochar on soil properties and plant growth. *Soil Sci* 177(6): 402–408. doi: 10.1097/SS.0b013e3182564202.
- SAS Institute Inc. 2017. SAS Institute. SAS Institute Inc., Cary, NC.
- Sastry, K.V.S., and D.W. Fuerstenau. 1973. Mechanisms of agglomerate growth in green pelletization. *Powder Technol.* 7(2): 97–105. doi: [https://doi.org/10.1016/0032-5910\(73\)80012-9](https://doi.org/10.1016/0032-5910(73)80012-9).
- Sharpley, A., Smith, S.J. 1994 Wheat tillage and water quality in the Southern plains. *Soil and Tillage Research.* 30 (1) 33-48. doi: [https://doi.org/10.1016/0167-1987\(94\)90149-X](https://doi.org/10.1016/0167-1987(94)90149-X).
- Sharpley, A. 1994. Managing agricultural phosphorus for protection of surface waters: Issues and options. *Journal of Environmental Quality.* 23: 437-451. doi: doi:10.2134/jeq1994.00472425002300030006x
- Sharpley, A.N., S. Herron, and T. Daniel. 2007. Overcoming the challenges of phosphorus-based management in poultry farming. *J. Soil Water* 62(6): 375–389.
- Slaton, N.A., K.R. Byre, M.B. Daniels, T.C. Daniel, R.J. Norman, et al. 2004. Nutrient input and removal trends for agricultural soils in nine geographic regions in Arkansas. *J. Environ. Qual.* 33(5): 1606–1615. doi: DOI: 10.2134/jeq2004.16.
- Sparks, D.L., A.L. Page, P.A. Helmke, R.H. Loeppert, P.N. Soltanpour, et al., editors. 1996. *Methods of Soil Analysis.* Soil Science Society of America, Inc. American Society of Agronomy, Inc., Madison, WI.
- Spellman, L. 1979. Features of a reciprocating spout broadcaster in the process of granular fertilizer application. Ph.D. dissertation. Mededelingen Landbouwhogeschool, Wageningen, Netherlands.
- Stewart, L., and Bandel, A. 1997. Uniform lime and fertilizer spreading. Cooperative Extension Service, University of Maryland.
- United States Environmental Protection Agency. 1996. Method 3050B: Acid digestion of sediments, sludges, and soils, Revision 2. U.S. EPA, Washington, DC.
- Walker, G.M., C.R. Holland, M.N. Ahmad, J.N. Fox, and A.G. Kells. 2000. Drum granulation of NPK fertilizers. *Powder Technol.* 107(3): 282–288. doi: [https://doi.org/10.1016/S0032-5910\(99\)00253-3](https://doi.org/10.1016/S0032-5910(99)00253-3).
- Whitehurst, B. 2018. Personal Communication.

Table 3.1 GPLA-Acd1 acidulation ratio calculations.

Acidulation %	Ratio (acid g : PLA g) (w/w)	P (g) added per (g) of 75% H₃P₀₄
H ₃ P ₀ ₄ %	GPLA-Acd H ₃ P ₀ ₄	P (g)
0	(0:50)	0
10	(5:50)	1.19
15	(7:50)	1.66
20	(10:50)	2.37
25	(12.5:50)	2.84
30	(15:50)	3.56
35	(17.5:50)	4.15
40	(20:50)	4.74
45	(22.5:50)	5.33
50	(25:50)	5.93

**Table 3.2 GPLA-Acd2
acidulation ratio calculations.**

Acidulation %	Ratio (acid g : PLA g) (w/w)
H₃P0₄ %	GPLA-Acd H₃P0₄
25	(12.5:50)
26	(13:50)
27	(13.5:50)
28	(14:50)
29	(14.5:50)
30	(15:50)

Table 3.3 EPA 3050B digested fertilizer total elemental analysis of fluidized bed fly (FB Fly), granulated poultry litter ash-bulk (GPLA-B), and granulation poultry litter ash-acidulation 2 (GPLA-Acd2).

Source†	g kg ⁻¹			
	P	Ca	Ca:P	pH
FB Fly	50.6 c‡	75.01 a	1.48 a	9.16
GPLA-B	90.47 b	60.06 b	0.67 b	5.53
GPLA-Acd2	101.97 a	55.85 c	0.55 c	4.85
LSD_{0.05}	5.30	4.05	0.03	0.20
<i>p-value</i>	<0.0001	<0.0001	<0.0001	<0.0001

† Fluidized bed fly (FB Fly) and granulated poultry litter ash (GPLA) originate from thermally converted broiler litter via fluidized combustion system in Rhodesdale, MD.

‡ Within columns, means followed by the same letter are not significantly different according to LSD (0.05).

Table 3.4 Fertilizer physical characteristics of granulated poultry litter ash-bulk (GPLA-B) compared to industry standard triple superphosphate (TSP) and original poultry litter ash (PLA), fluidized bed fly (FB Fly).

Fertilizer Product†	Bulk Density		Settling Rate (%)	Force (kgf)	Diameter (mm)	Attrition (%)
	Loose (g cm ⁻³)	Packed (g cm ⁻³)				
FB Fly	0.94 c‡	0.96 c	0.02	na§	na	na
TSP	1.13 a	1.14 a	0.02	5.95 a	2.86 b	0.0029
GPLA-B	1.01 b	1.03 b	0.02	4.53 b	3.73 a	0.0021
LSD 0.05	0.03	0.02	ns¶	0.61	0.61	ns
p-value	<0.0001	<0.0001	0.60	<0.0001	0.007	0.62

† Granulated poultry litter ash (GPLA) is granulated with phosphoric acid and FB Fly, that originated from thermally converted broiler litter via fluidized combustion system in Rhodesdale, MD. Triple superphosphate (TSP) is commercially sold phosphate fertilizer.

‡ Within columns, means followed by the same letter are not significantly different according to LSD (0.05).

§ na, not applicable.

¶ ns, nonsignificant.

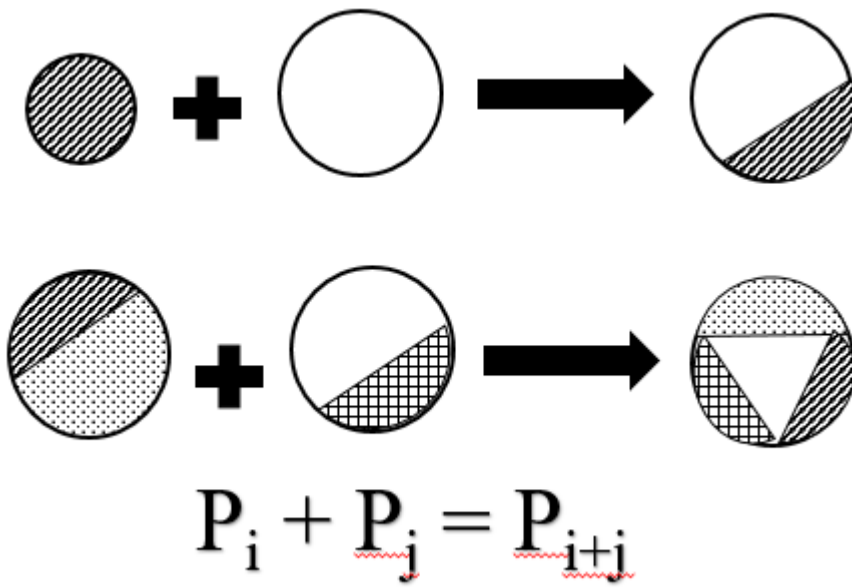


Figure 3.1 Diagram adapted from Sastry and Fuerstenau (1972) illustrating granulation via coalescence.

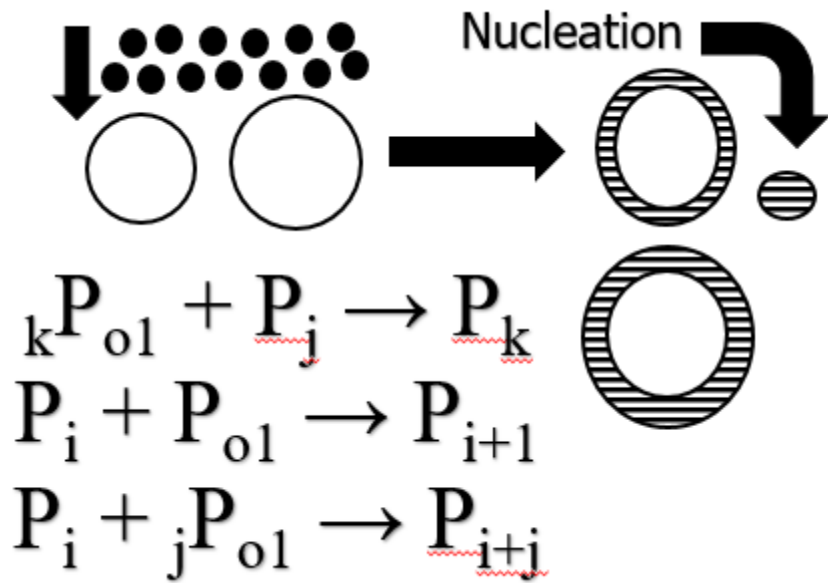
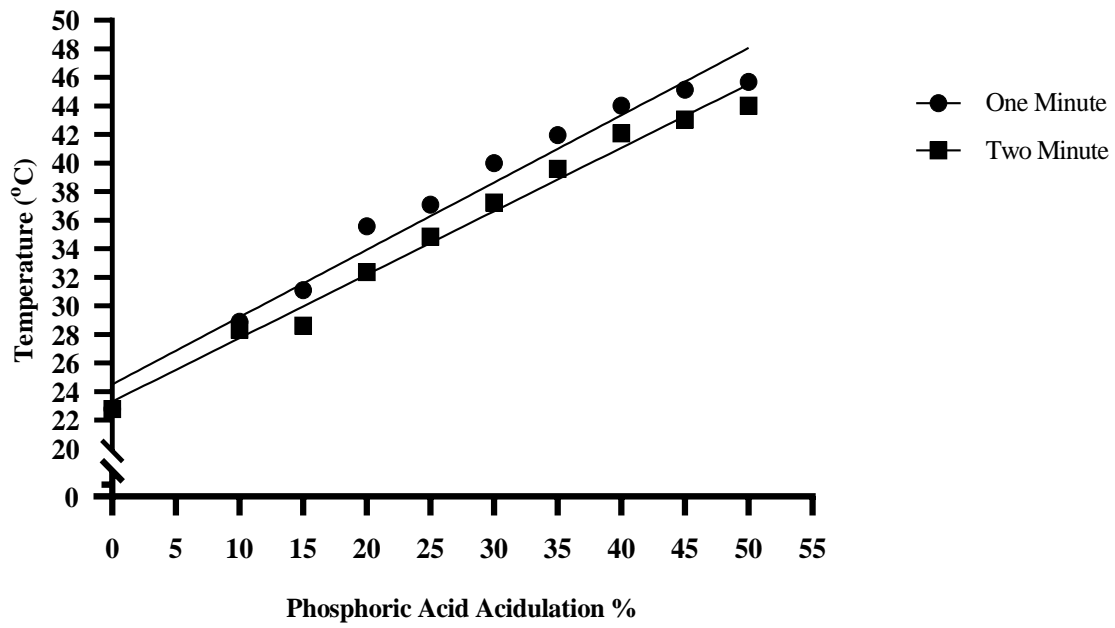


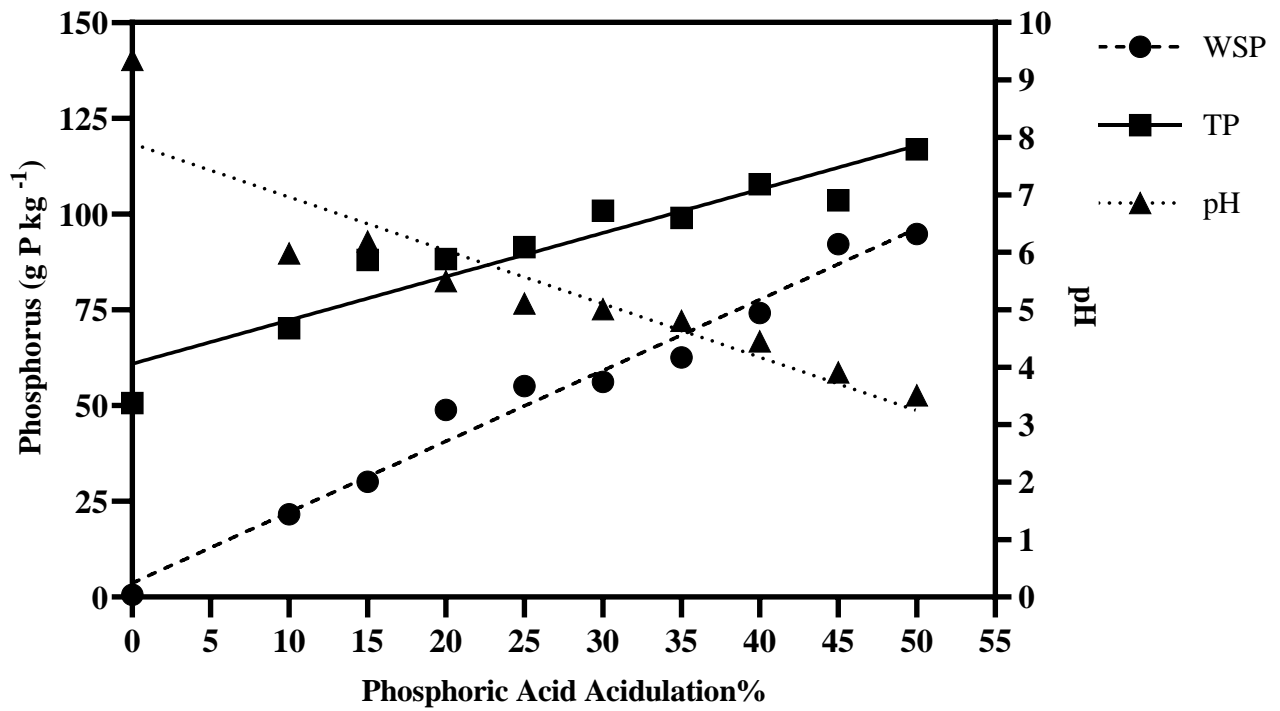
Figure 3.2 Diagram adapted from Sastry and Fuerstenau (1972) depicting nucleation, the first step in fertilizer granulation.



One-minute $C' = 24.5 + 0.49 \times \text{Acidulation\%}$ ($R^2=0.96$)

Two-minute $C' = 23.29 + 0.44 \times \text{Acidulation\%}$ ($R^2=0.98$)

Figure 3.3 Granulated poultry litter ash (GPLA-Acd1) phosphoric acid (H3PO4) effect on temperature (°C) recorded at one and two minutes during mixing.

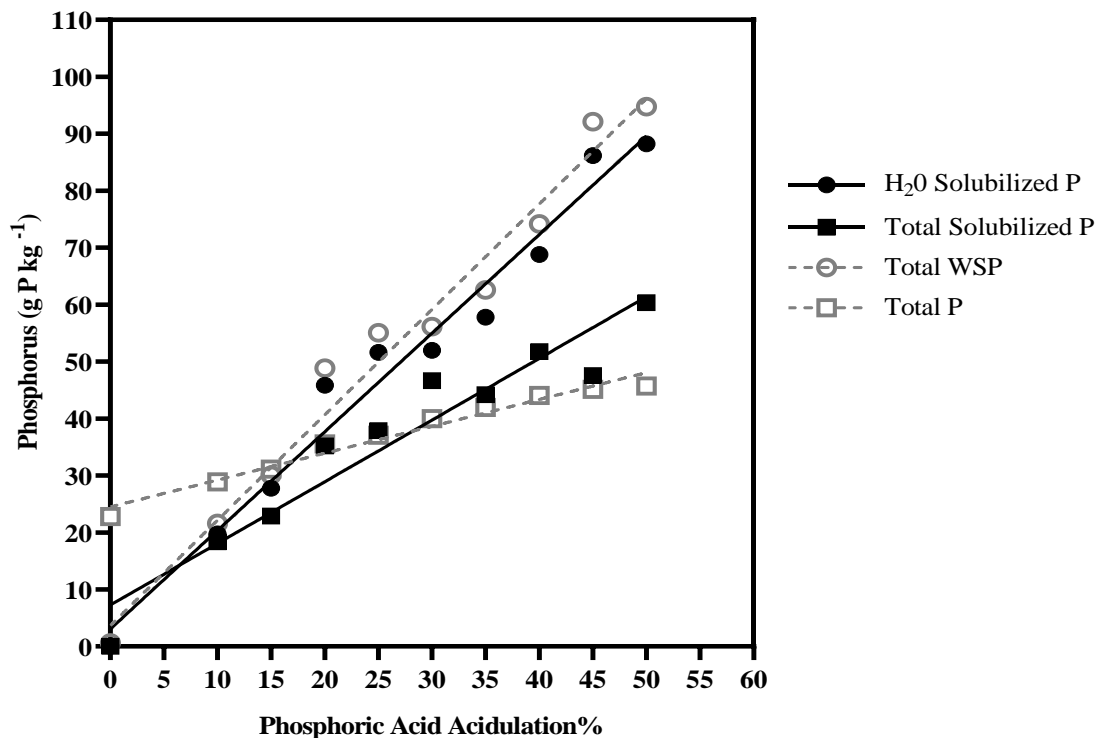


Water Soluble P (WSP) g kg⁻¹ = 3.63 + 1.85 x Acidulation% (R² = 0.96)

Total P (TP) g kg⁻¹ = 57.84 + 1.20 x Acidulation% (R² = 0.85)

pH = 7.89 - 0.09 x Acidulation% (R² = 0.82)

Figure 3.4 Phosphoric (H₃PO₄) acidulation effect on water soluble P (WSP), total P (TP) and pH for granulated poultry litter acidulation trial 1 (GPLA-Acd1).



$$\text{H}_2\text{O P Solubilized g kg}^{-1} = 3.06 + 1.73 \times \text{Acidulation \%} \quad (R^2 = 0.96)$$

$$\text{Total P Solubilized g kg}^{-1} = 7.25 + 1.08 \times \text{Acidulation \%} \quad (R^2 = 0.82)$$

Figure 3.5 Total and water soluble P solubilized by phosphoric acid (H₃PO₄) acidulation for granulated poultry litter ash acidulation trial 1 (GPLA-Acd1). Solubilized P in this calculation is defined as P amount previously unavailable that was increased by H₃PO₄. The calculation subtracts original P amount from original FB Fly of WSP 0.62 and TP 50.63 g P kg⁻¹ as well as subtracts P amount from each H₃PO₄ acidulation percentage.



Figure 3.6 Granulated Poultry Litter Ash acidulation trial 2 (GPLA-Acd2) visual effect on granule size.

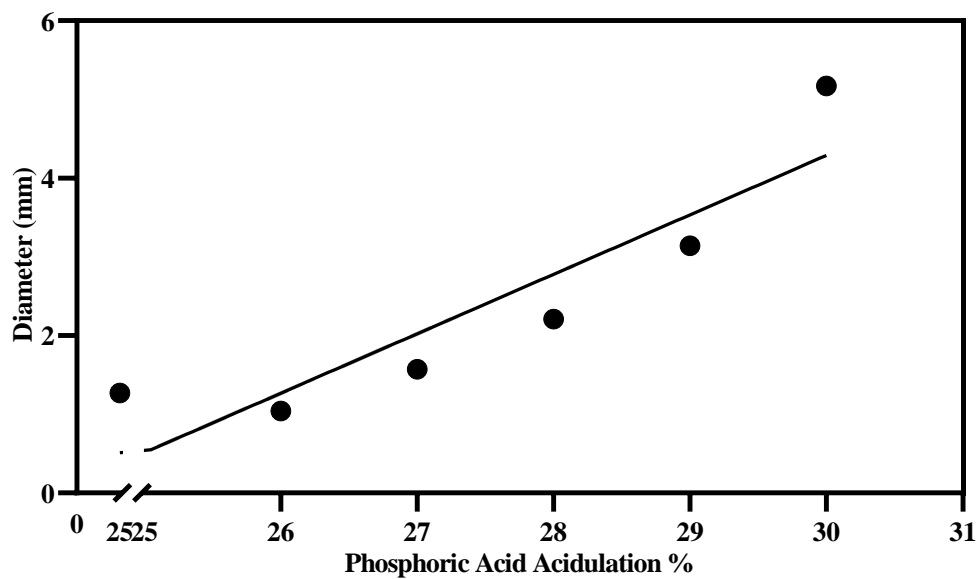


Figure 3.7 Granulated Poultry Litter Ash acidulation trial 2 (GPLA-Acd2) effect on granule size.

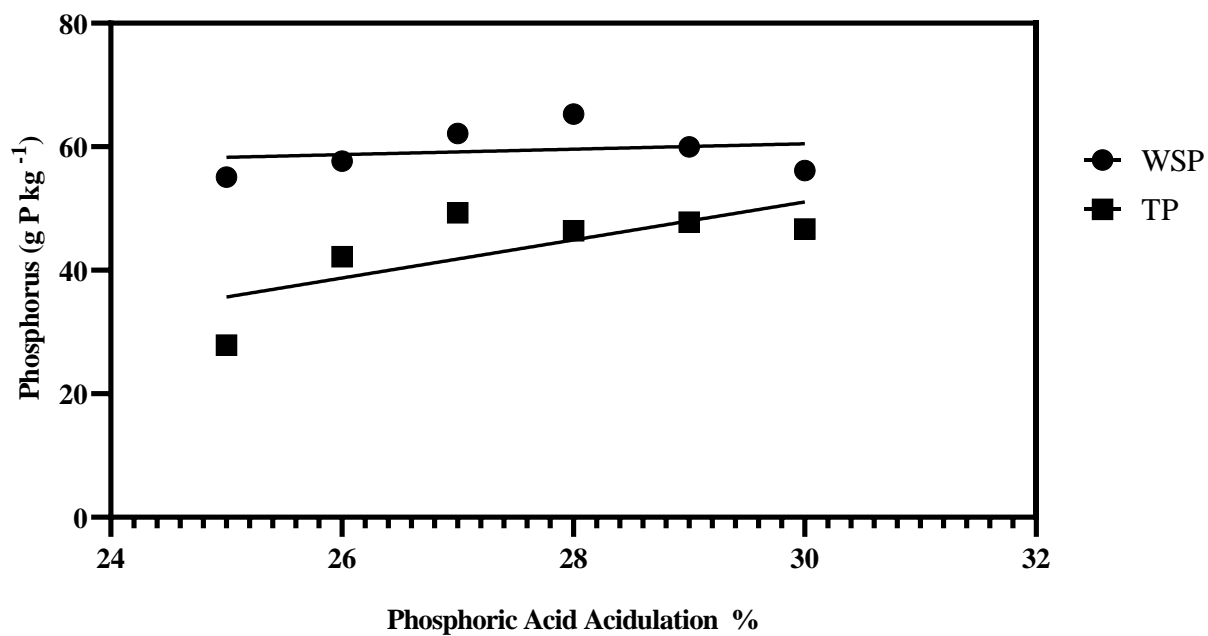


Figure 3.8 Granulated poultry litter ash acidulation trial 2 (GPLA-Acd 2) effect on water soluble (WSP) and total phosphorus (TP) (g P kg⁻¹).

Chapter 4: Delineating Factors influencing Poultry Litter Ash Nutrient Solubility

Abstract

Poultry litter ash (PLA), a product from manure-to-energy systems, is a solution addressing increased manure volumes by improving transportation logistics, repurposing poultry litter (PL) nutrients, and offers dual purpose as a fertilizer and an energy source. Manure thermo-conversion temperatures (171 to 593 °C) alter PLA nutrient solubility. Therefore, the main objective is to determine solubility fractions and factors effecting solubility of three PLA products [(fluidized bed bulk (FB Bulk), fluidized bed fly (FB Fly), and combustion Mix (CMix)], three manufactured co-products [(granulated poultry litter ash-bulk (GPLA-B), GPLA-Acd2, and ash coated urea (ACU)]. Fertilizer sources were extracted sequentially using deionized water, NaHCO₃, NaOH, HCl and acid digested using USEPA 3050B. Sequential extraction revealed decreased FB Bulk (0.42 to 0.96%), FB Fly (1.54 to 1.72%), and CMix (0.50 to 0.74) water soluble P when compared to PL (33.39%), TSP (74.52 to 91.39%), and GPLA (36.04%). A majority of PLA P was found in bound plant unavailable fractions (87.70 to 97.67%). Carbon (C) effect on PLA P was examined by ashing PLA samples in a muffle furnace at 550 °C. Differences in total C content negatively affected FB Bulk and CMix total P (1.30 and 4.56 g P kg⁻¹); however, muffle furnace temperatures increased FB Fly total P by 6.74 g P kg⁻¹. Particle size effect on solubility (> 2mm, > 0.84mm, > 0.25 mm, and <0.25mm) determined decreasing particle size increased solubility in CMix and FB Bulk. X-ray absorption near edge structure (XANES) spectroscopy identified Ca-phosphate species, monetite and brushite as species controlling solubility. Overall, understanding factors effecting nutrient solubility and plant availability is paramount to evaluate PLA derived co-products as alternative grain

fertilizers. In conclusion, to increase P solubility, PLA sources will need to be acidified to provide a readily water soluble P fertilizer source.

Introduction

A growing world population places pressure on both poultry and crop production industries to meet consumption demands. Challenges facing both agricultural sectors combine to provide a solution that can decrease reliance on finite nonrenewable rock phosphate (RP) while recycling increased poultry litter (PL) volumes. Elevated PL production presents environmental and agronomic challenges to identify alternative uses for increased manure volumes (Sharpley, 1994; Sims et al., 1998; Slaton et al., 2004). Alternatively, RP is a finite resource with quantity produced controlled by numerous geopolitical, environmental, financial, mining feasibility, and quality factors; therefore, new deposits or alternative phosphorus (P) sources will need to be identified to maintain sufficient crop production (Cordell et al., 2009; Ayding et al., 2010; Van Kauwenbergh et al., 2013; Scholz et al., 2013). Intertwining these challenges has created a potential solution that could create an efficient crop, manure, and renewable P cycle via manure-to-energy systems that densifies PL into poultry litter ash (PLA).

Often when manure is continually applied over long periods of time based on nitrogen (N) crop requirements, soil P concentrations will exceed crop needs due to disproportionate PL (3 N:1 P) N and P concentrations and crop uptake (8 N:1 P) (Sharpley, 1994; Howarth et al., 2002; Sharpley et al., 2007). An incubation study examining soil P availability in PL and biosolid amended soils concluded that when both sources are applied based on N rates, subsequent P soil concentrations will exceed crop requirements (Maguire et al., 2001). According to The Fertilizer Institute (2015), Virginia critical soil test P concentration, defined as a threshold concentration where fertilizer recommendations rates would typically drop to zero for most crops and/or little crop response to fertilizer would be expected, is 30 mg P kg⁻¹ based on Bray 1 P (24 mg P kg⁻¹ Mehlich-1 P). Exceeding critical P concentrations, 41.6% of the

Commonwealth's soils have P concentrations greater than 50 ppm P Bray 1 P ($> 44 \text{ mg P kg}^{-1}$ Mehlich-1 P) (The Fertilizer Institute, 2015). A mass balance calculation of P generated from livestock manures identified that 78% of US counties fall into lowest manure P production of less than 0 to 15 kg P ha⁻¹ while 22% of counties produced greater than 15 kg manure P ha⁻¹ (Maguire et al., 2007). The authors concluded that mass balance calculations demonstrated concentrated animal production and subsequent manure P is generated in a small percentage of counties across the US (Maguire et al. 2007). Livestock diet modification would reduce P amounts generated in manure as well as decrease manure P production categories of: 31 to 45, 46 to 60, and $> 60 \text{ kg P ha}^{-1}$ to 3, 1, and 1% (Maguire et al., 2007). More importantly regardless of diet modification, counties with a manure P deficit dominate the US (Maguire et al., 2007). Relative to crop P removal, surplus manure occurs in approximately 11% of US counties (Maguire et al., 2007).

A study conducted over nine years in a Virginia no-till crop rotation with PL applications revealed potential P soil buildup with repeated PL applications based on N requirements (Fleming-Wimer et al., 2018). Beginning soil test P values were rated "very high" at concentrations greater than 55 mg P kg⁻¹ and each year the control treatment revealed a 3 mg P kg⁻¹ year decline in a wheat (*Triticum aestivum L.*), soybean (*Glycine max*), and corn (*Zea Mays L.*) rotation (Fleming-Wimer et al., 2018). The study extrapolated crop rotation P drawdown rate, to estimate that it would take approximately fourteen years under the same crop rotation to reduce Mehlich-1 P soil concentrations to where P fertilization would be needed (Fleming-Wimer et al., 2018). Numerous studies examining manure-impacted legacy P soils are detailed by Qin and Shoiber, (2018). These researchers concluded manure applied based on N requirements oversupplied P, altered soil P dynamics, endangered environmental systems to non-

point solution, and required significant time to drawdown soil P concentrations (Qing and Shober, 2018). Although 41.6% of Virginia's soils exceed P concentrations greater than the 50 mg P kg⁻¹ threshold (Bray 1), a majority of state soils are below threshold levels but lack PL availability due spatial separation and associated transportation costs and/or lack of transportation subsidies (Pelletier et al., 2001; Slaton et al., 2004). Phosphorus nutrient management across Virginia is exacerbated by secluded poultry production regions, disproportionate N and P plant uptake and PL concentrations, as well as substantial soil P drawdown periods that created an unbalanced P cycle in need of manure redistribution (Sharpley, 1994; The Fertilizer Institute, 2015; Fleming-Wimer et al., 2018).

Examining links between P inputs and exports across the United States, the National Research Council created a dataset improving P source and balance estimates (Metson et al., 2017). On agricultural land across the United States, a net P accumulation rate of 7.5% year⁻¹ created 0.19 Tg P surplus with fertilizer contributing 74% of total P agricultural inputs (Metson et al., 2017). Nationally, 92.4% of total P applied (1.85 Tg inorganic P and 0.65 Tg manure P) was removed with crop harvest; however, removal rates varied across the U.S. and were influenced by proximity to confined animal feeding operations (CAFO) (Metson et al., 2017). Commonly, PL generated is sold or used as a fertilizer within a short distance of poultry operations (Pelletier et al., 2001). Poultry litter is not easily transported due to bulkiness, low nutrient density, and associated transportation cost beyond nutrient concentrated areas (Sharpley, 1994; Pelletier et al., 2001). Pelletier et al. (2001) concluded that PL can be transported and applied at competitive costs to commercial fertilizers within breakeven transportation distances outside of poultry production regions. Based upon PL nutrients, quantity transported is influenced by subsidy adoption rates and P soil requirements (Pelletier et al., 2001). Pelletier et

al.'s (2001) economic analysis calculated PL transported 122 to 161 km (76 to 100 miles) from the Shenandoah Valley would cost a subsidy program \$3.97 a ton; however, subsidy rates would be higher if PL production continued to increase creating surplus PL. Concluding the economic analysis, Pelletier et al. (2001) recommended investigating alternative PL uses to provide solutions for increased volumes.

A potential solution that meets recycling PL nutrients and increased transportation logistics due to increased bulk density was a PL co-product, PLA. Via manure-to-energy systems, PL was utilized as a fuel material to create steam or syngas while densifying PL and associated nutrients into PLA. Collectively, PLA studies cited favorable PL nutrient densification and P and K concentrations four to seven times greater than PL (Bock, 2004; Reiter and Middleton, 2016). Codling et al. (2002) recorded total P concentrations of PLA ranging 76.0 to 114.0 g P kg⁻¹ which was two to three times more concentrated than PL (22.0 to 27.0 g P kg⁻¹). Manure thermo-conversion temperatures condensed PL nutrients into PLA, but decreased PLA nutrient solubility (Codling et al., 2002; Codling, 2006; Pagliari et al., 2010; Wells, 2013; Middleton, 2015). Wells (2013) found increasing combustion temperatures decreased P dissolution; at 500, 700, and 1000° C, P dissolution was 1,062, 369, and 0.75 mg P L⁻¹, respectively. Novak et al. (2016) noted variable biochar characteristics based upon temperature, concluding that as temperature increased from 400 to 500° C organic material volatilized. Temperatures above 500 to 700° C caused non-volatile structures to stack and form into turbostratic crystalline-aromatic sheets (Keiluweit et al., 2010; Novak et al., 2016). Decreased PLA P dissolution prompted further research to determine optimum application for crop growth (Codling et al., 2002; Codling, 2006; Pagliari et al., 2010). In a greenhouse scenario, lower PLA solubility is a positive attribute tested to reduce P nutrient leaching compared to triple

superphosphate (TSP) (Wells, 2013). Poultry litter ash applications reduced greenhouse losses of dissolved reactive phosphorus (DRP) and effluent-total phosphorus losses by 92% and 69% compared to TSP, respectively (Wells, 2013). Adams (2005) found PLA particle size affects on total nutrient concentrations. Phosphorus, potassium, magnesium, and calcium as well as micronutrients' total concentrations increased as particle size decreased (Adams, 2005). As particle size decreased in the order of > 2 mm, < 2 mm, and < 0.25 mm, total P concentrations increased by 79, 98, and 104 g P kg⁻¹, for each particle size respectively (Adams, 2005). Despite slow release or controlled release N fertilizers, predominately P and K industry fertilizers are noted for immediate crop availability through readily water soluble fractions. Codling (2006), utilizing a modified Hedley sequential extraction, identified water soluble PLA P fractions as 1.45%, labile fraction averaged 17%, and bound plant unavailable HCl fraction resulted as 82% of total inorganic P. Balancing agronomic and environmental standards, low PLA solubility could be interpreted as a negative agronomic characteristic but a positive feature for reducing P bioavailability to sensitive watersheds.

Physiochemical processes that govern P fractions in soils are ubiquitous, but vital in maintaining balance between crop production and environmental preservation. Both physiochemical and biogeochemical dynamics interacted to drastically influence P fractionation in soil systems (Stewart, 1991). To determine P sinks, numerous sequential extraction procedures exist to determine P fractionation in soils, sediments, and organic P from manure sources (Dou et al., 2000; Ajiboye et al., 2004; Kovar and Pierzynski, 2009; Wang et al., 2013; Qin and Shober, 2018). Overall, inorganic P fractionation techniques gradually increase extractant harshness to solubilize P forms (Kovar and Pierzynski, 2009; Wang et al., 2013; Qin and Shober, 2018). Although sequential extraction results are criticized for operationally defined P fractions

represented by variations in extractant harshness, sequential fractionation provided a qualitative representation of P pools that extends beyond agronomic and environmental soil testing results (Qin and Shober, 2018).

Phosphorous biogeochemistry is diverse with soil P concentrations largely controlled by Al, Fe, and Ca phosphates adsorption sites or soil minerals. Common P minerals in acidic soils include variscite ($\text{AlPO}_4 \cdot 2 \text{H}_2\text{O}$) and strengite (FePO_4) with low solubility (McBride, 1994; Havlin et al., 2014). Once soil P is in plant available forms (H_2PO_4^- or HPO_4^{2-}), inorganic P forms can react with Al, Fe, Mg or Ca by adsorbing to exposed mineral surfaces or precipitate as secondary compounds (Havlin et al., 2014). Orthophosphate ions and availability are influenced by pH (Lindsay, 1979; McBride, 1994; Chow and Eanes, 2001; Havlin et al., 2014). Under alkaline conditions, HPO_4^{2-} is dominant while H_2PO_4^- is dominant species under acidic conditions. Secondary precipitated P compounds or P fixation depends largely on sorption mineral surface type and soil pH (McBride, 1994; Havlin et al., 2014).

Generalized into three fractions, P is found in soil solution, labile, and stable or fixed (Scheckel et al., 2013; Havlin et al., 2014; Qin and Shober, 2018). Phosphorus fractionation techniques are designed to accommodate numerous soil conditions (i.e. alkaline or acidic soils), P fertilizer soil transformations, and manure P fractions (Dou et al., 2000; Kovar and Pierzynski, 2009). Fractionation schemes categorize proposed P fractions associated with extraction utilized to solubilize P forms, and as referenced by Wang et al. (2013), there are numerous protocols with many P categories and delineations. Phosphorus categories represented by sequential extraction derive from three main P (soil solution, labile, and stable or fixed) fractions found in soil systems (Havlin et al., 2014; Qin and Shober, 2018). Adopting P sequential extraction techniques to fractionate PLA P sinks, Codling, (2006) modified Hedley et al.'s (1982) protocol to determine

PLA P fractions. The study concluded that most PLA P is found in hydrochloric (HCl) fractions and largely plant unavailable (Codling, 2006).

Poultry litter ash is chemically and physically altered from original PL nutrient sources. High conversion temperatures alter PLA nutrient chemistry, drastically decreasing nutrient solubility into slowly or completely unavailable forms. Although present PLA studies consistently confirm increased PLA nutrient concentrations and densification, the same studies concluded that a potential agronomic obstacle is decreased nutrient solubility (Codling et al., 2002; Codling, 2006; Pagliari et al., 2010; Wells, 2013; Middleton, 2015). Poultry litter ash nutrient concentration and solubility are highly dependent upon thermo-conversion system, temperature, PL type (poultry layers vs broilers), and poultry feed nutrition (Kunkle et al., 1981; Codling et al., 2002; Coufal et al., 2006; Middleton, 2015). Due to cited decreased PLA P solubility, the following objectives were designed to: 1) Determine PLA solubility fractions and factors effecting solubility; 2) Examine PLA carbon influence on water soluble and total P; 3) Address PLA particle size effect on water soluble P; and 4) Identify PLA P species via X-ray absorption near edge structure spectroscopy allowing reference to species formation diagrams and solubility.

Materials and Methods

P Solubility Using Sequential Extractions

Poultry litter ash fertilizers were subjected to a modified Hedley sequential extraction as detailed by Codling (2006) to characterize operationally defined inorganic P fractions in PLA and P fertilizers (Table 4.1). Original sequential extraction methods were designed for soil P fractionation, which capitalized on reagents increasing harshness to solubilize P forms (Dou et al., 2000; Codling, 2006; Kovar and Pierzynski, 2009; Wang et al., 2013). Sequential extraction

began with 0.3 g of fertilizer sample that was extracted with 30 ml reagent. Reagents from least to most harsh included: deionized H₂O, 0.5 M NaHCO₃, 0.1M NaOH, 1.0 M HCl, and acid digestion via USEPA 3050B (United States Environmental Protection Agency, 1996; Codling, 2006).

Three poultry litter ash products, ash coated urea (ACU), and industry fertilizers (TSP and PL) were sequentially extracted. Alterations to Codlings (2006) extraction protocol included a change in shake time from 16 h to 1 h, centrifuge for 15 minutes at 12,000 rpm, and final acid digestion according to USEPA method 3050B utilizing HNO₃-H₂O₂ instead of H₂SO₄-HNO₃ to ensure efficient P colorimetric detection as S and P have overlapping peaks (United States Environmental Protection Agency, 1996; Dou et al., 2000; Wiel, 2003). A 0.45 nitrocellulose membrane filter was used for water soluble P and remaining extractants were filtered through Whatman 42 (2.5 µm) filter paper (Kovar and Pierzynski, 2009). Four replications were subjected to sequential extraction and then analyzed via inductively coupled plasma spectroscopy (ICP-AES) (ICP-AES; CirOS Vision Model, Spectro Analytical).

Phosphorus Species and Solubility Identification via XANES Spectroscopy

All XANES spectroscopic work was conducted at beam line 9-BM of the Argonne National Laboratory Advanced Photon Source in Lemont, IL with assistance from colleagues at the University of Delaware, Maryland, and USEPA. All sample spectra photon energy was used at 2150 eV in a double crystal monochromator in helium (He) atmosphere. Sample preparation included grinding fertilizers into fine powder via agate mortar and pestle mixed with polyvinylpyrrolidone (PVP) followed by pellet pressing into a 7-mm diameter. Pellets were attached to an eight-carousel sample holder by double-sided C tape before spectra collection. Poultry litter ash samples were collected in K-edge XANES spectra using fluorescence mode with multiple scans (3-8) per sample and then averaged to improve signal-to-noise ratios.

Phosphorus reference standards were collected with similar protocols as described by Qin et al., (2018) in total electron yield (TEY) mode using an electron yield detector to minimize sample adsorption. Multiple scans per sample were collected (2-5) for each sample and averaged. Standard spectra were normalized with a two normalization order from a pre-edge of -50 to -10 eV and normalization range of 15 to 115 eV. Additional standards' spectra that were collected in previous studies were included in linear combination fitting (Shober et al., 2006; Qin et al., 2018). Poultry litter ash K-edge spectra were compared to 15 standards in our spectra library (Table 4.2).

Spectra data processing was conducted using Athena software (Ravel and Newville, 2005). Raw PLA sample spectra were normalized with a normalization order of two from a pre-edge of -29 to -7 and -29.5 to -19.5 eV and normalization range of 15 to 110 and 15 to 120 eV corresponding to white line peak. All sample spectrums' electron binding energy (E_0) were assigned to maximum peak of the first derivative. Linear combination fitting (LCF) was utilized to identify spectra standards comprising PLA P samples. Goodness of fit determined by residual factor (R-factor) and reduced chi-square produced by Athena LCF were utilized to evaluate model accuracy in describing sample spectra (Ravel and Newville, 2005). Residual factor (R-factor) generated by Athena LCF are utilized to determine goodness of fit, with smaller values indicating best spectral fitting of library standards (Qin et al., 2018). Initially, all standards were selected for LCF and were sequentially eliminated based upon standard weight contributing to the model. Standard samples contributing < 10% of LCF spectra were removed until all remaining standards describing the model contributed at least 10% or greater (Qin et al., 2018). Reference standard spectra E_0 was allowed to shift up to + or - 1 eV during LCF.

Poultry Litter Ash and Industry Fertilizer Mehlich-1 P Extractions

Three PLA (CMix, FB Fly, and FB Bulk), manufactured GPLA, and industry standard TSP were extracted via Mehlich-1 soil extraction protocols to determine solubility of remaining soil applied materials for future soil tests (Mehlich, 1953). Five grams of each fertilizer were extracted with Mehlich-1 solution followed by analysis via ICP-AES for total elemental analysis (Mehlich, 1953; Maguire and Heckendorn, 2005).

Muffle Furnace Protocol

Carbon concentration was measured according to Revell et al. (2012) by ashing PLA fertilizers in triplicate in a muffle furnace at 550 °C for 24 h followed by weight change determinations, water extraction, and final EPA 3050B digest to determine total measurable P (United States Environmental Protection Agency, 1996). Changes in water soluble P (WSP) were performed in triplicate in 100:1 ratio (50 ml DDI water to 0.5 g fertilizer) as recommended for manure and biosolid water extractable P by Kleinman et al. (2012) with filtration through a 2.5 µm quantitative filter (Whatman 42) (Zirkler et al., 2012).

Particle Size Effect on Water Soluble Phosphorus

Five hundred grams of PLA (FB Fly, FB Bulk, and CMix) were sieved through a 10 (2 mm), 20 (0.841 mm) and 60 (0.250 mm) mesh screen as described by Adams, (2005). Ash passing through each screen was weighed, recorded, and samples collected for WSP analysis (Kleinman et al., 2012). Water soluble P was extracted in 100:1 ratio (50 ml DDI water to 0.5 g ash) in four replications as recommended for manure and biosolid water extractable P by Kleinman et al. (2012) with filtration through a 2.5 µm quantitative filter (Whatman 42) (Zirkler et al., 2012).

Statistical Analysis

Sequential extraction, Mehlich-1, total C effect, and particle size water extractions were subjected to analysis of variance conducted with the General Linear Model procedure (PROC GLM) in SAS Enterprise Guide 7.1 at 5% significance level (SAS Institute Inc., 2017).

Additionally, Fishers protected least significant difference (LSD) tests were used to separate statistically significant means at $LSD_{0.05}$. X-ray absorption near edge structure spectroscopy spectra were analyzed via Athena XAS data linear combination fitting (LCF) software (Ravel and Newville, 2005).

Results and Discussion

Poultry Litter Ash and Industry Standard Fertilizer Characteristics prior to Sequential Extraction

Poultry litter ash total P prior to sequential extraction included increasing concentrations that ranged FB Bulk ($44.95 \text{ g P kg}^{-1}$), FB Fly ($50.60 \text{ g P kg}^{-1}$), CMix ($69.89 \text{ g P kg}^{-1}$), ACU (5.38 g P kg^{-1}) and GPLA 90.47 to $101.97 \text{ g P kg}^{-1}$ (Table 4.3). Average GPLA P concentrations, a manufactured product from FB Fly, was approximately 1.9 times more concentrated than original FB Fly source and approximately one times less than industry standard TSP (TSP; approximately $200.97 \text{ g P kg}^{-1}$). Potassium PLA concentrations prior to sequential extraction decreased in the order of CMix $128.59 \text{ g K kg}^{-1}$, FB Fly $119.15 \text{ g K kg}^{-1}$, GPLA 93.91 to $102.2 \text{ g K kg}^{-1}$, FB Bulk $62.57 \text{ g K kg}^{-1}$, and ACU $13.98 \text{ g K kg}^{-1}$ and were significantly lower analysis K sources than muriate of potash concentrations of approximately $516.67 \text{ g K kg}^{-1}$. Poultry litter ash pH values were 9.16, 10.21, 10.50, 9.07, 4.86, 5.53 for FB Fly, FB Bulk, and CMix, ACU, GPLA-Acd2, and GPLA-B, respectively. Industry standard fertilizers had significantly lower pH readings due to acidification that occurred to phosphate minerals during fertilizer production with TSP's average pH recorded at 3.14.

Poultry Litter Ash and Industry Standards Fertilizers Characteristics after Sequential Extraction

As expected, TSP had higher total inorganic P with $208.74 \text{ g P kg}^{-1}$ followed by CMix $65.74 \text{ g P kg}^{-1}$, FB Fly $54.56 \text{ g P kg}^{-1}$, FB Bulk $47.33 \text{ g P kg}^{-1}$, PL $18.95 \text{ g P kg}^{-1}$, and ACU 6.52 g P kg^{-1} with an $LSD_{0.05}$ of 9.71 g P kg^{-1} (Table 4.4). Total P fraction is a summation from

each extraction including H₂O, NaHCO₃, NaOH, HCl, and USEPA 3050B acid digest. Water soluble P presented as percent soluble of total P (%S_p of total P), identified all three PLA fertilizers (FB Fly, FB Bulk and CMix) with significantly less water soluble P than industry fertilizers at 1.54, 0.96, and 0.50 % S_p of total P, respectively. Both TSP and PL had significantly higher water soluble P of 74.52 and 33.39 %S_p of total P. Dou et al. (2000) found a majority of PL P was extracted by H₂O (49% P), followed by HCl (25% P), NaHCO₃ (19% P) , and NaOH (5% P) (Codling, 2006). Similarly, if labile (H₂O and NaHCO₃) and bound P (NaOH, HCl, EPA 3050B Digest) fractions were segregated by each reagent, PL fractionation follows a similar trend including H₂O (32.8% P) being greatest followed by HCl (29.4% P), NaHCO₃ (30.3% P), and NaOH (4.7% P) (data not shown). Ash coated urea (ACU) surprisingly resulted in significantly higher WSP at 9.12 %S_p of total P. Ash coated urea (CO(NH₂)₂) is created by coating FB Fly onto a urea granule with a binder developed and patented by Whitehurst and Associates; which will not be fully disclosed. Significant differences between ACU (9.12 %S_p of total P) and FB Fly (1.54%S_p of total P) water solubility can potentially be explained by several hypothesized factors in the ACU manufacturing process. First, FB Fly ash is sieved down prior to coating urea granules that potentially demonstrated smaller ash particle sizes resulting in greater surface reactivity, subsequently resulting in greater water solubility (Adams, 2005). Alternatively, coating binder is slightly acidic, possibly lowering FB Fly pH from 9.16 to 9.07 and increasing P solubility. Labile P fractions followed a similar trend with TSP and PL providing significantly higher labile P than all three PLA fertilizers. Bound P fractions revealed all PLA fertilizers (FB Fly, FB Bulk and CMix) had significantly higher bound P at 87.7, 97.37, and 93.27% Bp of total P compared to TSP and PL (22.02 and 36.86% Bp of total P, respectively). Similar trends between PLA and TSP P fractions were found in sequential

extraction experiment 2 (Table 4.5). Granulated poultry litter ash, manufactured from FB Fly, resulted in significantly higher total, water soluble, and labile P fractions when compared to three non-treated PLA products. However, 51.47 B_p% of total P remained in plant unavailable fractions. Water soluble and labile P fractions were significantly improved due to granulation process (GPLA 36.04 %S_p of total P and 48.53 %L_p of Total P) when compared to original FB Fly P fractions of 1.72 %S_p of total P and labile 11.71 %L_p of Total P. Fractions highlight drastically lower GPLA dissolution and total P when compared to commercial TSP (36.04 vs. 91.39 %S_p of total P and 77.34 g P kg⁻¹ vs. 176.13 g P kg⁻¹ total P) translating into a lower analysis slow release GPLA P fertilizer source. However, the question remains regarding time needed to adequately acidulate particles in acidic soil systems for plant uptake.

Overall PLA P solubility resulted in the greatest P concentration found in the following fractions: Bound P > Labile P > Water Soluble P and are in agreeance with Codling (2006) sequential extraction results. Decreased PLA P solubility identified in sequential extractions is an obstacle for utilizing unmanufactured PLA fertilizers as readily available and comparable P source for crop production. Granulated poultry litter ash is an improved alternative source providing greater total, water soluble, and labile P when compared to PLA.

Although sequential extraction procedures were designed to address P fractions, K fractionation revealed majority of PLA K is found in water soluble and labile K pools. Poultry litter ash water soluble K ranged from 51.87 to 79.6% S_k of total K across experiments three and four (Table 4.6 and 4.7). Poultry litter K had significantly higher water soluble (87.61% S_k of total K) and labile K (98.53% L_k of total K) and significantly less bound K (1.47% B_k of total K) compared to PLA. The only noted negative effects to PLA K nutrient densification is gaseous K losses identified by Middleton (2015) mass balance equation and further supported by higher K

concentrations in FB Fly (collected in the exhaust) as opposed to FB Bulk (collected in thermo-conversion system bed). However, PLA ability to provide K is unhindered by thermo-conversion temperatures and is a readily available K plant source.

X-ray Absorption Near Edge Structure Spectroscopic PLA P Species Solubility

Spectra linear combination fitting (LCF) identified Ca, Al, Mg, and Fe phosphate species present across PLA examined (Table 4.8). Identifying P species that comprised PLA, allowed reference to formation ($\log K^\circ$) and solubility constants ($-\log K_{sp}$) that aid in explaining reduced P solubility results and interpretation of species that control solubility are found in table 4.2 (Lindsay, 1979; Chow and Eanes, 2001). The XANES LCF species results were interpreted utilizing formation and solubility constants to explain P solubility and availability.

Beginning with most soluble Ca-phosphate species, monocalcium phosphate ($\text{Ca}(\text{H}_2\text{PO}_4)_2 \cdot \text{H}_2\text{O}$; $\log K^\circ -1.15$) was identified in FB Bulk LCF results (Lindsay, 1979; Chow and Eanes, 2001; Ervin, 2019). However, elemental Ca to P molar ratios failed to support LCF results of monocalcium phosphate comprising FB Bulk P species (Table 4.9). Elemental ratios are utilized to support or disqualify XANES qualitative identification of species, based upon what is stoichiometrically possible due to total elemental analysis results (Shober et al., 2006). Likewise, solubility experiments corroborate FB Bulk decreased solubility and do not support soluble monocalcium detection.

Brushite ($\text{CaHPO}_4 \cdot 2\text{H}_2\text{O}$; $\log K^\circ 0.63$; $-\log K_{sp} 6.59$) was the second most soluble (second least stable) Ca-phosphate species and was detected in FB Fly (25.7%) and GPLA (33.2%) LCF weight percentage (Lindsay, 1979; Chow and Eanes, 2001). Additionally, GPLA acidified from FB Fly had higher brushite and monetite weight percentage describing spectra models, translating into a more soluble Ca-phosphate species when compared to FB Fly original P species (Lindsay, 1979; Chow and Eanes, 2001). Monetite (CaHPO_4 ; $\log K^\circ 0.30$; $-\log K_{sp}$

6.90) was the third most soluble Ca-phosphate species and was detected in FB Bulk, CMix, and GPLA (Lindsay, 1979; Chow and Eanes, 2001). Supporting LCF monetite identification, Toor et al. (2005) XANES analysis of broiler litter detected monetite presence that was supported by Ca:P ratios ranging from 1.12 to 1.71. Poultry litter ash Ca:P ratios analyzed within the current study of 1.15 to 1.37 fall within monetite and brushite thresholds. Further supporting dicalcium phosphates species detected (monetite and brushite), Peak et al. (2002) identified dicalcium phosphate species as predominate P species of unamended PL. Therefore, based on support from literature and stoichiometric ratios, monetite and brushite are predominate Ca-phosphate species controlling PLA solubility.

It was hypothesized that insoluble Ca-phosphate minerals predominantly composed PLA species due to alkaline pH values, high Ca concentrations, Ca:P ratios, and thermal conversion temperatures creating an environment for recalcitrant minerals to precipitate and would ultimately explain decreased P solubility results (Lindsay, 1979; Shober et al., 2006). Contrary to this hypothesis and findings from Shober et al. (2006) and Toor et al. (2005), XANES PL and biochar analysis did not identify insoluble Ca-phosphate minerals including octacalcium ($\text{Ca}_8\text{H}(\text{PO}_4)_6 \cdot 2.5 \text{H}_2\text{O}$), beta-tricalcium phosphate ($\beta\text{-Ca}_3(\text{PO}_4)_2$), hydroxyapatite ($\text{Ca}_5(\text{PO}_4)_3\text{OH}$), and fluorapatite ($\text{Ca}_5(\text{PO}_4)_3\text{F}$). Lack of recalcitrant Ca-phosphate species identified was also reported in other studies examining PL, alum-treated PL, and biosolids through XANES and solid-state P-31 nuclear magnetic resonance (NMR) (Frossard et al., 1994; Peak et al., 2002; Hunger et al., 2004). Although literature and stoichiometric results supported soluble monetite and brushite findings, solubility results do not support soluble Ca-phosphate species present.

Reverting to principles governing P solid-solution equilibriums, pH must be discussed to aid interpreting results. Changes in pH can drastically alter magnitude to which Ca-phosphate minerals can dissolve in a unit of solution (Lindsay, 1979; Chow and Eanes, 2001). Especially in soil systems with a pH range between 6.0 to 6.5, solubility diagrams illustrated several Ca, Al, and Fe-phosphate minerals can coexist and maintain approximately $10^{-3.25}$ M $\text{H}_2\text{PO}_4^{-1}$ concentration (Lindsay, 1979). Examining solubility diagrams, as pH decreased brushite and monetite P concentrations increased as supported by acidic sequential extracting solution (HCl) and slightly acidic Mehlich-1 extraction solutions that ultimately solubilized more P than a DI water (Lindsay, 1979). Decreased pH values below solubility constants of monetite ($-\log K_{sp}$ 6.90) and brushite ($-\log K_{sp}$ 6.59) will favor mineral dissolution and release more P. Therefore, decreased solubility found in current experiments and reported in numerous field studies is speculated to be caused by: 1) lack of acidic soil conditions (below mineral K_{sp} constants) and 2) antagonistic effects from PLA alkalinity altering microenvironment pH and subsequently reducing P solubility (Codling, 2006; Pagliari et al., 2010; Middleton, 2015).

Magnesium phosphate species bobierite ($\text{Mg}_3(\text{PO}_4)_2 \cdot 8 \text{H}_2\text{O}$; $14.45 \log K^\circ$) identified in FB Fly, FB Bulk, and GPLA were the only Mg-phosphate species found by spectra fitting (Lindsay, 1979). Molar Mg to P stoichiometric ratios failed to support evidence of bobierite detected in PLA samples. Bobierite's Mg:P ratio of 1.5:1 was not supported by PLA total elemental stoichiometric ratios that ranged from 0.27 to 0.86 (Mg:P). Fluidized bed fly LCF model contained greatest weight percentage of varscite (55.9 %, $\text{AlPO}_4 \cdot 2 \text{H}_2\text{O}$; $-2.50 \log K^\circ$) and was the only Al species detected in PLA spectra (Lindsay, 1979). Additionally, CMix LCF detected 10.3% non-crystalline (amorphous) Fe-phosphate describing spectra. Varscite and amorphous Fe-phosphate detection was surprising due to PLA alkalinity. Aluminum to P molar

ratios calculated from total elemental digest failed to support varscite Al to P ratio (1:1). Shober et al. (2006) also found contradictory results between XANES Al species detection and Al:P stoichiometric ratios of PL samples and biosolids. Aligning with Shober et al. (2006), we hypothesize that soil artifacts from PL cleanout may introduce more Al and Fe than expected thus resulting in minor species detected in PLA sources. Aluminum and Fe species are not thought to be main species or cations controlling P solubility in PLA.

Stoichiometric Ca:P ratios and literature supported monetite and brushite identification in XANES LCF PLA analysis as species controlling P solubility. Furthermore, pH of solution or environment will be the ultimate governing principle influencing monetite and brushite dissolution, plant availability, and soil longevity.

Poultry Litter Ash and Industry Fertilizers Mehlich-1 P Extractions

Poultry litter ash fertilizers had significantly lower Mehlich-1 extractable P compared to TSP (Table 4.10). Among PLA fertilizers, manufactured GPLA had significantly higher P (1913.9 mg P kg⁻¹) followed by FB Bulk, FB Fly, and CMix. Considering GPLA is granulated from FB Fly with phosphoric acid (H₃PO₄) and has resulted in significantly higher Mehlich-1 extractable P (1913.9 mg P kg⁻¹ vs. 160.3 mg P kg⁻¹ for GPLA and FB Fly, respectively), one would expect GPLA dissolution ratios to differ. Examining Ca:P ratios, FB Fly and GPLA resulted in similar extraction ratios of 0.02 and 0.03 mg P kg⁻¹, respectively. Similar Ca:P extractant ratios corroborate XANES results of a shared Ca-phosphate species (brushite) unaffected by manufacturing process, causing stoichiometric or congruent dissolution ratios. Supporting a shared Ca-phosphate species between GPLA and FB Fly is supported by XANES LCF with only brushite (CaHPO₄·2H₂O) describing FB Fly (25.7%) and GPLA (33.2%) spectra. Combustion Mix resulted in the highest Ca:P (2.94:1) extraction ratio, explaining decreased P (28.7 mg P kg⁻¹) extracted. No significant differences were detected between PLA's and GPLA

K extraction results. Mehlich-1 PLA results aligned with decreased solubility noted in other studies and supported XANES detection and interpretation of pH influenced monetite and brushite solubility (Codling, 2006; Pagliari et al., 2010; Middleton, 2015). Mehlich-1 PLA extraction is important to establish margins that acidic extracting solutions may incorrectly influence soil test data of PLA fertilized soils. Dilute double acid method is the accepted soil testing procedure in acidic southern soils (Sparks et al., 1996; Maguire and Heckendorn, 2005). However, Mehlich-1 extracting solution (0.05 M HCl + 0.0125 M H₂SO₄) is unsuitable for calcareous soils as well as soils previously receiving highly alkaline rock phosphate applications due to acidic extracting solutions overestimating plant available P (Sparks et al., 1996). It is expected that Mehlich-1 soils test results of PLA amended soils will overestimate plant available P as seen in Pagliari et al. (2010) study testing turkey manure ash amended soils that increased Bray 1 soil test P regression slopes to five times greater than other fertilizer sources tested. In contrast to the same study, Olsen P extractions supported plant growth results and revealed soil levels were greater with fertilizer treatments than TMA (Pagliari et al., 2010). Differences in soil test P levels were explained by low pH Bray 1 solution likely solubilizing Ca-phosphate forms and subsequently overestimating TMA amended soil availability (Pagliari et al., 2010). As noted by Yost et al., (1982) when comparing soil extractant (Mehlich-1, Bray 1, and Olsen) results of rock phosphate and P fertilizer amended soils, the ideal soil extraction procedure would result in a curve relating yield and extractable P values. However, Mehlich-1, Bray 1, and Olsen soil extraction results failed to meet these criteria and as expected more P was extracted by Mehlich-1 followed by Bray 1 and Olsen (Yost et al., 1982). Overall, interpreting PLA amended soil test results should consider extractant solution as a major factor overestimating plant available P. Furthermore, when testing alkaline fertilizer materials like PLA, calibrating margins to which

Mehlich-1 inflates soil test results should be included to correctly predict plant available P from PLA amended soils.

Muffle Furnace

Examining characteristics effecting P solubility beyond P speciation was included to determine if C content effected P solubility. Carbon effect was examined by muffle furnacing PLA sources to determine C loss' impact on water soluble and total P. Upon ashing PLA samples at 550°C for 24 h, weight loss across samples averaged 0.21 g (Table 4.11). Combustion mix resulted in significantly higher weight (0.37 g) and C (38.20 g C kg⁻¹) loss than FB Fly and FB Bulk (LSD_{0.05} = 0.02 g and 24.14 g C kg⁻¹, respectively). As expected, organic material volatilized explaining CMix and FB Fly weight and C loss due to increasing temperatures as supported by Wells (2013), Novak et al. (2016), and Keiluweit et al. (2010). Fluidized bed bulk ash was minimally impacted by MF and recorded only a 0.33 g C kg⁻¹ decrease in C content. This is not surprising due to FB Bulk origin from a fluidized sand bed and initially low C content of 0.77 g C kg⁻¹. Differences in total P after MF were significant (*p*-value 0.04); however, FB Fly total P increased on average by 6.74 g P kg⁻¹ while FB Bulk and CMix total P decreased by 1.30 and 4.56 g P kg⁻¹, respectively. Increased FB Fly total P can potentially be explained by decreasing C content and dilution effect on total P concentration resulting in increased total P detected. Poultry litter ash samples followed similar WSP trends resulting in significantly higher concentrations prior to muffle furnacing. Differences due to MF decreased WSP in the order of FB Bulk 0.62 g P kg⁻¹, FB Fly 0.61 g P kg⁻¹, and CMix 0.58 g P kg⁻¹. We speculated increased temperatures would decrease all P parameters measured due to non-volatile structures stacking and forming turbostratic crystalline structures as recorded (Keiluweit et al., 2010; Novak et al., 2016; Wells 2013). However, this was not the case for FB Fly total P that increased after MF

from the C dilution effect. Overall, MF temperatures reduced C concentration and water soluble P. Therefore, C is not thought to be a major element controlling or reducing P solubility.

Particle Size Effect on Water Soluble Phosphorus

Fluidized bed fly ash particles greater than 2 mm and 0.84 mm produced significantly greater WSP than FB Bulk and CMix at each respective particle size (Table 4.12 and 4.13). Majority of FB Fly particle size distribution contained particles less than 0.25 mm contributing 68.01% ash by weight. Fluidized bed bulk primary particle size distribution included particles greater than 0.25 mm (71.65% ash weight). Statistically lower CMix WSP (0.29 g P kg⁻¹) was identified in largest particle size (>2 mm) representing 26% by ash weight size distribution. Decreased availability increased with particle size in the order of: less than 0.25 mm (1.45 g P kg⁻¹), greater than 0.25 mm (1.04 g P kg⁻¹), greater than 0.84 mm (0.62 g P kg⁻¹), greater than 2 mm (0.29 g P kg⁻¹) (LSD_{0.05} 0.57 g P kg⁻¹) (Table 4.13). Significant differences in FB Bulk and FB Fly particle size effect on WSP were undetected. However, FB Bulk WSP followed similar numerical trend as CMix. Contrastingly to FB Bulk and CMix increasing WSP with decreasing particle size trend, FB Fly resulted in numerically greater WSP of larger particles 0.84 mm (1.64 g P kg⁻¹) and 2 mm (1.48 g P kg⁻¹) when compared to particles greater and less than 0.25 mm. Supporting CMix and FB Bulk trends in WSP, Adams, (2005) found as PLA particle size decreased total nutrient concentrations increased. Phosphorous concentrations increased with decreasing particle size (> 2mm, <2 mm, and < 0.25 mm) in the order of: 79, 98, and 104 g P kg⁻¹ (Adams, 2005). Particle size has been cited as a major factor effecting P fertilizers water solubility and plant availability (Engelstad and Hellums, 1993). Smaller particle sizes increases surface area exposed to soil as well as influences availability and soil volume affected by fertilizer (Engelstad and Hellums, 1993). Collectively, particle size can influence P solubility as noted in significant and numerical differences detected in CMix and FB Bulk. In

conclusion, PLA particle size distribution is a useful physical characteristic that can be utilized to interpret and explain PLA P solubility.

Conclusions

Phosphorus fractions from sequential extraction identified that most PLA P is in bound plant unavailable fractions with little labile and WSP. Granulated poultry litter ash water, labile, and total P were significantly higher than other PLA sources tested due to additional and solubilized P from H_3PO_4 granulation. X-ray absorption near edge structure spectroscopy identified brushite, the second most soluble Ca-phosphate species, in both GPLA (16.8%) and FB Fly (18.4%) which recorded greatest WSP among PLA and manufactured PLA in sequential extraction. Additionally, dicalcium phosphate species, brushite and monetite, were identified as dominate P species controlling P solubility. However, reduced P solubility found in PLA extractions did not support these moderately soluble species that were detected by XANES, leading to the conclusion that pH will ultimately control brushite and monetite P solubility. Therefore, the authors concluded that the XANES species identification is correct; however, pH changes will govern species and subsequently availability. Ultimately, TSP had greater total P and solubility compared to all other P sources tested. Poultry litter ash sources when compared to PL contained higher total P but lower solubility. Lastly, particle size impacted solubility trends with decreasing PLA particle size increasing surface area contact and subsequently increasing solubility in CMix and FB Bulk WSP. Collectively, understanding solubility fractions requires understanding PLA species, carbon effects, and particle size influence on nutrient solubility and furthermore potential as an alternative fertilizer source. In conclusion, to increase P solubility PLA sources will need to be acidified to provide a readily water soluble P fertilizer source.

Acknowledgements

This research used resources of the Advanced Photon Source, a U.S. Department of Energy (DOE) Office of Science User Facility operated for the DOE Office of Science by Argonne National Laboratory under Contract No. DE-AC02-06CH11357. Funding for this work was provided in part by the Virginia Agricultural Experiment Station and the Hatch program of the National Institute of Food and Agriculture, US Department of Agriculture, and National Fish and Wildlife Foundation project number 0602.16.053565.

References

- Adams, Z. 2005. Comparison of broiler litter, broiler litter ash with reagent grade materials as sources of plant nutrients. M.S. thesis, Auburn University, AL.
- Ajiboye, B., O.O. Akinremi, and G.J. Racz. 2004. Laboratory characterization of phosphorus in fresh and oven-dried organic amendments. *J. Environ. Qual.* 33(3): 1062–1069.
- Ayding, I., F. Aydin, A. Saydut, G.E. Bakirdere, and C. Hamamci. 2010. Hazardous metal geochemistry of sedimentary phosphate rock used for fertilizer (Mazıdag, SE Anatolia, Turkey). *Microchem. J.* 96: 247–251. doi: 10.1016/j.microc.2010.03.006.
- Bock, B.R. 2004. Poultry litter to energy: Technical and economic feasibility. TVA Public Power Institute, Muscle Shoals, AL.
- Chow, L.C., and E.D. Eanes, editors. 2001. Octacalcium Phosphate. Karger Medical and Scientific Publishers, Giathersburg, MD.
- Codling, E.E. 2006. Laboratory characterization of extractable phosphorus in poultry litter and poultry litter ash. *Soil Sci.* 171(11): 858–864. doi: 10.1097/01.ss.0000228059.38581.97.
- Codling, E.E., R.L. Chaney, and J. Sherwell. 2002. Poultry litter ash as a potential phosphorus source for agricultural crops. *J. Environ. Qual.* 31(3): 954–61.
- Cordell, D., J.-O. Drangert, and S. White. 2009. The story of phosphorus: Global food security and food for thought. *Tradit. Peoples Clim. Change* 19(2): 292–305. doi: 10.1016/j.gloenvcha.2008.10.009.
- Coufal, C.D., C. Chavez, P.R. Niemeyer, and J.B. Carey. 2006. Measurement of broiler litter production rates and nutrient content using recycled litter. *Poult. Sci.* 85(3): 398–403. doi: 10.1093/ps/85.3.398.
- Dou, Z., J.D. Toth, D.T. Galligan, C.F. Ramberg, and J.D. Ferguson. 2000. Laboratory procedures for characterizing manure phosphorus. *J. Environ. Qual.* 29(2): 508–514. doi: 10.2134/jeq2000.00472425002900020019x.
- Engelstad, O.P., and D.T. Hellums. 1993. Water solubility of phosphate fertilizers: Agronomic aspects- a literature review. *Int. Fertil. Dev. Cent.* (17). <http://eprints.icrisat.ac.in/12719/1/RP-%208105.pdf>.
- Ervin, C.R. 2019. Poultry litter ash as an alternative fertilizer source for corn. Ph.D. dissertation, Virginia Polytechnic and State University, Painter, VA.
- Fleming-Wimer, C., M.S. Reiter, R.O. Maguire, and S. Phillips. 2018. Long-Term impacts of poultry litter on soil pH and phosphorus in no-till. *Better Crops* 102(2): 21–221. doi: <https://doi.org/10.24047/BC102221>.

- Frossard, E., P. Tekely, and J.Y. Grimal. 1994. Characterization of phosphate species in urban sewage sludges by high resolution solid-state ^{31}P NMR. *Eur. J. Soil Sci.* 45(4): 403–408. doi: <https://doi.org/10.1111/j.1365-2389.1994.tb00525.x>.
- Havlin, J., S. Tisdale, W. Nelson, and J. Beaton. 2014. *Soil Fertility and Fertilizers: An Introduction to Nutrient Management*. 8th ed. Pearson, New Jersey.
- Hedley, M.J., J.W.B. Stewart, and B.S. Chauhan. 1982. Changes in Inorganic and Organic Soil Phosphorus Fractions Induced by Cultivation Practices and by Laboratory Incubations. *Soil Sci Soc Am J.* <https://dl-sciencesocieties-org.ezproxy.lib.vt.edu/publications/sssaj/pdfs/46/5/SS0460050970> (accessed 23 September 2017).
- Howarth, R.W., A. Sharples, and D. Walker. 2002. Sources of nutrient pollution to coastal waters in the United States: Implications for achieving coastal water quality goals. *Estuaries Res. Found.* 25(4b): 565–676. doi: <https://doi.org/10.1007/BF02804898>.
- Hunger, S., H. Cho, J.T. Sims, and D.L. Sparks. 2004. Direct speciation of phosphorus in alum-amended poultry litter: Solid-state ^{31}P NMR investigation. *Environ. Microbiol.* 38(3): 674–681. doi: <https://doi.org/10.1021/es034755s>.
- Keiluweit, M., P.S. Nico, M.G. Johnson, and M. Kleber. 2010. Dynamic molecular structure of plant biomass-derived black carbon (biochar). *Environ. Sci. Technol.* 44(4): 1247–1253. doi: [10.1021/es9031419](https://doi.org/10.1021/es9031419).
- Kleinman, P., K.S. Blunk, R. Bryant, L. Saportio, D. Beegle, et al. 2012. Managing manure for sustainable livestock production in the Chesapeake Bay Watershed. *J. Soil Water Conserv.* 67(2): 54–61. doi: [10.2489/jswc.67.2.54A](https://doi.org/10.2489/jswc.67.2.54A).
- Kovar, J.L., and G.M. Pierzynski. 2009. *Methods of Phosphorus Analysis for Soils, Sediments, Residuals, and Waters*.
- Kunkle, W.E., L.E. Carr, T.A. Carter, and E.H. Bossard. 1981. Effect of flock and floor type on the levels of nutrients and heavy metals in broiler litter. *Poult. Sci.* 60(6): 1160–1164. doi: <https://doi.org/10.3382/ps.0601160>.
- Lindsay, W.L. 1979. *Chemical Equilibria in Soils*. The Blackburn Press, Caldwell, NJ.
- Maguire, R.O., and S.E. Heckendorn. 2005. *Laboratory Procedures; Virginia Tech Soil Testing Laboratory*. <https://vtechworks.lib.vt.edu/handle/10919/55039> (accessed 19 June 2017).
- Maguire, R.O., J.T. Sims, S.K. Dentel, F.J. Coale, and J.T. Mah. 2001. Relationships between biosolids treatment process and soil phosphorus availability. *J. Environ. Qual.* 30(3): 1023–1033. doi: [10.2134/jeq2001.3031023x](https://doi.org/10.2134/jeq2001.3031023x).
- Maguire, R.O., D.A. Crouse, and S.C. Hodges. 2007. Diet modification to reduce phosphorus surpluses: A mass balance approach. *J. Environ. Qual.* 36: 1235–1240. doi: [10.2134/jeq2006.0551](https://doi.org/10.2134/jeq2006.0551).

- McBride, M.B. 1994. *Environmental Chemistry of Soils*. Oxford University Press, New York.
- Mehlich, A. 1953. Determination of P, Ca, Mg, K, and NH₄. N. C. Soil Test Div. Raleigh NC.
- Metson, G.S., J. Lin, J.A. Harrison, and J.E. Compton. 2017. Linking terrestrial phosphorus inputs to riverine export across the United States. *Water Res.* doi: 10.1016/j.watres.2017.07.037.
- Middleton, A.J. 2015. Nutrient availability from poultry litter co-products. M.S. thesis, Virginia Polytechnic and State University, Blacksburg, VA.
- Novak, J.M., J.A. Ippolito, R.D. Lentz, K.A. Spokas, C.H. Bolster, et al. 2016. Soil health, crop productivity, microbial transport, and mine spoil response to biochars. *Bioenerg Res* 9: 454–464. doi: DOI 10.1007/s12155-016-9720-8.
- Pagliari, P., C. Rosen, J. Strock, and M. Russelle. 2010. Phosphorus availability and early corn growth response in soil amended with turkey manure ash. *Commun. Soil Sci. Plant Anal.* 41(11): 1369–1382. doi: 10.1080/00103621003759379.
- Peak, D., J.T. Sims, and D.L. Sparks. 2002. Solid-state speciation of natural and alum-amended poultry litter using XANES spectroscopy. *Environ. Sci. Technol.* 36(20): 4253–4261. doi: 10.1021/es025660d.
- Pelletier, B.A., J. Pease, and D. Kenyon. 2001. Economic analysis of Virginia poultry litter transportation. *Va. Tech.* <https://scholar.lib.vt.edu/ejournals/vaes/01-1.pdf> (accessed 22 December 2016).
- Qin, Z., and A. Shober. 2018. The challenges of managing legacy phosphorus losses from manure-impacted agricultural soils. *Curr. Pollut. Rep.* 4(4): 265–276. doi: <https://doi.org/10.1007/s40726-018-0100-1>.
- Qin, Z., A.L. Shober, K.G. Scheckel, C.J. Penn, and K.C. Turner. 2018. Mechanisms of phosphorus removal by phosphorus sorbing materials. *J. Environ. Qual.* 47(5): 1232–1241. doi: 10.2134/jeq2018.02.0064.
- Ravel, B., and M. Newville. 2005. ATHENA, ARTEMIS, HEPHAESTUS: Data analysis for X-ray absorption spectroscopy using IFEFFIT. *J. Synchrotron Radiat.* 12(4): 537–541. doi: doi.org/10.1107/S0909049505012719.
- Reiter, M.S., and A. Middleton. 2016. Nutrient availability from poultry litter co-products. Virginia Tech University, Painter, VA.
- Revell, K.T., R.O. Maguire, and F.A. Agblevor. 2012. Influence of poultry litter biochar on soil properties and plant growth. *Soil Sci* 177(6): 402–408. doi: 10.1097/SS.0b013e3182564202.
- SAS Institute Inc. 2017. SAS Institute. SAS Institute Inc., Cary, NC.

- Scheckel, K.G., G.L. Diamond, M.F. Burgess, J.M. Klotzbach, M. Maddaloni, et al. 2013. Amending soils with phosphate as means to mitigate soil lead hazard: A critical review of the state of the science. *J. Toxicol. Environ. Health* 16(6): 337–380. doi: <https://doi.org/10.1080/10937404.2013.825216>.
- Scholz, R.W., A.E. Ulrich, M. Eilitta, and A. Roy. 2013. Sustainable use of phosphorus: A finite resource. *Sci. Total Environ.* 461: 799–803. doi: <https://doi.org/10.1016/j.scitotenv.2013.05.043>.
- Sharpley, A. 1994. Managing Agricultural Phosphorus for Protection of Surface Waters: Issues and Options. <https://dl-sciencesocieties-org.ezproxy.lib.vt.edu/publications/jeq/pdfs/23/3/JEQ0230030437> (accessed 19 December 2016).
- Sharpley, A.N., S. Herron, and T. Daniel. 2007. Overcoming the challenges of phosphorus-based management in poultry farming. *J. Soil Water* 62(6): 375–389.
- Shober, A.L., D.L. Hesterberg, J.T. Sims, and S. Gardner. 2006. Characterization of phosphorus species in biosolids and manures using XANES spectroscopy. *J. Environ. Qual.* 35(6): 1983–1993. doi: 10.2134/jeq2006.0100.
- Sims, J.T., R.R. Simard, and B.C. Joern. 1998. Phosphorus loss in agricultural drainage: Historical perspective and current research. *J. Environ. Qual.* 27(2): 277–293. doi: 10.2134/jeq1998.00472425002700020006x.
- Slaton, N.A., K.R. Byre, M.B. Daniels, T.C. Daniel, R.J. Norman, et al. 2004. Nutrient input and removal trends for agricultural soils in nine geographic regions in Arkansas. *J. Environ. Qual.* 33(5): 1606–1615. doi: DOI: 10.2134/jeq2004.16.
- Sparks, D.L., A.L. Page, P.A. Helmke, R.H. Loeppert, P.N. Soltanpour, et al., editors. 1996. *Methods of Soil Analysis*. Soil Science Society of America, Inc. American Society of Agronomy, Inc., Madison, WI.
- Stewart, B.A., editor. 1991. *Advances in Soil Science*. Springer-Verlag New York Inc.
- The Fertilizer Institute. 2015. Soil test levels in North America. <http://soiltest.ipni.net/charts/distribution> (accessed 24 July 2017).
- Toor, G., D.J. Peak, and T.J. Sims. 2005. Phosphorus speciation in broiler litter and turkey manure produced from modified diets. *J. Environ. Qual.* 34(2): 687–97. doi: 10.2134/jeq2005.0687.
- United States Environmental Protection Agency. 1996. Method 3050B: Acid digestion of sediments, sludges, and soils, Revision 2. U.S. EPA, Washington, DC.
- Van Kauwenbergh, S.J., M. Stewart, and R. Mikkelsen. 2013. World reserves of phosphate rock... a dynamic and unfolding story. *Better Crops* 97(3): 18–20.

- Wang, C., Y. Zhang, H. Li, and J.R. Morrison. 2013. Sequential extraction procedures for the determination of phosphorus in sediment. *Jpn. Soc. Limnol.* 14: 147–157. doi: 10.1007/s10201-012-0397-1.
- Wells, D. 2013. Poultry litter ash as a phosphorus source for greenhouse crop production. Ph.D. dissertation, Louisiana State University, Baton Rouge, LA.
- Wiel, H. 2003. Determination of elements by ICP-AES and ICP-MS. *Natl. Inst. Public Health Environ.*
- Yost, R.S., G.C. Naderman, E.J. Kamprath, and E. Lobato. 1982. Availability of rock phosphate as measured by an acid tolerant pasture grass and extractable phosphorus. *Agron. J.* 74(3): 462–468. doi: doi:10.2134/agronj1982.00021962007400030016x.
- Zirkler, D., F. Lang, and M. Kaupenjohann. 2012. “Lost in Filtration”--The separation of soil colloids from larger particles. *Colloids Surfaces Physicochemical Engineering Asp.* 399: 35–40. doi: 10.1016/j.colsurfa.2012.02.021.

Table 4.1 Sequential extraction operationally defined P fractions and data notation explanation.

Fraction	Total P	Water Soluble P	Labile P	Bound P
Extraction	(H ₂ O + NaHCO ₃ + NaOH + HCl + EPA 3050 B Digest)	(H ₂ O)	(NaHCO ₃ + H ₂ O)	(NaOH + HCl + EPA 3050 B Digest)
Fraction notation	Total P (%)	% S _P of Total P	% L _P of Total P	% B _P of Total P

Table 4.2 Phosphorus K-XANES spectra phosphate standards used in linear combination fitting.

Standard	Formula	Formation Constant $\log K^\dagger$
Aluminum Phosphate Species		
Phosphate sorbed to Alumina hydroxide‡	$\text{Al}(\text{OH}_3)\text{PO}_4$	-§
Wavelite	$\text{Al}_3(\text{PO}_4)_2(\text{OH},\text{F})_3 \cdot 5 \text{H}_2\text{O}$	
Varscite	$\text{AlPO}_4 \cdot 2 \text{H}_2\text{O}$	-2.50
Calcium Phosphate Species		
Monocalcium phosphate	$\text{Ca}(\text{H}_2\text{PO}_4)_2$	-1.15
Brushite (Dicalcium phosphate dihydrate)	$\text{CaHPO}_4 \cdot 2 \text{H}_2\text{O}$	0.63
Monetite (Dicalcium phosphate anhydrous)	CaHPO_4	0.30
Octacalcium phosphate	$\text{Ca}_4\text{H}(\text{PO}_4)_3 \cdot 2.5 \text{H}_2\text{O}$	11.76
Beta-tricalcium phosphate	$\beta\text{-Ca}_3(\text{PO}_4)_2$	10.18
Hydroxyapatite	$\text{Ca}_5(\text{PO}_4)_3\text{OH}$	14.46
Fluorapatite	$\text{Ca}_5(\text{PO}_4)_3\text{F}$	-0.21
Iron Phosphate Species		
Non-crystalline iron phosphate (FePAmp)	-	-
Strengtite	$\text{FePO}_4 \cdot 2 \text{H}_2\text{O}$	-6.85
MnFeP	-	-
Magnesium and Phosphate Species		
Bobierrite	$\text{Mg}_3(\text{PO}_4)_2 \cdot 8 \text{H}_2\text{O}$	14.10
Newberryite	$\text{MgHPO}_4 \cdot 3 \text{H}_2\text{O}$	1.38

† Formation constant ($\log K^\circ$) relating two species is numerically equal to the pH at which the reacting species have equal activities for various phosphate reactions at 25 °C. Solubility constants adapted from Chemical Equilibria in Soils by Lindsay (1979).

‡ Phosphorus standard preparation, synthesis, and spectra utilized for LCF are described in supplemental information by Qin et al. (2018).

§ Unknown equilibrium constant.

Table 4.3 Poultry litter ash and co-products total elemental analysis via EPA 3050 B.

Source	Al	Ca	Fe	K	Mg	Na	P	S	Ca:P	pH
	g kg⁻¹									
FB Fly†	7.65 b‡	75.01 b	5.49 b	119.15 b	20.76 b	40.65 a	50.60 d	30.50 a	1.48 c	9.16 c
FB Bulk	5.79 c	72.89 b	4.32 c	62.57 e	19.11 c	25.62 d	44.95 e	22.00 c	1.62 b	10.21 b
CMix	17.72 a	123.73 a	13.22 a	128.59 a	47.18 a	31.87 c	69.89 c	24.27 b	1.77 a	10.50 a
GPLA-B	7.25 bc	60.06 c	5.98 b	102.20 c	19.16 c	34.76 b	90.47 b	25.91 b	0.67 d	5.53 d
GPLA-Acd2	5.78 c	55.85 c	4.20 c	93.91 d	16.34 d	32.17 c	101.97 a	22.16 c	0.55 e	4.85 e
ACU	0.81 d	8.07 d	0.69 d	13.98 f	2.14 e	4.71 e	5.38 f	1.69 d	1.50 c	9.07 c
LSD_{0.05}	1.49	4.70	0.55	6.26	1.25	1.55	4.34	2.05	0.03	0.13
p-value										
Source	<0.0001	<0.0001	<0.0001	<0.0001	<0.0001	<0.0001	<0.0001	<0.0001	<0.0001	<0.0001

† Fluidized bed fly (FB Fly), fluidized bed bulk (FB Bulk), and granulated poultry litter ash (GPLA) originate from thermally converted broiler litter via fluidized combustion system in Rhodesdale, MD. Combustion Mix (CMix) originates from broiler litter thermally converted via a combustion system in Lancaster county, PA.

‡ Within columns, means followed by the same letter are not significantly different according to LSD (0.05).

Table 4.4 Experiment 1: Sequential poultry litter ash, triple superphosphate (TSP), and poultry litter (PL) extraction delineating operationally defined P fractions.

P Fertilizer Source†	Total P (g P kg⁻¹)	% S_P of Total P	% L_P of Total P	B_P % of Total P
TSP	208.74 a‡	74.52 a	77.98 a	22.02 f
PL	18.95 d	33.39 b	63.14 b	36.86 e
ACU	6.52 e	9.12 c	25.55 c	74.45 d
FB Fly	54.56 c	1.54 d	12.30 d	87.7 c
FB Bulk	47.33 c	0.96 d	2.63 f	97.37 a
CMix	65.74 b	0.50 d	6.73 e	93.27 b
LSD_{0.05}	9.71	2.49	2.68	2.68
<i>p-value</i>				
Source	<0.0001	<0.0001	<0.0001	<0.0001

† Fluidized bed fly (FB Fly), fluidized bed bulk (FB Bulk), and granulated poultry litter ash (GPLA) originate from thermally converted broiler litter via fluidized combustion system in Rhodesdale, MD. Combustion Mix (CMix) originates from broiler litter thermally converted via a combustion system in Lancaster county, PA.

‡ Within columns, means followed by the same letter are not significantly different according to LSD (0.05).

Table 4.5 Experiment 2: Sequential poultry litter ash, granulated poultry litter ash (GPLA), and triple superphosphate (TSP) extraction delineating operationally defined P fractions.

P Fertilizer Source†	Total P (g P kg⁻¹)	% S_P of Total P	% L_P of Total P	B_P % of Total P
TSP	176.13 a‡	91.39 a	93.08 a	6.92 f
ACU	7.13 e	4.56 c	18.24 c	81.76 d
FB Fly	44.51 d	1.72 d	11.71 d	88.29 c
FB Bulk	41.54 d	0.42 e	2.34 f	97.67 a
CMix	62.44 c	0.74 e	5.90 e	94.10 b
GPLA	77.34 b	36.04 b	48.53 b	51.47 e
LSD_{0.05}	4.73	0.97	1.72	1.72
<i>p</i>-value				
Source	<0.0001	<0.0001	<0.0001	<0.0001

† Fluidized bed fly (FB Fly), fluidized bed bulk (FB Bulk), and granulated poultry litter ash (GPLA) originate from thermally converted broiler litter via fluidized combustion system in Rhodesdale, MD. Combustion Mix (CMix) originates from broiler litter thermally converted via a combustion system in Lancaster county, PA.

‡ Within columns, means followed by the same letter are not significantly different according to LSD (0.05).

§ ns, nonsignificant.

Table 4.6 Experiment 3: Sequential poultry litter ash poultry litter extraction delineating operationally defined K fractions.

K Fertilizer Source[†]	Total K (g K kg⁻¹)	% S_k of Total K	% L_k of Total K	B_k % of Total K
PL	48.43 b‡	87.61 a	98.53 a	1.47 c
FB Fly	132.83 a	73.31 b	77.49 b	22.51 b
FB Bulk	69.63 b	73.84 b	75.16 b	24.84 b
CMix	115.05 a	51.87 c	55.21 c	44.78 a
LSD_{0.05}	25.76	12.67	11.69	11.69
<i>p-value</i>				
Source	0.0001	0.001	0.0001	0.0001

[†] Fluidized bed fly (FB Fly), fluidized bed bulk (FB Bulk), and granulated poultry litter ash (GPLA) originate from thermally converted broiler litter via fluidized combustion system in Rhodesdale, MD. Combustion Mix (CMix) originates from broiler litter thermally converted via a combustion system in Lancaster county, PA.

[‡] Within columns, means followed by the same letter are not significantly different according to LSD (0.05).

Table 4.7 Experiment 4: Sequential poultry litter ash poultry litter extraction delineating operationally defined K fractions.

K Fertilizer Source†	Total K (g K kg⁻¹)	% S_k of Total K	% L_k of Total K	B_k % of Total K
GPLA	87.43 c‡	84.15 a	92.47 a	7.53 c
FB Fly	109.15 b	77.94 a	83.32 b	16.68 b
FB Bulk	60.23 d	79.60 a	82.36 b	17.64 b
CMix	131.45 a	55.85 b	60.75 c	39.25 a
LSD_{0.05}	14.58	6.88	6.02	6.02
<i>p-value</i>				
Source	<0.0001	<0.0001	<0.0001	<0.0001

† Fluidized bed fly (FB Fly), fluidized bed bulk (FB Bulk), and granulated poultry litter ash (GPLA) originate from thermally converted broiler litter via fluidized combustion system in Rhodesdale, MD. Combustion Mix (CMix) originates from broiler litter thermally converted via a combustion system in Lancaster county, PA.

‡ Within columns, means followed by the same letter are not significantly different according to LSD (0.05).

Table 4.8 Linear combination fitting (LCF) weight percentage of standards describing poultry litter ash P spectra fitting.

Standard Species	Monetite (CaHPO₄)	Bobierrite (Mg₃(PO₄)₂ · 8 H₂O)	Brushite (CaHPO₄·2H₂O)	Monocalcium P Ca(H₂PO₄)₂ · H₂O	Varscite (AlPO₄ · 2H₂O)	FeAmorP	Residual Factor (R)	Chi-Square
Source†	% of total P							
FB Fly	-‡	18.4	25.7	-‡	55.9	-‡	0.002614	0.25
FB Bulk	34.4	39.5	-‡	10.6	15.5	-‡	0.003873	0.32
CMix	76.8	-‡	-‡	-‡	12.9	10.3	0.004215	0.05
GPLA	50.0	16.8	33.2	-‡	-‡	-‡	0.01	0.75

† Fluidized bed fly (FB Fly), fluidized bed bulk (FB Bulk), and granulated poultry litter ash (GPLA) originate from thermally converted broiler litter via fluidized combustion system in Rhodesdale, MD. Combustion Mix (CMix) originates from broiler litter thermally converted via a combustion system in Lancaster County, PA.

‡ Species was not detected in Athena linear combination fitting (LCF). Standards were sequentially eliminated when standard described < 10% of LCF spectra.

Table 4.9 Selected poultry litter ash elemental properties that were used for XANES analysis.

Source [†]	Total					Molar Ratio			
	g kg ⁻¹					mol mol			
	P	Al	Ca	Mg	Fe	Al:P	Ca:P	Mg:P	Fe:P
FB Fly	50.60	7.65	75.01	20.76	5.49	0.17	1.15	0.52	0.06
FB Bulk	44.95	5.79	72.89	19.11	4.32	0.15	1.25	0.54	0.05
CMix	69.89	17.72	123.73	47.18	13.22	0.29	1.37	0.86	0.10
GPLA-B	90.47	7.25	60.6	19.16	5.98	0.09	0.52	0.27	0.04

[†] Fluidized bed fly (FB Fly), fluidized bed bulk (FB Bulk), and granulated poultry litter ash (GPLA) originate from thermally converted broiler litter via fluidized combustion system in Rhodesdale, MD. Combustion Mix (CMix) originates from broiler litter thermally converted via a combustion system in Lancaster county, PA.

Table 4.10 Poultry litter ash and triple superphosphate Mehlich-1 fertilizer extraction.

Source†	P	Ca	Ca:P	K
	mg P kg⁻¹			
TSP	4703.4 a‡	393.1 a	0.08 b	991.9 b
GPLA	1913.9 b	40.4 b	0.02 c	3848.6 a
FB Bulk	236.9 c	20.1 c	0.08 b	3435.8 a
FB Fly	160.3 d	4.7 e	0.03 c	3686.7 a
CMix	28.7 e	8.4 d	0.29 a	3501.8 a
LSD 0.05	51.6	2.3	0.02	1,312.6
p-value				
Source	<0.0001	<0.0001	<0.0001	<0.0025

† Fluidized bed fly (FB Fly), fluidized bed bulk (FB Bulk), and granulated poultry litter ash (GPLA) originate from thermally converted broiler litter via fluidized combustion system in Rhodesdale, MD. Combustion Mix (CMix) originates from broiler litter thermally converted via a combustion system in Lancaster county, PA.

‡ Within columns, means followed by the same letter are not significantly different according to LSD (0.05).

Table 4.11 Muffle furnace (550 °C) effect on poultry litter ash carbon loss and changes in total and water soluble P.

Source†	Weight loss (g)	Before Muffle Furnace Carbon	After Muffle Furnace Carbon	Difference in Carbon Content	Before Muffle Furnace H ₂ O Soluble P	After Muffle Furnace H ₂ O Soluble P	Difference in H ₂ O Soluble P	Total P Before Muffle Furnace	Total P After Muffle Furnace	Total P Difference
	g	g C kg ⁻¹			g P kg ⁻¹					
FB Fly	0.22 b‡	16.97 ab	0.57 b	16.40 ab	1.15	0.53 a	-0.61	46.77 b	53.51 b	6.74
FB Bulk	0.03 c	0.77 b	0.43 b	0.33 b	0.74	0.12 b	-0.62	43.43 b	42.14 b	-1.30
CMix	0.37 a	38.20 a	1.93 a	36.27 a	0.67	0.09 b	-0.58	74.17 a	69.6 a	-4.56
LSD 0.05	0.02	24.14	0.20	24.10	ns§	0.12	ns	9.98	19.5	ns
<i>p-value</i>										
Source	<0.0001	0.03	<0.0001	0.04	0.06	0.0009	0.95	0.002	0.04	0.53

† Fluidized bed fly (FB Fly) and fluidized bed bulk (FB Bulk) originate from thermally converted broiler litter via fluidized bed combustion system in Rhodesdale, MD. Combustion Mix (CMix) originates from broiler litter thermally converted via combustion system in Lancaster county, PA.

‡ Within columns, means followed by the same letter are not significantly different according to LSD (0.05).

§ ns, nonsignificant.

Table 4.12 Poultry litter ash particle size distribution and particle size effect on water soluble P.

Size	> 2mm	> 0.84 mm	> 0.25 mm	< 0.25 mm
Source†	Ash Weight (%)	Ash Weight (%)	Ash Weight (%)	Ash Weight (%)
FB Bulk	0.73	24.69	71.65	2.87
FB Fly	0.9	1.49	29.24	68.01
CMix	26.0	17.12	23.27	33.34

† Fluidized bed fly (FB Fly) and fluidized bed bulk (FB Bulk) originate from thermally converted broiler litter via fluidized bed combustion system in Rhodesdale, MD. Combustion Mix (CMix) originates from broiler litter thermally converted via combustion system in Lancaster county, PA.

‡ Within columns, means followed by the same letter are not significantly different according to LSD (0.05).

Table 4.13 Poultry litter ash particle size effect on water soluble P.

PLA Source†‡	FB Bulk	FB Fly	CMix
Mesh Size	g P kg ⁻¹		
> 2 mm	0.73 a§	1.48 a	0.29 b
> 0.84 mm	0.69 a	1.64 a	0.62 b
> 0.25 mm	0.87 a	0.99 b	1.04 a
< 0.25 mm	1.03 a	1.45 a	1.45 a

† Fluidized bed fly (FB Fly) and fluidized bed bulk (FB Bulk) originate from thermally converted broiler litter via fluidized bed combustion system in Rhodesdale, MD. Combustion Mix (CMix) originates from broiler litter thermally converted via combustion system in Lancaster county, PA.

‡ Interaction term, size, and source p-values were significant 0.02, 0.0004, and 0.04, respectively.

§ Within columns, means followed by the same letter are not significantly different according to LSD 0.05 = 0.57 g P kg⁻¹.

Chapter 5: Poultry Litter Ash as an Alternative Nutrient Source for Corn Production

Abstract

Investigating poultry litter ash (PLA) as an alternative crop fertilizer is a potential solution to balance poultry and crop regional nutrient cycling. As the expanding world population places pressure on the poultry industry to meet consumption demands, heightened poultry litter (PL) production presents a challenge to identify alternative uses for increased volumes. Poultry litter ash, a co-product from manure-to-energy systems, is an alternative phosphorus (P) and potassium (K) source enhancing transportation logistics, repurposing PL nutrients, and offers dual purpose as a fertilizer and an energy source when compared to PL. In effort to test PLA products as P, K, and PLA fortified nitrogen (N) sources, corn (*Zea Mays L.*) field studies were initiated across eastern Virginia. Three separate nutrient studies were implemented testing P, K, and N response to PLA fertilizer compared to industry standards of PL, urea ($\text{CO}(\text{NH}_2)_2$), triple superphosphate ($\text{Ca}(\text{H}_2\text{PO}_4)_2$), and muriate of potash (KCl). In total, three PLA [(fluidized bed bulk (FB Bulk), fluidized bed fly (FB Fly), and combustion Mix (CMix)], one PLA coated urea (ash coated urea, ACU), and one granulated PLA (GPLA) were compared in each respective nutrient study. Plant parameters were collected to determine P, K, or N fertilizer effects on corn growth included yield, grain concentrations, vegetative and reproductive tissue analysis, and Mehlich-1 extraction post-harvest. For P, PL recorded highest yield in both years as compared to PLA and confirmed P solubility concerns for PLA. The K response study found that PLA K is a comparable nutrient source and improved plant parameters when compared to control; therefore, K was plant available in our soil system. For N, eighteen out of twenty-one plant parameters examined found similar ACU and urea effects on N concentrations and were higher than the no-fertilizer control. Therefore, ACU is a comparable N

source to urea, but offered no greater benefit. Overall, PLA is a suitable co-product as-is for K, and can be effectively combined with N to formulate a multi-nutrient product, but must be further processed to increase P solubility and availability.

Introduction

Disproportional nutrient distribution within the USA is caused by large distances between crop and livestock production areas. Crop regions generally remain in a nutrient deficient status while surplus nutrients from manure build in livestock production regions due to transportation difficulties. For instance, in 2016, poultry produced in the DELMARVA area consumed more than 3.11 million metric tons of grain that consistently exceeded grain amounts produced in the region, causing average corn (*Zea Mays L.*) and soybean (*Glycine max L.*) imports to total 354,000 and 202,000 metric tons, respectively (Delmarva Poultry Industry, 2017). In a mass balance manure P study, Maguire et al. (2007) found that relative to crop P removal approximately 11% of US counties were in a P surplus. Although a minority of counties across the US contain surplus P nutrients, 22% and 9% generate greater than 15 and 30 kg manure P ha⁻¹ illustrating intense animal and subsequent manure production is concentrated in certain counties across the US. Phosphorus associated with imported grains is metabolized into meat and eggs exported for consumption, while undigested P is found in considerable quantities in PL (9 to 22 g P kg⁻¹ total P) (Havlin et al., 2014). Unlike grain, PL is rarely shipped more than 80 to 160 km beyond the original source due to low bulk density per nutrient value (0.37 g cm³ and ~9 to 22 g P kg⁻¹) as compared to commercial fertilizers like TSP (1.09 g cm³ and ~201 kg P kg), causing PL to be land applied in close proximity to poultry production (Pelletier et al., 2001; Reiter and Daniel, 2013; Havlin et al., 2014). Rarely PL nutrients are redistributed to crop production regions where soils are left in a nutrient deficit state relying on mined and synthetic fertilizers (i.e. Coastal Plain regions of Virginia) to replace grain removed nutrients.

The anticipated increase in PL production, due to growing world populations and increased consumption demands, prompted economic analysis by Pelletier et al. (2001) to

examine economic feasibility and PL transportation logistics to redistribute nutrients from concentrated to nutrient deficit areas within the Commonwealth. Pelletier et al. (2001) concluded that PL can be transported and applied at competitive costs to commercial fertilizers within the breakeven transportation distance. Results calculated PL transported 122 to 161 km from the Shenandoah Valley would cost a subsidy program \$3.97 metric ton⁻¹ (in 2019, due to inflation rate, transportation would cost approximately \$5.75 ton⁻¹) (Pelletier et al., 2001). The study concluded research investigating alternative PL uses beyond a transportation subsidy program are necessary (Pelletier et al., 2001). In effort to redistribute PL, manure-to-energy systems were investigated as an alternative method to convert PL into PLA condensing P nutrients 4 to 10 times while creating a green energy source (Crozier et al., 2009; Pagliari et al., 2009; Codling, 2013; Reiter and Middleton, 2016). Densifying nutrients into PLA increases shipping potential; however, PLA fine particulate physical characteristics compounded with confirmed decreased nutrient solubility are major obstacles for PLA adoption as a viable fertilizer which can aid in PL nutrient redistribution (Codling, 2006; Crozier et al., 2009; Reiter and Middleton, 2016).

Higher bulk density and increased PLA nutrient concentrations resulted in nutrient densities ten to seventeen times greater than PL and have potential as a viable fertilizer sources (Bock, 2004). There are numerous studies reporting PLA nutrient concentration ranges. In a study comparing eleven methods of thermo-conversion systems, Middleton (2015) found P concentrations were 4 to 7 times concentrated, potassium (K) 2.5 to 5.0 times concentrated, and sulfur (S) 2 to 3 times concentrated when compared to fresh PL. Total elemental concentrations varied between 9.4 to 104.9 g P kg⁻¹, 32.03 to 42.49 g K kg⁻¹, and 9.06 to 162.58 g S kg⁻¹ (Middleton, 2015). Codling et al. (2002) found that extractable P was two to three times concentrated and ranged from 76 to 114 g P kg⁻¹ compared to PL concentrations 22.0 to 27 g P

kg⁻¹. Trace elements found in PL included copper, arsenic, selenium, lead, mercury, and cadmium with average concentrations 319, 35, 3.4, 0.31, 0.55 mg kg⁻¹, respectively (Kunkle et al., 1981). Trace elements in PL vary due to poultry nutrition, poultry production type, and PL management (Kunkle et al., 1981; Gupta and Charles, 1999).

Current PLA studies confirmed nutrients within PL co-products are more concentrated than original PL sources and further testing is needed to determine optimum application for crop growth (Codling, 2006; Pagliari et al., 2010; Middleton, 2015). In a greenhouse study comparing PLA effectiveness to industry standard potassium phosphate (KP) (~227.1 g P kg⁻¹ and 283 g K kg⁻¹) wheat dry matter yields harvested at boot stage were equal for both soils amended with PLA and KP (Codling et al., 2002). In the same study, soils treated amended with PLA, resulted in numerically higher P plant tissue concentrations than KP (Codling et al., 2002). Alfalfa (*Medicago sativa*) production on Minnesota sandy and silt loam soils demonstrated that turkey manure ash (TMA) was an effective nutrient source in the second year of production with yields similar to industry fertilizer and greater than control (Pagliari et al., 2009). However, Pagliari et al. (2009) found that tissue P concentrations results contradicted Codling et al.'s (2002) greenhouse experiment which reported increased plant P concentrations with PLA compared to commercial fertilizer. Reiter et al. (2004) found that soybean and wheat had equal yields and plant tissue concentrations for crops grown on silt loam soils in Arkansas production systems using broiler PLA when compared to industry fertilizer sources.

Although past research consistently confirms PL co-products are more concentrated than original PL sources, the same studies conclude PLA has lower nutrient solubility than traditional inorganic fertilizers and is a potential agronomic obstacle (Codling et al., 2002; Codling, 2006; Pagliari et al., 2010; Wells, 2013; Middleton, 2015). Thermo-conversion systems' high

temperatures decrease PLA nutrient solubility and effectively renders nutrients, especially P, partially or completely unavailable within a growing season (Middleton, 2015). A greenhouse experiment by Wells (2013) compared nutrient leaching of PLA and triple super phosphate (TSP) as a fertilizer source. In this study, PLA applications reduced dissolved reactive phosphorus (DRP) and effluent-total phosphorus (TP) losses by 92% and 69% when compared to TSP, respectively (Wells, 2013). Codling (2006) utilized a modified Hedley fractionation technique to compare extractable fractions of PLA with PL. Overall, soluble inorganic PLA P extracted by H₂O accounted for only 1.45% of total inorganic P, whereas 82% of total inorganic P was removed with the harsher and largely insoluble HCl extraction (Codling, 2006). Comparatively, water extractions for inorganic P for PL was 55% while PLA was only 1.45%, highlighting changes in inorganic P solubility due to thermal-conversion temperatures (Codling, 2006).

Low solubility is a negative attribute for crop uptake but a positive characteristic as a dissolved pollutant. An early corn response study referenced slower P dissolution rates from TMA as the cause for decreased corn growth at 24 days after emergence when compared to TSP (Pagliari et al., 2010). However, 38 to 52 days after emergence there was no significant difference in stalk height or diameter, which the authors attributed to increased P dissolution with time as opposed to increased corn root systems (Pagliari et al., 2010). Turkey manure ash and TSP supplied similar quantities of plant available P with similar net P uptake 52 days after emergence (Pagliari et al., 2010). Lower P solubility in TMA caused slower plant development that did not compensate for the 7 to 8-week interval of reduced P availability when compared to increases in dry matter accumulated by industry fertilizer treatments (Pagliari et al., 2010). Ultimately the authors conclude, that corn fertilized with TMA was unable to compensate for

initial low P availability (Pagliari et al., 2010). In North Carolina, granulated animal waste by-product (AWP) efficacy was tested across three experimental systems including a greenhouse study with low P soil, a long-term research site with preexisting soil P gradients, and agricultural fields with prior P fertilization (Crozier et al., 2009). The study across P gradients illustrated lower P solubility in AWP, but Crozier et al. (2009) stated that lower solubility may not be an agronomic constraint with repeated application of AWP increasing residual P concentrations and lower dissolution rates reducing environmental concerns. Crozier et al. (2009) concluded that in general AWP was an effective P source and over time availability would increase. The researchers also cited that differences in water soluble P should have minimal impacts on yield since 90% of maximum yield was reached with <50% water soluble P fertilizer (Prochnow et al., 2008).

Manure-to-energy systems' high conversion temperatures effectively recycle PL but reduce PLA nutrient solubility and subsequent plant availability (Reiter et al., 2004; Codling, 2006; Crozier et al., 2009; Pagliari et al., 2010). Therefore, objectives are to determine PLA and PLA coated urea (Ash Coated Urea, ACU) products as N, P, and K nutrient sources. Our objectives were to: 1) Compare PLA and P industry standard fertilizers effect on corn productivity parameters; 2) Determine PLA effectiveness as K fertilizer sources compared to muriate of potash (KCL); and 3) Determine PLA coated urea effects on N plant growth parameters.

Materials and Methods

Experimental Design

Field studies were initiated in Spring 2017 and 2018 on sandy loam soils to test PLA P, K, and ash coated urea (ACU) nutrient availability (Table 5.1) (Ervin, 2019). Between 2017 and

2018 sites were conducted in the same VA counties but not at the same site locations. Poultry litter ash sources' pH and total elemental analysis via USEPA 3050B digestion are detailed in Table 5.2 (United States Environmental Protection Agency, 1996). More information regarding nutrient sources can be found in Middleton (2015). Studies consisted of four replications of 13 P, 6 K, and 5 N treatments (Table 5.3). Phosphorus fertilizer treatments were arranged in a 2 factor (source \times rate) factorial randomized complete block design and surface broadcast at 0, 9.8, 19.6, and 29.3 kg P ha⁻¹ application rates with each treatment balanced for K and N. Similarly, K and N fertilizer treatments were conducted in randomized complete block designs with fertilizer source as the main factor. Potassium treatments were surface applied at 29.3 kg K ha⁻¹ rates. Nitrogen fertilizer treatments were applied at-planting (56 kg ha⁻¹) and side-dressed (112 kg ha⁻¹) at V6 growth stage for a total of 168 kg N ha⁻¹. In 2018, two additional treatments were added to examine alternating N source at starter and side dress effect on corn productivity.

Sample Analysis

Plant tissue samples collected at V6, R1, and grain harvested at physiological maturity (R6) were dried and ground to pass a 2 mm sieve prior to plant analysis (Brann et al., 2009; Campbell, 2013). Grain harvested at physiological maturity was analyzed for moisture and corrected to 15.5% moisture. Total P and K plant and grain concentrations were digested according to USEPA 3050B protocol and analyzed via inductively coupled plasma spectroscopy (ICP-AES) (ICP-AES; CirOS Vision Model, Spectro Analytical) (United States Environmental Protection Agency, 1996). Total nitrogen was analyzed via combustion procedure using the Dumas method with a Vario EL Cube (Elementar Americas, Mt. Laurel, NJ, USA) (Bremner, 1996).

Soil pre-implementation and post-harvest were analyzed via Mehlich-1 extraction (Mehlich, 1953). Soil samples taken 0-15 cm were air-dried and ground using a hammer mill to

pass through a 2 mm screen. Five-grams of soil were extracted with 25 ml of Mehlich-1 solution and shaken for 5 minutes on a reciprocating shaker at 180 rpm. Following filtration through filter paper (Whatman 42), samples were analyzed via ICP-AES for nutrient concentrations (Mehlich, 1953; Maguire and Heckendorn, 2005).

Statistical Analysis

The P corn field study was analyzed using general linear model procedures (PROC GLM) with SAS Enterprise Guide version 7.15 (SAS Institute Inc., 2017). Phosphorus control was replicated once per block, consequently when analyzing interaction terms separately, experimental design violates balancing properties that each treatment must be assigned to the same number of experimental units (EU). Adhering to project objectives to compare PLA sources to commercial P fertilizers, control was removed from analysis and will be reported as an average. Site, P source, and rates were analyzed as fixed effects while replication was a random effect. Fishers Protected least significant difference (LSD) was used to separate statistically significant means at p -value < 0.10 . If rate p -value was significant or below trend threshold (p -value < 0.20), yield, plant tissue, and soil data were subjected to simple linear regression procedures (PROC REG) using SAS Enterprise Guide version 7.15 (SAS Institute Inc., 2017). Potassium and N data were analyzed using general linear model procedures (PROC GLM) in SAS enterprise Guide 7.15 with source as a main factor.

Results and Discussion

Phosphorus

Phosphorus Source and Rate Effects on Corn Yield

In 2017, corn yields (3,708 kg ha⁻¹) were well below Virginia's average of 9,164 kg ha⁻¹ (Table 5.4) (National Agricultural Statistics Service, 2018). Below normal yields were attributed to a combination of drought, mechanical harvesting error, and sites with initial low soil P and K

concentrations creating nutrient deficiencies not overcome during the growing season even though additional fertilizer was applied. Phosphorus rates in Dinwiddie were below trend threshold (p -value < 0.20) and identified higher yields when $19.6 \text{ kg P ha}^{-1}$ was applied as compared to 0 or 9.8 kg P ha^{-1} (4371 and $5589 \text{ kg grain ha}^{-1}$, respectively; $\text{LSD}_{0.10} = 1160 \text{ kg grain ha}^{-1}$; data not shown). A significant source \times rate interaction in Accomack (p -value 0.09) showed PL yields were significantly higher than other sources tested (Table 5.5). Poultry litter when averaged across all five 2017 field sites resulted in higher yields ($4,343 \text{ kg ha}^{-1}$) followed by CMix, FB Bulk, TSP, and no fertilizer P control. Numerically, PL treatments resulted in greatest increase in yields as supported by Middleton (2015). However, lack of statistical differences aligns with equal soybean (*Glycine max L.*) and wheat (*Triticum aestivum L.*) yields found by Reiter et al. (2004) between PLA and commercial fertilizer sources on silt loam soils in Arkansas.

Site differences were significant; therefore, each site yield will be discussed separately (Table 5.6 and 5.7). The ESAREC had highest yield ($13,206 \text{ kg ha}^{-1}$) across 2018 sites. Only Dinwiddie and ESAREC yields resulted in significant source p -values (0.003 and 0.09) and followed similar trends. Poultry litter resulted in similar yields as TSP at Dinwiddie and significantly higher yields at ESAREC. Increases in yield due to PL applications in both years was also observed by Middleton (2015) corn and Slaton et al. (2013) soybean response studies in comparison to industry fertilizer sources. Slaton et al. (2013) concluded PL yield increases were attributed to P and K fertilization, although additional PL macro and micro nutrients cannot be fully discounted as influencing factors. Poultry litter ash yields (FB Bulk and GPLA) were significantly less than PL and TSP in Dinwiddie on a medium P testing soil ($10.7 \text{ mg P kg}^{-1}$), but higher than no P additions ($8,887 \text{ kg grain ha}^{-1}$). The potential for corn response to P

fertilizers sources were expected at Dinwiddie due to medium low P soils. Differences in yield were detected between PLA and commercial fertilizer sources corroborating cited reduced PLA P availability reducing yield potential in PLA fertilized plots (Codling, 2006; Pagliari et al., 2010). However, TSP and PLA resulted in similar yields at the ESAREC which can be explained by initially high soil test P ($137.2 \text{ mg P kg}^{-1}$) although all P sources resulted in higher corn yields than no-fertilizer at ESAREC and Dinwiddie. Across all sites, P rate was insignificant with a *p*-value of 0.37 and above trend threshold (*p*-value 0.20) to be evaluated by SLR.

Phosphorus Source and Rate Effect on Plant Tissue and Grain P Concentrations

The magnitude to which decreased PLA P solubility effected early plant growth in 2017, was apparent in MM data as well as visually noticeable at Caroline and Essex sites where anthocyanin accumulation signified severe P deficiencies at V6 (Table 5.8 a, b and 5.9). Averaged across P rates, source's impact on mature leaf (V6) tissue P concentrations did not identify significant differences. Additionally, P critical nutrient concentrations were below sufficiency thresholds (3.0 to 4.5 g P kg^{-1}) across all fertilizer sources at Dinwiddie and Caroline field sites indicating that crops may have reduced yield potential due to a lack of fertility (Havlin et al., 2014). Slow PLA P availability is an undesirable characteristic for soils testing low (0 - 6 mg P kg^{-1} Mehlich-1) to medium (6 to 18 mg P kg^{-1}) like Caroline, Essex, and Dinwiddie sites. Corn P partitioning indicated approximately half of plant P uptake occurs before tasseling (VT) and remaining half of total P uptake occurred after VT and silking (R1) (Bender et al., 2013). Therefore, it is vital that alternative P fertilizers be readily available if plant productivity is not to be compromised on low P soils. As Pagliari et al. (2010) highlighted, 52 days after emergence no differences in height and stalk diameter were detected, suggesting TMA P becomes more plant available with time (Bierman and Rosen, 1994; Codling et al., 2002). Although P release increased with time, Pagliari et al. (2010) preemptively suggested that TMA did not compensate

for initial decreased P availability. High soil test P levels at the ESAREC ($83.5 \text{ mg P kg}^{-1}$) prevented an early season P deficiency from occurring and allowed more time for PLA P dissolution. Although time-dependent PLA dissolution is an intuitive conclusion, eight of fourteen total plant parameters tested, even at ESAREC, revealed that no-fertilizer P controls had numerically higher P concentrations than PLA. Therefore, surface soil chemistry may be altered from additions of PLA co-products in no-till situations where soil P remains exposed. Future research to calibrate and provide recommendations for slowly plant available manure ash sources in no-till situations is necessary (Sharpley and Smith, 1994; Codling et al., 2002; Crozier et al., 2009; Pagliari et al., 2010; Middleton, 2015; Fleming-Wimer et al., 2018).

Differences in corn ear leaf (CE) were detected at Caroline, ESAREC, and Essex field sites. Generally, PL and TSP fertilizer sources had higher CE P concentrations than CMix and FB Bulk ash. These results support those reported by Bireman and Rosen (1994) where responses in corn and lettuce tissue P from incinerated sewage sludge increased when soil P was limiting. Lower CE P concentrations across PLA sources tested is explained by decreased P dissolution from animal waste ash products due to thermal conversion temperatures (Codling et al., 2002; Codling, 2006; Pagliari et al., 2010; Ervin, 2019). Slow PLA P dissolution when compared to PL and TSP contributed to decelerated initial plant development, as observed in MM results, and subsequently affected total tissue concentrations accumulated through a growing season. Pagliari et al. (2010) identified this trend in an early corn P response study testing turkey manure ash (TMA) effect on tissue concentration, plant height, and stalk diameter. At 24 and 31 days after corn emergence, fertilizer amended soils significantly increased height and stalk diameter when compared to TMA treatments (Pagliari et al., 2010).

Rate was significant on Essex and Caroline CE P concentrations (p -value 0.08 and 0.03, respectively) (Table 5.9). Averaged across all P sources at both Essex and Caroline, at least 19.6 kg P ha⁻¹ was needed to reach highest tissue P concentrations. However, CE P concentrations were still below critical nutrient concentrations necessary for optimal yields (3.0 to 4.0 g P kg⁻¹) (Havlin et al., 2014).

Dinwiddie corn grain concentrations in 2017 had a significant source × rate impact; however, all sources were found to be similar. In Essex, higher corn grain concentrations were seen with TSP and PL (3.71 and 3.49 g P kg⁻¹) than with CMix sources (3.05 g P kg⁻¹; LSD_{0.10} = 0.32 g P kg⁻¹). Regarding rates, a linear trend demonstrated low solubility and more P fertility needed to reach maximum P grain concentration. A need for more P fertilizer from PLA sources supported mixed responses identified in other studies due to PLA decreased solubility and elemental variability (Codling et al., 2002; Reiter et al., 2004; Pagliari et al., 2009; Middleton, 2015). Source and rate main effects in Caroline corn grain P concentrations demonstrated greater plant uptake for both PL and TSP as compared to PLA sources and the no-fertilizer control.

In 2018 collectively, FB Bulk resulted in consistently lower plant tissue and grain P concentrations due to lower solubility even though they were applied to acidic soil systems (Table 5.10 and 5.11). In general, PLA failed to improve plant parameters when compared to TSP and PL and is not a suitable fertilizer in forms directly generated by manure-to-energy facilities. Granulated poultry litter ash that had acidifying binding agents demonstrated slightly improved availability on plant parameters tested compared to FB Bulk unamended forms. Most mature leaf P concentrations produced significant albeit contrasting differences in trends detected across sources at ESAREC, Essex, and Dinwiddie sites. At two sites (ESAREC and Essex), no-fertilizer P controls were similar to TSP and is further indication of PL and PLA

sources negatively impacting surface P solubility by adding high pH products to soil's concentrated P layer in no-till systems (Sharpley and Smith, 1994; Fleming-Wimer et al., 2018). Likewise, at early MM stages, PL was not yet mineralized and plant available so MM tissue was typically equal to or lower than PLA sources. These differences would later dissipate as PL released P nutrients into plant available forms which did not happen for PLA sources. Plant tissue trends were similar to 2017 results for CE with more soluble PL and TSP sources generally having higher CE P values.

Corn grain P resulted in similar responses as 2017 in Dinwiddie and Essex with PL and/or TSP having higher grain P concentrations compared to PLA sources. It was hypothesized that acidifying FB Fly ash into GPLA would increase P water solubility (original ash FB Fly 1.72% soluble of total P vs. GPLA 36.04% soluble of Total P) translating into differences detected in corn field trial parameters (Ervin, 2019). However, granulation benefits did add to field applicability but did little for increasing actual solubility for plant uptake since nearly all plant parameters in 2018 had statistically similar values for GPLA and FB Bulk.

Phosphorus Sources Effect on Mehlich-1 Soil Test P after Harvest

Mehlich-1 soil test P concentrations in 2017 were significant across site; therefore, sites will be discussed separately (Table 5.12 and 5.13). Fluidized bed bulk ash applications at Dinwiddie resulted in similar soil test P levels (8.7 mg P kg⁻¹) as TSP (5.9 mg P kg⁻¹) and significantly higher levels than PL (4.9 mg P kg⁻¹), CMix (3.9 mg P kg⁻¹), and the no-fertilizer P Control (4.1 mg P kg⁻¹) (LSD_{0.10} = 3.2 mg P kg⁻¹). The Accomack and Caroline source × rate interaction was significant. Accomack FB Bulk (17.5 mg P kg⁻¹) resulted in higher P concentrations post-harvest, than all other sources; however, this was not the case for Caroline Mehlich-1 results. As expected, highest Mehlich-1 extractable P concentrations were generally found following application of 29.3 kg P ha⁻¹ averaged across P sources (Table 5.14 and 5.15).

Soil test results showed PLA sources increased soil concentrations but did not translate into agronomic benefits, ultimately questioning if PLA applications are beneficial or further complicate nutrient management efforts due to low solubility.

In 2018, soil concentrations were significant across site; therefore, sites will be discussed separately where source effect on soil test P was only significant in Dinwiddie and Essex (Table 5.16 and 5.17). Granulated poultry litter ash and PL were similar and resulted in significantly lower Dinwiddie soil test P concentrations after harvest than TSP (8.4 mg P kg⁻¹), FB Bulk (8.3 mg P kg⁻¹), and P control (6.7 mg P kg⁻¹) (LSD_{0.10} = 1.7 mg P kg⁻¹). Essex generally mirrored Dinwiddie with FB Bulk having highest soil test P concentrations. Overall, FB Bulk resulted in numerically or significantly higher Mehlich-1 P concentrations than other P sources at 8 out of 9 field sites. Although Mehlich-1 P concentrations increased, yield and plant parameters did not. This points to conclusions established by Reiter et al. (2004) and Crozier et al. (2009) that, manure ash sources increased soil residual P concentrations but were relatively unavailable to crops during the first growing season. Applying more insoluble P sources may benefit the environment in the short-term by reducing possible WSP losses; however, producers may be applying P sources that are not beneficial to the current crop but ultimately raising their overall soil test P values.

Soil chemical properties affected by PLA present a myriad of factors that explain and influence Mehlich-1 soil test P results that should be considered when interpreting soil data. Biochar, a low temperature and oxygen produced thermally converted soil amendment, was investigated for its potential to act as soil P sorbing agent on legacy P soils (Novak and Watts, 2005; Yingxue et al., 2019). Although biochar and PLA differ by thermal conversion processes, similar chemical characteristics including Ca-phosphate species (monetite; CaHPO₄ and

brushite; $\text{CaHPO}_4 \cdot 2\text{H}_2\text{O}$), pH, submicron porosity size and structure, and functional groups could enhance surface chemistry to adsorb soil P (Antunes et al., 2018; Yingxue et al., 2019). Potential PLA P sorption effect could be one of two factors explaining numerically and significantly higher PLA amended soil test P results across 2017 and 2018 sites. Bierman and Rosen (1994) identified increases in soil pH, Bray and Olsen extractable P, and ammonium acetate extractable Ca and Mg with increasing incinerated ash sewage sludge rates. Turkey manure ash amended soils increased Bray 1 soil test P regression slopes to five times greater than other fertilizer sources tested (Pagliari et al., 2010). Contrastingly within the same study, Olsen P extractions revealed soil concentrations were greater with fertilizer treatments than TMA, supporting plant growth results (Pagliari et al., 2010). Differences in soil test P concentrations were explained by low pH Bray 1 solution likely solubilizing Ca-phosphate forms and subsequently overestimating TMA amended soil availability. Dilute double acid method is the accepted soil testing procedure in acidic southern soils (Sparks et al., 1996; Maguire and Heckendorn, 2005). However, Mehlich-1 extracting solution (0.05 M HCl + 0.0125 M H_2SO_4) is unsuitable for calcareous soils as well as soils previously receiving highly alkaline rock phosphate ($\text{Ca}_{10}(\text{PO}_4)_6\text{F}_2$) applications due to acidic extracting solutions overestimating plant available P (Sparks et al., 1996). Combustion mix, FB Fly, and FB Bulk sources have pH values of 9.16, 10.21, and 10.50, respectively. Bray-1 and Mehlich-1 correlate well due to slightly acidic extracting solutions, therefore; our second hypothesized factor influencing higher PLA amended soil test P values is caused by acidic extracting solutions overestimating plant available P as seen in other studies (Bierman and Rosen, 1994; Sparks et al., 1996; Pagliari et al., 2010). FB Bulk and CMix fertilizers extracted by Mehlich-1 resulted in 240 and 30 mg P kg^{-1} , respectively (Ervin, 2019). Difficulty in discerning soil P available portions represented by Mehlich-1 extractions is caused

by pH effects, Mehlich-1 acidic solution, crop uptake, and potential antagonistic P sorption effects. Consequently, future studies utilizing acidic soil extraction on manure ash amended soils should evaluate these characteristics to measure influence upon soil test results.

Potassium

Potassium Source Effect on Corn Yield

Corn yield varied by year and site; therefore, yield data will be presented separately (Table 5.18 and 5.19). Significant differences amongst K sources was only detected in Essex 2018 site with highest yield achieved with muriate of potash (KCl) at 13,771 kg ha⁻¹. Across site years, three of eight sites followed similar trends with KCl producing highest grain yields. Amongst PLA sources, FB Fly averaged numerically higher yields (8,409 kg ha⁻¹) across site years when compared to CMix (7,966 kg ha⁻¹) and FB Bulk (7,982 kg ha⁻¹). Potassium yield results generally reflect previous solubility data that demonstrated K solubility from PLA is suitable as-is from the manure-to-energy system and is not largely bound in recalcitrant forms like P.

Potassium Source Effect on Plant Tissue and Grain K Concentrations

Most mature corn leaf K concentrations collected at V6 resulted in significant differences in 2017 Caroline and 2018 Dinwiddie sites. Combustion Mix, KCl and PL generally had highest MM concentrations in Caroline 2017 and Dinwiddie 2018 sites (Tables 5.20 a, b and 5.21). In most cases for both years, the no-fertilizer K control was numerically or statistically lower than fertilized sources. Most mature leaf were sampled 45 to 85 days after emergence and were within PLA K 56 day dissolution intervals concluded in Middleton's (2015) PLA incubation study (Havlin et al., 2014). By 56 days, CMix [denoted as Ash 4 by Middleton (2015)] K availability increased to 88% K comparable to PL. Therefore, PLA K availability increased with time and aligned with early K uptake by plants. Potassium critical nutrient concentration for V6 most

mature leaf (20 to 35 g K kg⁻¹) were met by all K sources across all sites and years (Schulte and Kelling, 1985; Havlin et al., 2014). Collectively, PLA provided sufficient K across plant parameters tested, and supports results from Pagliari et al. (2009) which concluded turkey manure ash as a comparable K source to potassium chloride. Initial K availability is vital for sufficient corn growth and could be detrimental if availability was reduced since two-thirds of corn K uptake occurs by VT and R1 so most K must be available during vegetative growth. Based upon plant parameter results, PLA provided available K sufficient for sustaining season long growth.

Corn ear leaf collected at R1 identified significant differences only at Accomack in 2017 with FB Fly (17.20 g K kg⁻¹), FB Bulk (17.03 g K kg⁻¹), CMix (16.65 g K kg⁻¹), and KCl (16.28 g K kg⁻¹) producing similar K concentrations that were higher than the no-fertilizer K control (14.78 g K kg⁻¹). Corn ear leaf critical K thresholds of 20 to 30 g K kg⁻¹ were not achieved by any K sources tested at Caroline 2017 and Accomack 2017 so more fertilizer was likely warranted to reach optimal yields (Schulte and Kelling, 1985; Havlin et al., 2014).

Potassium source effect on plant tissue and grain concentrations differed between years and sites. Significant differences in corn grain concentrations were detected in 2017 Caroline and Accomack and 2018 Dinwiddie sites. Poultry litter across all three sites produced significantly greater grain K (4.67, 4.75, and 4.08 g K kg⁻¹ for Caroline, Accomack, and Dinwiddie, respectively) concentrations than PLA, depending on site. Collectively, based upon plant parameter results, PLA provided available K sufficient for sustaining season long growth.

Potassium Source Effect on Mehlich-1 Soil Test K after Harvest

Soil test K concentrations differed across site and year; therefore, K source effect on soil will be discussed separately (Table 5.22 and 5.23). Significant differences detected in Caroline 2017 revealed greater K concentrations on PL amended soils (92.6 mg K kg⁻¹) when compared

to FB Fly (57.4 mg K kg⁻¹), CMix (61.3 mg K kg⁻¹), and KCl (51.9 mg K kg⁻¹) post-harvest. Numerical differences in soil test K revealed that all PLA sources increased K concentrations beyond no-fertilizer K controls. Unlike PLA P, K provided by PLA is not thought to negatively impact soil K availability or Mehlich-1 extractable K, since K structures are largely water soluble within the soil system. Previous work revealed water soluble K structures when compared to PL (84.15% water soluble of total K), FB Fly (77.94% water soluble of total K), and FB Bulk (82.36% water soluble of total K) were similar (LSD_{0.05} 6.88% water soluble of total K) (Ervin, 2019).

Nitrogen

Nitrogen Source Effect on Corn Yield

Nitrogen treatments differed by years; therefore, 2017 and 2018 data were analyzed and discussed separately. Site and source were significant in 2017 yield and were analyzed separately identifying yield differences at Accomack, Caroline, Dinwiddie, and ESAREC sites (Table 5.24 and 5.25). All sites, except Caroline, identified ACU and urea yields significantly higher than N control. In 2018, two additional treatments were added to examine alternating N source at starter and side dress effect on corn productivity. Yield differed across site; therefore, sites were analyzed separately (Table 5.26 and 5.27). Only Dinwiddie produced significantly lower ACU/urea yields (4,995 kg ha⁻¹) than other N treatments, excluding N control (LSD_{0.10} = 411 kg ha⁻¹). However, yield at ESAREC and Essex failed to identify any differences between N source at starter or side dress. All 2018 N treatments yielded significantly higher than N control. Overall, ash coated urea offered no benefit to corn productivity compared to urea alone.

Nitrogen Source Effect on Plant Tissue and Grain N Concentrations

In 2017, MM leaf concentrations were significantly affected at Caroline and Essex and demonstrated contrasting differences (Table 5.28 a and b). Caroline MM concentrations resulted

in significant differences between ACU and urea, however no differences were found between Essex MM concentrations. Critical N concentrations at V6 of 35 to 45 g N kg⁻¹ were met by ACU and urea sources at Caroline and ESAREC (Schulte and Kelling, 1985; Havlin et al., 2014). Likewise, Essex CE concentrations resulted in no significant differences between ACU and urea. Nitrogen source effect on grain N concentrations occurred at Dinwiddie and ESAREC. Generally, all N fertilized plots MM concentrations were more than no-fertilizer control plots with no significant difference observed between ACU or urea.

In 2018, MM leaf concentrations followed similar trends as seen in 2017 with all N sources meeting N threshold levels (35 to 45 g N kg⁻¹) (Schulte and Kelling, 1985; Havlin et al., 2014) (Table 5.29). Across all sites CE leaf N concentrations followed similar trends with all N sources resulting in significantly higher concentrations than N control. Corn ear leaf critical N concentrations (28 to 25 g N kg⁻¹) were reached or exceeded across all sites and N source except ACU at Dinwiddie (26.7 g N kg⁻¹) (Schulte and Kelling, 1985; Havlin et al., 2014). Significant difference in grain N concentrations were identified at Dinwiddie and ESAREC; however, similar to previous results, no major differences between N sources were observed.

Collectively across plant parameters, eighteen out of twenty-one plant parameters examined found similar ACU and urea effects on N concentrations. Therefore, ACU is a comparable N source to urea. Noticeable differences due to volatility inhibitors in ACU binder had little to no effect on parameters examined. That is not to completely disqualify ACU as a controlled or volatility inhibited N source as two plant parameters examined are worth mentioning. Caroline yield and MM found ACU increasing N concentrations significantly above urea, suggesting there is potential ACU characteristics that improve N availability and stability.

However, the study cannot conclusively support ACU superiority over urea and more research is needed.

Conclusions

In general, differences were observed regarding PLA as a fertilizer source whether P or K was the nutrient of interest. For P, PLA chemical characteristics effecting P solubility and subsequent plant availability determined that unprocessed PLA will likely not be suitable as a P fertilizer when initially applied. Granulated PLA improved plant response parameters in response to P rate when compared to insoluble FB Bulk supporting hypothesized increased availability. For K, PLA K is a comparable nutrient source and improved plant parameters when compared to no-fertilizer control and often produced similar results to PL and KCl. Regarding formulation with urea to provide a N fertilizer choice, PLA hinted at improved plant parameters when formulated with urea but more research is needed. In conclusion, farmers utilizing PLA sources can consider these materials suitable K fertilizers as-is, but more processing is needed if being utilized as a P fertilizer in Mid-Atlantic farming systems.

Acknowledgements

This research used resources of the Advanced Photon Source, a U.S. Department of Energy (DOE) Office of Science User Facility operated for the DOE Office of Science by Argonne National Laboratory under Contract No. DE-AC02-06CH11357. Funding for this work was provided in part by the Virginia Agricultural Experiment Station and the Hatch program of the National Institute of Food and Agriculture, US Department of Agriculture, and National Fish and Wildlife Foundation project number 0602.16.053565.

References

- Antunes, E., M. Jacob, G. Brodie, and P. Schneider. 2018. Isotherms, kinetics and mechanism analysis of phosphorus recovery from aqueous solution by calcium-rich biochar produced from biosolids via microwave pyrolysis. *J. Environ. Chem. Eng.* 6(1): 395–403. doi: <https://doi.org/10.1016/j.jece.2017.12.011>.
- Bender, R.R., J.W. Haegele, and F.E. Below. 2015. Modern Soybean Varieties' Nutrient Uptake Patterns. *Agron. J.* 99(2): 7–10.
- Bender, R.R., J.W. Haegele, M.L. Ruffo, and F.E. Below. 2013. Modern Corn Hybrids' Nutrient Uptake Pattern. *Agron. J.* 97(1): 7–10.
- Bierman, P.M., and C.J. Rosen. 1994. Sewage sludge incinerator ash effects on soil chemical properties and growth of lettuce and corn. *Commun. Soil Sci. Plant Anal.* 25(13–14): 2409–2437. doi: 10.1080/00103629409369197.
- Bock, B.R. 2004. Poultry litter to energy: Technical and economic feasibility. TVA Public Power Institute, Muscle Shoals, AL.
- Brann, D.E., A.O. Abaye, P.R. Peterson, D.R. Chalmers, D.L. Whitt, et al. 2009. *Agronomy Handbook*. <https://vtechworks.lib.vt.edu/handle/10919/48840> (accessed 3 May 2017).
- Bremner, J.M. 1996. Nitrogen-total. *Methods of Soil Analysis Part 3- Chemical Methods*. SSSA, Madison, WI.
- Campbell, Ray.C., editor. 2013. *Southern Cooperative Series Bulletin: Sufficiency Ranges for Plant Analysis in the Southern Region of the United States*. <http://www.ncagr.gov/agronomi/saaesd/scsb394.pdf> (accessed 28 July 2017).
- Codling, E.E. 2006. Laboratory characterization of extractable phosphorus in poultry litter and poultry litter ash. *Soil Sci.* 171(11): 858–864. doi: 10.1097/01.ss.0000228059.38581.97.
- Codling, E.E. 2013. Phosphorus and arsenic uptake by corn, wheat, and soybean from broiler litter ash and egg layer manure ash. *J. Plant Nutr.* 36(7): 1083–1101. doi: 10.1080/01904167.2013.776079.
- Codling, E.E., R.L. Chaney, and J. Sherwell. 2002. Poultry litter ash as a potential phosphorus source for agricultural crops. *J. Environ. Qual.* 31(3): 954–61.
- Crozier, C.R., J.L. Havlin, G.D. Hoyt, J.W. Rideout, and R. McDaniel. 2009. Three experimental systems to evaluate phosphorus supply from enhanced granulated manure ash. *Agron. J.* 101(4): 880–888. doi: 10.2134/agronj2008.0187x.
- Delmarva Poultry Industry. 2017. *Delmarva meat chickens, soybeans, and corn production and use*. <http://www.dpichicken.org/facts/facts-figures.cfm> (accessed 30 August 2018).
- Ervin, C.R. 2019. Poultry litter ash as an alternative fertilizer source for corn. Ph.D. dissertation, Virginia Polytechnic and State University, Painter, VA.

- Fleming-Wimer, C., M.S. Reiter, R.O. Maguire, and S. Phillips. 2018. Long-Term impacts of poultry litter on soil pH and phosphorus in no-till. *Better Crops* 102(2): 21–221. doi: <https://doi.org/10.24047/BC102221>.
- Gupta, G., and S. Charles. 1999. Trace elements in soils fertilized with poultry litter. *Poult. Sci.* 78(12): 1695–1698. doi: 10.1093/ps/78.12.1695.
- Havlin, J., S. Tisdale, W. Nelson, and J. Beaton. 2014. *Soil Fertility and Fertilizers: An Introduction to Nutrient Management*. 8th ed. Pearson, New Jersey.
- Kunkle, W.E., L.E. Carr, T.A. Carter, and E.H. Bossard. 1981. Effect of flock and floor type on the levels of nutrients and heavy metals in broiler litter. *Poult. Sci.* 60(6): 1160–1164. doi: <https://doi.org/10.3382/ps.0601160>.
- Maguire, R.O., and S.E. Heckendorn. 2005. *Laboratory Procedures; Virginia Tech Soil Testing Laboratory*. <https://vtechworks.lib.vt.edu/handle/10919/55039> (accessed 19 June 2017).
- Maguire, R.O., D.A. Crouse, and S.C. Hodges. 2007. Diet modification to reduce phosphorus surpluses: A mass balance approach. *J Environ. Qual.* 36: 1235–1240. doi: 10.2134/jeq2006.0551.
- Mehlich, A. 1953. Determination of P, Ca, Mg, K, and NH₄. N. C. Soil Test Div. Raleigh NC.
- Middleton, A.J. 2015. Nutrient availability from poultry litter co-products. M.S. thesis, Virginia Polytechnic and State University, Blacksburg, VA.
- National Agricultural Statistics Service. 2018. 2018 State Agriculture Overview. NASS USDA.
- Novak, J.M., and D.W. Watts. 2005. An Alum-Based Water Treatment Residual Can Reduce Extractable Phosphorus Concentrations in Three Phosphorus-Enriched Coastal Plain Soils. *J. Environ. Qual.* 34(5): 1820–1827. doi: 10.2134/jeq2004.0479.
- Pagliari, P.H., C.J. Rosen, and J.S. Strock. 2009. Turkey manure ash effects on alfalfa yield, tissue elemental composition, and chemical soil properties. *Commun. Soil Sci. Plant Anal.* 40(17–18): 2874–2897. doi: 10.1080/00103620903173863.
- Pagliari, P., C. Rosen, J. Strock, and M. Russelle. 2010. Phosphorus availability and early corn growth response in soil amended with turkey manure ash. *Commun. Soil Sci. Plant Anal.* 41(11): 1369–1382. doi: 10.1080/00103621003759379.
- Pelletier, B.A., J. Pease, and D. Kenyon. 2001. Economic analysis of Virginia poultry litter transportation. *Va. Tech.* <https://scholar.lib.vt.edu/ejournals/vaes/01-1.pdf> (accessed 22 December 2016).
- Prochnow, L.I., S.H. Chien, G. Carmona, E.F. Dillard, and J. Henao. 2008. Plant availability of phosphorus in four superphosphate fertilizers varying in water-insoluble phosphate compounds. *Soil Sci. Soc. Am. J.* 72(2): 462–470. doi: 10.2136/sssaj2006.0421.

- Reiter, M.S., and T.C. Daniel. 2013. Binding agents effect on physical and chemical attributes of nitrogen-fortified poultry litter and biosolid granules. *Am. Soc. Agric. Biol. Eng.* 56(5): 1695–1702. doi: 10.12031/trans.56.9979.
- Reiter, M.S., T.S. Daniel, N.A. Slaton, C.E. Wilson, C.H. Tingle, et al. 2004. Poultry litter ash and raw litter residual effects on wheat and soybeans in an Eastern Arkansas rice, wheat, and soybean rotation. *Wayne E Sabbe Ark. Soil Fertil. Stud.* 2004: 72–77.
- Reiter, M.S., and A. Middleton. 2016. Nutrient availability from poultry litter co-products. Virginia Tech University, Painter, VA.
- SAS Institute Inc. 2017. SAS Institute. SAS Institute Inc., Cary, NC.
- Schulte, E.E., and K.A. Kelling. 1985. *Plant Analysis: A Diagnostic Tool*. Purdue University, West Lafayette, IN.
- Sharpley, A.N., and S.J. Smith. 1994. Wheat tillage and water quality in the Southern plains. *Soil Tillage Res.* 30(1): 33–48. doi: [https://doi.org/10.1016/0167-1987\(94\)90149-X](https://doi.org/10.1016/0167-1987(94)90149-X).
- Slaton, N.A., T.L. Roberts, B.R. Golden, J.W. Ross, and R.J. Norman. 2013. Soybean Response to Phosphorus and Potassium Supplied as Inorganic Fertilizer or Poultry Litter. *Agron. J.* 105(3): 812–820.
- Soil Survey Staff, Natural Resource Conservation Unit, United States Department of Agriculture. Web Soil Survey. <https://websoilsurvey.sc.egov.usda.gov/>.
- Sparks, D.L., A.L. Page, P.A. Helmke, R.H. Loeppert, P.N. Soltanpour, et al., editors. 1996. *Methods of Soil Analysis*. Soil Science Society of America, Inc. American Society of Agronomy, Inc., Madison, WI.
- United States Environmental Protection Agency. 1996. Method 3050B: Acid digestion of sediments, sludges, and soils, Revision 2. U.S. EPA, Washington, DC.
- Wells, D. 2013. Poultry Litter Ash as a Phosphorus Source for Greenhouse Crop Production. <http://etd.lsu.edu/docs/available/etd-04152013-121245/> (accessed 5 February 2017).
- Yingxue, L., D. Xu, Y. Guan, K. Yu, and W. Wang. 2019. Phosphorus sorption capacity of biochars from different waste woods and bamboo. *Int. J. Phytoremediation* 21(2): 145–151. doi: 10.1080/15226514.2018.1488806.

Table 5.1 Poultry litter ash corn field site locations, soil series, nutrient concentrations, and studies conducted in Virginia in 2017 and 2018.

Year	Location	Soil Series†	P	K	P Study	K Study	N Study
			mg kg ⁻¹				
2017	Accomack Co., Va. (37° 6'N; -75° 8'W)	sandy loam (coarse-loamy, mixed, semiactive, thermic Aquic Hapludults)	12.1 M	122.7 H	X	X	X
	Caroline Co., Va. (37° 9'N; -77° 5'W)	Kempsville-Emporia fine sandy loam (fine-loamy, siliceous, subactive, thermic Typic Hapludults)	1.8 L-	131.0 H	X	X	X
	Dinwiddie Co., Va. (36° 9'N; -77° 5'W)	Roanoke loam fine (mixed semiactive, thermic Typic Endoaquults)	7.2 M-	22.4 L	X	X	X
	Eastern Shore Agricultural and Research Extension Center (ESAREC), Painter, Va. (37° 5'N; -75° 8'W)	Bojac Sandy Loam (coarse-loamy, mixed, semiactive, thermic Typic Hapludults)	83.5 VH	119.8 H	X	X	X
	Essex Co., Va. (37° 8'N; -76° 8'W)	Pamunkey fine sandy loam (fine-loamy, mixed, semiactive, thermic Ultlic Hapludalfs)	8.4 M-	114.2 H	X	X	X
2018	Dinwiddie Co., Va. (36° 9'N; -77° 5'W)	Emporia sandy loam (mixed semiactive, thermic Typic Endoaquults)	10.7 M-	107.5 H	X	X	X
	Eastern Shore Agricultural and Research Extension Center (ESAREC), Painter, Va. (37° 5'N; -75° 8'W)	Bojac Sandy Loam (coarse-loamy, mixed, semiactive, thermic Typic Hapludults)	26.8 H	137.2 H	X	X	X
	Essex Co., Va. (37° 8'N; -76° 8'W)	Pamunkey loam (mixed semiactive, thermic Typic Endoaquults)	18.7 H-	115.9 H	X	X	X
	Mecklenburg Essex Co., Va. (36° 9'N; -78° 0'W)	Appling sandy loam (fine, kaolinitic, thermic Typic Kanhapludults)	35.6 H	206.3 VH	X		

† Source: Web Soil Survey (Soil Survey Staff, Natural Resource Conservation Unit, United States Department of Agriculture)

Table 5.2 Total elemental analysis of broiler litter converted into poultry litter ash (PLA) via fluidized bed combustion system in Rhodesdale, MD producing fluidized bed fly (FB Fly), fluidized bed bulk (FB Bulk), granulated poultry litter ash (GPLA), and ash coated urea (ACU) and from combustion thermo-conversion system in Lancaster county, PA producing combustion mix (CMix).

Source	Al	N	Ca	Fe	K	Mg	Na	P	S	Ca:P	pH
	g kg ⁻¹										
FB Fly†	7.65 b‡	2.58 b	75.01 b	5.49 b	119.15 b	20.76 b	40.65 a	50.60 d	30.50 a	1.48 c	9.16 c
FB Bulk	5.79 c	0.55 b	72.89 b	4.32 c	62.57 e	19.11 c	25.62 d	44.95 e	22.00 c	1.62 b	10.21 b
CMix	17.72 a	2.38 b	123.73 a	13.22 a	128.59 a	47.18 a	31.87 c	69.89 c	24.27 b	1.77 a	10.50 a
GPLA-B	7.25 bc	2.70 b	60.06 c	5.98 b	102.20 c	19.16 c	34.76 b	90.47 b	25.91 b	0.67 d	5.53 d
GPLA-Acd2	5.78 c	2.28 b	55.85 c	4.20 c	93.91 d	16.34 d	32.17 c	101.97 a	22.16 c	0.55 e	4.85 e
ACU	0.81 d	456.38 a	8.07 d	0.69 d	13.98 f	2.14 e	4.71 e	5.38 f	1.69 d	1.50 c	9.07 c
LSD_{0.05}	1.49	3.59	4.70	0.55	6.26	1.25	1.55	4.34	2.05	0.03	0.13
p-value											
Source	<0.0001	<0.0001	<0.0001	<0.0001	<0.0001	<0.0001	<0.0001	<0.0001	<0.0001	<0.0001	<0.0001

† Fluidized bed fly (FB Fly), fluidized bed bulk (FB Bulk), and granulated poultry litter ash (GPLA) originate from thermally converted broiler litter via fluidized combustion system in Rhodesdale, MD. Combustion Mix (CMix) originates from broiler litter thermally converted via a combustion system in Lancaster county, PA.

‡ Within columns, means followed by the same letter are not significantly different according to LSD (0.05).

Table 5.3 Poultry litter ash phosphorus (P), potassium (K), and nitrogen (N) field study treatments in 2017 and 2018 for Virginia corn field studies.

Phosphorus				
Year	2017		2018	
Treatment Number	P Source	P Rate kg P ha⁻¹	P Source	P Rate kg P ha⁻¹
1	P Control	0	P Control	0
4	FB Bulk	9.8	FB Bulk	9.8
5	FB Bulk	19.6	FB Bulk	19.6
6	FB Bulk	29.3	FB Bulk	29.3
7†	CMix	9.8	GPLA	9.8
8†	CMix	19.6	GPLA	19.6
9†	CMix	29.3	GPLA	29.3
10	PL	9.8	PL	9.8
11	PL	19.6	PL	19.6
12	PL	29.3	PL	29.3
13	TSP	9.8	TSP	9.8
14	TSP	19.6	TSP	19.6
15	TSP	29.3	TSP	29.3

Potassium		
Treatment Number	K Source	K Source
2	K Control	K Control
16	FB Fly	FB Fly
17	FB Bulk	FB Bulk
18	CMix	CMix
19	PL	PL
20	KCl	KCl

Nitrogen		
Treatment Number	N Source (Source (planting/sidedress))	N Source (Source (planting/sidedress))
3	N Control	N Control
21	ACU / ACU	ACU / ACU
22	Urea / Urea	Urea / Urea
23†	na	Urea / ACU
24†	na	ACU / Urea

† Treatment source differed between site years.

Table 5.4 Corn yield response to P control, poultry litter (PL), triple superphosphate (TSP), combustion mix (CMix), and fluidized bed bulk (FB Bulk) sources averaged over P rate in 2017.

All 2017 Sites	
P Source	kg ha ⁻¹
P Control†	2,089
PL	4,343
TSP	3,916
CMix	4,222
FB Bulk	3,970
LSD_{0.10}	ns§
<i>p-value</i>	
(Site × P Source × P Rate)	0.68
(Site × P Source)	0.83
(Site × P Rate)	0.66
(P Source × P Rate)	0.99
Site	<0.0001
P Source	0.51
P Rate	0.25

† P Control data is averaged and was not subjected to ANOVA due to unbalanced replication.

‡ Within columns, means followed by the same letter are not significantly different according to LSD (0.10).

§ ns, non-significant at the 0.10 probability level.

Table 5.5 Corn yield response to P control, poultry litter (PL), triple superphosphate (TSP), combustion mix (CMix), and fluidized bed bulk (FB Bulk) sources averaged over P rate in 2017 sites.

Site	Dinwiddie	ESAREC	Essex	Accomack	Caroline	
P Source	kg ha⁻¹					
P Control†	4,372	5,409	3,363	1,576	2,861	
PL	6,263	4,693	3,803	3,644 a‡	3,311	
TSP	5,658	5,015	3,419	1,966 b	3,519	
CMix	5,987	5,397	3,976	2,212 b	3,536	
FB Bulk	6,123	4,978	3,367	2,176 b	3,206	
LSD_{0.10}	ns	ns	ns	444	ns	
<i>p-value</i>						
(P Source × P Rate)		0.53	0.64	0.37	0.09	0.25
P Source		0.89	0.52	0.71	<0.0001	0.93
P Rate		0.18	0.86	0.22	0.38	0.33

† P Control data is averaged and was not subjected to ANOVA due to unbalanced replication.

‡ Within columns, means followed by the same letter are not significantly different according to LSD (0.10).

§ ns, non-significant at the 0.10 probability level.

Table 5.6 Corn yield response to P control, poultry litter (PL), triple superphosphate (TSP), granulated poultry litter ash (GPLA), and fluidized bed bulk (FB Bulk) sources averaged over rate in 2018.

		All 2018 Sites
P Sources	kg ha ⁻¹	
P Control†		10,312
PL		10,717
TSP		10,520
GPLA		10,380
FB Bulk		10,662
	LSD_{0.10}	ns§
<i>p-value</i>		
(Site × P Source × P Rate)		0.96
(Site × P Source)		0.35
(Site × P Rate)		0.89
(P Source × P Rate)		0.53
Site		<0.0001
P Source		0.77
P Rate		0.70

† P Control data is averaged and was not subjected to ANOVA due to unbalanced replication.

‡ Within columns, means followed by the same letter are not significantly different according to LSD (0.10).

§ ns, non-significant at the 0.10 probability level.

Table 5.7 Corn yield response to P control, poultry litter (PL), triple superphosphate (TSP), granulated poultry litter ash (GPLA), and fluidized bed bulk (FB Bulk) sources averaged over rate in 2018 sites.

Site	Dinwiddie	ESAREC	Essex	Mecklenburg
P Sources	kg ha⁻¹			
P Control†	8,887	12,586	10,456	9,318
PL	11,271 a‡	13,612 a	10,187	7,797
TSP	10,875 a	13,046 b	9,7422	8,419
GPLA	10,211 b	13,069 b	10,422	7,818
FB Bulk	10,013 b	13,097 b	11,175	8,364
LSD_{0.10}	577	422	ns	ns
<i>p-value</i>				
Site				
(P Source × P Rate)	0.51	0.58	0.88	0.35
P Source	0.003	0.09	0.44	0.73
P Rate	0.88	0.80	0.66	0.31

† P Control data is averaged and was not subjected to ANOVA due to unbalanced replication.

‡ Within columns, means followed by the same letter are not significantly different according to LSD (0.10).

§ ns, non-significant at the 0.10 probability level.

Table 5.8a Most mature V6 corn leaf (MM), corn ear leaf (CE), and corn grain P concentrations as effected by P sources ((fluidized bed bulk (FB Bulk), combustion mix (CMix), poultry litter (PL), and triple superphosphate (TSP)) averaged over rate in 2017.

Site Plant Parameter	-----Accomack-----		-----Caroline-----			-----Dinwiddie-----		
	CE	Grain	MM	CE	Grain	MM	CE	Grain
P Sources	Tissue Concentrations g P kg⁻¹							
P Control†	2.70	3.80	2.16	1.95	1.83	2.24	2.27	1.43
PL	2.82	4.21	2.16	2.66 a‡	2.47 a	2.12	2.19	1.84 a
TSP	3.04	4.08	2.23	2.54 ab	2.50 a	2.19	2.32	1.98 a
CMix	2.76	3.97	2.08	2.26 c	2.18 b	2.07	2.09	1.78 a
FB Bulk	2.79	3.82	2.12	2.31 bc	2.06 b	2.07	2.11	1.62 a
LSD 0.10	ns§	ns	ns	0.24	0.17	ns	ns	0.57
<i>p-value</i>								
(P Source × P Rate)	0.55	0.80	0.23	0.98	0.51	0.18	0.77	0.04
P Source	0.30	0.13	0.30	0.03	0.0001	0.68	0.21	0.05
P Rate	0.17¶	0.98	0.13	0.03	0.0001	0.06	0.49	0.59

† P Control data is averaged and was not subjected to ANOVA due to unbalanced replication.

‡ Within columns, means followed by the same letter are not significantly different according to LSD (0.10).

§ ns, non-significant at the 0.10 probability level.

¶ Represents a trend found across P rate (P-Value < 0.20). Represents a trend found across P rate (P-Value < 0.20).

Table 5.8b Most mature V6 corn leaf (MM), corn ear leaf (CE), and corn grain P concentrations as effected by P sources ((fluidized bed bulk (FB Bulk), combustion mix (CMix), poultry litter (PL), and triple superphosphate (TSP)) averaged over rate in 2017.

Site	-----ESAREC-----			-----Essex-----		
Plant Parameter	MM	CE	Grain	MM	CE	Grain
P Sources	Tissue Concentrations g P kg⁻¹					
P Control†	3.65	4.75	5.20	3.40	2.45	3.45
PL	3.65	4.92 a	4.91	3.72	2.55 ab	3.49 ab
TSP	3.62	4.64 ab	4.79	3.54	2.62 a	3.71 a
CMix	3.55	4.56 ab	4.94	3.60	2.24 c	3.05 c
FB Bulk	3.44	4.32 b	4.91	3.47	2.40 bc	3.23 bc
LSD 0.10	ns	0.34	ns	ns	0.20	0.32
<i>p-value</i>						
(P Source × P Rate)	0.30	0.40	0.79	0.58	0.45	0.41
P Source	0.65	0.04	0.85	0.78	0.02	0.008
P Rate	0.54	0.69	0.96	0.49	0.08	0.07

† P Control data is averaged and was not subjected to ANOVA due to unbalanced replication.

‡ Within columns, means followed by the same letter are not significantly different according to LSD (0.10).

§ ns, non-significant at the 0.10 probability level.

¶ Represents a trend found across P rate (P-Value < 0.20). Represents a trend found across P rate (P-Value < 0.20).

Table 5.9 Most mature V6 corn leaf (MM), corn ear leaf (CE), and corn grain P concentrations as effected by phosphorus (P) rate 0, 9.8, 19.6, and 29.3 kg P ha⁻¹ averaged over P sources in 2017.

Site	-Accomack-	----- Caroline -----		--Dinwiddie--	-----Essex-----		
Plant Parameter	CE	MM	CE	Grain	MM	CE	Grain
Rate (kg P ₂ O ₅ ha ⁻¹)	Tissue Concentrations g P kg ⁻¹						
0†	2.70	2.16	1.95	1.83	2.24	2.45	3.45
9.8	2.79	2.07	2.27 b‡	2.13 b	1.99 b	2.32 b	3.15 b
19.6	2.76	2.18	2.44 ab	2.24 b	2.13 ab	2.47 ab	3.44 a
29.3	3.01	2.19	2.62 a	2.53 a	2.22 a	2.56 a	3.53 a
LSD 0.10	ns§	ns	0.21	0.14	0.16	0.18	0.28
<i>p-value</i> (P Source × P Rate)	0.55	0.23	0.98	0.51	0.18	0.45	0.41
P Source	0.30	0.30	0.03	0.0001	0.68	0.02	0.008
P Rate	0.17¶	0.13	0.03	0.0001	0.06	0.08	0.07

† P Control data is averaged and was not subjected to ANOVA due to unbalanced replication.

‡ Within columns, means followed by the same letter are not significantly different according to LSD (0.10).

§ ns, non-significant at the 0.10 probability level.

¶ Represents a trend found across P rate (P-Value < 0.20). Represents a trend found across P rate (P-Value < 0.20).

Table 5.10 Most mature V6 corn leaf (MM), corn ear leaf (CE), and corn grain phosphorus (P) concentrations as effected by P sources including: P control, fluidized bed bulk (FB Bulk), granulated poultry litter ash (GPLA), poultry litter (PL), and triple superphosphate (TSP) averaged over P rate in 2018.

Site	-----Dinwiddie-----			-----ESAREC-----			-----Essex-----			-----Mecklenburg-----		
Plant Parameter	MM	CE	Grain	MM	CE	Grain	MM	CE	Grain	MM	CE	Grain
P Sources	Tissue Concentrations g P kg ⁻¹											
P Control†	3.80	2.53	2.22	5.08	4.15	3.63	4.25	3.43	3.88	3.48	3.33	3.83
PL	4.11 b‡	2.44 b	2.43 a	4.91 b	3.74 c	4.00	4.06 b	3.18 b	3.37 b	3.67	3.17	3.77
TSP	4.54 a	2.88 a	2.67 a	5.25 a	4.32 a	3.85	4.41 a	3.53 a	3.95 a	3.89	3.22	3.59
GPLA	4.04 b	2.33 bc	2.23 b	5.13 ab	4.10 b	3.72	4.07 b	3.27 b	3.44 b	3.58	3.48	3.29
FB Bulk	3.75 c	2.16 c	2.23 b	5.29 a	3.89 bc	3.80	4.05 b	3.10 b	3.33 b	3.50	3.12	3.45
LSD_{0.10}	0.28	0.20	0.19	0.29	0.22	ns§	0.24	0.25	0.35	ns	0.24	ns
<i>p-value</i>												
(P Source × P Rate)	0.33	0.54	0.47	0.69	0.99	0.84	0.17	0.45	0.22	0.15	0.05	0.59
P Source	0.0004	<0.0001	0.02	0.09	0.0008	0.28	0.04	0.06	0.02	0.36	0.15	0.17
P Rate	0.03	0.44	0.001	0.72	0.50	0.78	0.18¶	0.26	0.33	0.41	0.13	0.36

† P Control data is averaged and was not subjected to ANOVA due to unbalanced replication.

‡ Within columns, means followed by the same letter are not significantly different according to LSD (0.10).

§ ns, non-significant at the 0.10 probability level.

¶ Represents a trend found across P rate (P-Value < 0.20).

Table 5.11 Most mature V6 corn leaf (MM), corn ear leaf (CE), and corn grain phosphorus (P) concentrations as effected by P rate 0, 9.8, 19.8, 29.3 kg P ha⁻¹ averaged over P sources in 2018.

Site	-----Dinwiddie-----		-----Essex-----		--Mecklenburg--
Plant Parameter	MM	Grain	MM		CE
Rate (kg P ha ⁻¹)	Tissue Concentrations g P kg ⁻¹				
0†	3.80	2.22	4.25		3.33
9.8	3.94 b‡	2.16 c	4.03		3.08 b
19.6	4.07 b	2.38 b	4.26		3.28 a
29.3	4.33 a	2.55 a	4.16		3.37 a
LSD 0.10	0.24	0.16		ns§	0.24
<i>p-value</i>					
(P Source × P Rate)	0.33	0.47	0.17		0.05*
P Source	0.0004	0.02	0.04		0.15
P Rate	0.03	0.001	0.18¶		0.13

† P Control data is averaged and was not subjected to ANOVA due to unbalanced replication.

‡ Within columns, means followed by the same letter are not significantly different according to LSD (0.10).

§ ns, non-significant at the 0.10 probability level.

¶ Represents a trend found across P rate (P-Value < 0.20).

Table 5.12 Mehlich-1 soil test (0-15 cm) phosphorus (P) levels as effected by P sources ((fluidized bed bulk (FB Bulk), combustion mix (CMix), poultry litter (PL), and triple superphosphate (TSP)) averaged over P rate in 2017.

Site	All 2017 Sites
Phosphorus Source	mg P kg ⁻¹
P Control†	23.1
PL	22.4
TSP	22.2
CMix	20.2
FB Bulk	23.6
	LSD 0.10
	ns§
<i>p-value</i>	
(Site × P Source × P Rate)	0.96
(Site × P Source)	0.82
(Site × P Rate)	0.46
(P Source × P Rate)	0.94
Site	<0.0001
P Source	0.49
P Rate	0.008 ¶

† P Control data is averaged and was not subjected to ANOVA due to unbalanced replication.

‡ Within columns, means followed by the same letter are not significantly different according to LSD (0.10).

§ ns, non-significant at the 0.10 probability level.

¶ Represents a trend found across P rate (P-value <0.20).

Table 5.13 Mehlich-1 soil test (0-15 cm) phosphorus (P) levels as effected by P sources ((fluidized bed bulk (FB Bulk), combustion mix (CMix), poultry litter (PL), and triple superphosphate (TSP)) averaged over P rate in 2017 sites.

Site	Accomack	Caroline	Dinwiddie	ESAREC	Essex
Phosphorus Source	mg P kg⁻¹				
P Control†	12.1	4.6	4.1	86.2	8.5
PL	10.9 b	9.9 a	4.9 b‡	79.4	6.6
TSP	11.0 b	10.3 a	5.9 ab	74.5	9.1
CMix	11.4 b	7.8 a	3.9 b	69.7	8.4
FB Bulk	17.5 a	9.9 a	8.7 a	70.6	11.3
LSD_{0.10}	4.2	2.56	3.2	ns	ns
<i>p-value</i>					
Site					
(P Source × P Rate)	0.06	0.078	0.81	0.92	0.60
P Source	0.07	0.49	0.08	0.73	0.11
P Rate	0.13¶	0.003	0.53	0.18	0.17

† P Control data is averaged and was not subjected to ANOVA due to unbalanced replication.

‡ Within columns, means followed by the same letter are not significantly different according to LSD (0.10).

§ ns, non-significant at the 0.10 probability level.

¶ Represents a trend found across P rate (P-value <0.20).

Table 5.14 Mehlich-1 soil test (0-15 cm) phosphorus (P) levels as effected by P rate 0, 9.8, 19.6, 29.3 kg P ha⁻¹ averaged over P sources in 2017.

Site Rate (kg P ha ⁻¹)	All 2017 Sites mg P kg ⁻¹
0†	23.1
9.8	19.4 c‡
19.6	21.5 bc
29.3	25.3 a
LSD 0.10	3.0
<i>p-value</i>	
(Site × P Source × P Rate)	0.96
(Site × P Source)	0.82
(Site × P Rate)	0.46
(P Source × P Rate)	0.94
Site	<0.0001
P Source	0.49
P Rate	0.008 §

† P Control data is averaged and was not subjected to ANOVA due to unbalanced replication.

‡ Within columns, means followed by the same letter are not significantly different according to LSD (0.10).

§ Represents a trend found across P rate (P-Value < 0.20).

Table 5.15 Mehlich-1 soil test (0-15 cm) phosphorus (P) levels as effected by P rate 0, 9.8, 19.6, 29.3 kg P ha⁻¹ averaged over P sources in 2017 sites.

Site	Accomack	Caroline	ESAREC	Essex
Rate (kg P ha ⁻¹)	mg P kg ⁻¹			
0†	12.1	4.6	86.2	8.5
9.8	11.8 a	7.5 b	65.8	7.2
19.6	10.7 b	8.2 b	73.4	9.1
29.3	15.6 a	12.7 a	81.4	10.3
LSD_{0.10}	4.2	2.6	ns	ns
<i>p-value</i>				
Site				
(P Source × P Rate)	0.06	0.078	0.92	0.60
P Source	0.07	0.49	0.73	0.11
P Rate	0.14¶	0.003	0.18	0.17

† P Control data is averaged and was not subjected to ANOVA due to unbalanced replication.

‡ Within columns, means followed by the same letter are not significantly different according to LSD (0.10).

§ ns, non-significant at the 0.10 probability level.

¶ Represents a trend found across P rate (P-Value < 0.20).

Table 5.16 Mehlich-1 soil test (0-15 cm) phosphorus (P) levels as effected by P sources ((fluidized bed bulk (FB Bulk), granulated poultry litter ash (GPLA), poultry litter (PL), and triple superphosphate (TSP)) averaged over P rate in 2018.

Site	All 2018 Sites
Phosphorus Source	mg P kg ⁻¹
P Control†	18.5
PL	15.4 b‡
TSP	19.7 a
GPLA	17.5 ab
FB Bulk	20.7 a
	LSD 0.10
	3.2
<i>p-value</i>	
(Site × P Source × P Rate)	0.65
(Site × P Source)	0.89
(Site × P Rate)	0.74
(P Source × P Rate)	0.14
Site	<0.0001
P Source	0.04
P Rate	0.84

*Significant at the 0.10 probability level.

** Significant at the 0.05 probability level.

*** Significant at the 0.001 level.

† P Control data is averaged and was not subjected to ANOVA due to unbalanced replication.

‡ Within columns, means followed by the same letter are not significantly different according to LSD (0.10).

§ ns, non-significant at the 0.10 probability level.

¶ Represents a trend found across P rate (P-Value < 0.20).

Table 5.17 Mehlich-1 soil test (0-15 cm) phosphorus (P) levels as effected by P sources ((fluidized bed bulk (FB Bulk), granulated poultry litter ash (GPLA), poultry litter (PL), and triple superphosphate (TSP)) averaged over P rate in 2018 sites.

Site	Dinwiddie	ESAREC	Essex	Mecklenburg
Phosphorus Source	mg P kg⁻¹			
P Control†	6.7	23.1	25.8	21.2
PL	6.3 b	25.4	13.2 c	16.6
TSP	8.4 a	31.9	21.0 a	17.3
GPLA	6.1 b	26.2	19.3 b	18.5
FB Bulk	8.3 a	33.6	20.6 a	20.4
LSD_{0.10}	1.7	ns§	5.5	ns
<i>p-value</i>				
(P Source × P Rate)	0.69	0.49	0.32	0.35
P Source	0.03	0.15	0.07	0.91
P Rate	0.81	0.72	0.18¶	0.81

† P Control data is averaged and was not subjected to ANOVA due to unbalanced replication.

‡ Within columns, means followed by the same letter are not significantly different according to LSD (0.10).

§ ns, non-significant at the 0.10 probability level.

¶ Represents a trend found across P rate (P-Value < 0.20).

Table 5.18 Corn yield response to potassium (K) sources K control, fluidized bed fly (FB Fly), fluidized bed bulk (FB Bulk), combustion mix (CMix), poultry litter (PL), and muriate of potash (KCL) in 2017 and 2018.

Site	Across Site Year	All Sites	
Year	Both	2017	2018
K Source	Yield (kg ha ⁻¹)		
KControl	8,356	4,662	11,513
FB Fly	8,409	4,829	11,103
FB Bulk	7,982	3,925	11,313
CMix	7,966	4,158	11,537
PL	8,560	4,786	11,482
KCl	8,747	4,316	12,718
LSD 0.10	ns‡	ns	ns
<i>p-value</i>			
(Year × Site × Source)	0.86	na§	na
(Year × Site)	0.01	na	na
(Year × Source)	0.31	na	na
(Site × Source)	0.62		
Year	<0.0001	na	na
Site	<0.0001	<0.0001	<0.0001
Source	0.41	0.43	0.44

† Within columns, means followed by the same letter are not significantly different according to LSD (0.10).

‡ ns, non-significant at the 0.10 probability level.

§ na, not applicable.

Table 5.19 Corn yield response to potassium (K) sources K control, fluidized bed fly (FB Fly), fluidized bed bulk (FB Bulk), combustion mix (CMix), poultry litter (PL), and muriate of potash (KCL) in 2017 and 2018.

Site	Accomack	Caroline	Dinwiddie		ESAREC		Essex	
Year	2017	2017	2017	2018	2017	2018	2017	2018
K Source	Yield (kg ha ⁻¹)							
KControl	2,359	5,355	5,193	10,797	5,932	13,924	4,472	9,827 b†
FB Fly	3,223	4,409	6,204	10,479	5,100	13,482	4,418	9,353 b
FB Bulk	2,747	2,296	5,063	10,564	5,597	13,302	4,714	10,064 b
CMix	3,998	3,606	4,322	10,698	5,573	13,518	3,289	10,397 b
PL	3,138	3,876	6,875	10,825	5,729	13,389	4,313	10,217 b
KCl	3,322	3,973	3,924	11,249	5,611	13,133	4,795	13,771 a
LSD 0.10	ns	ns	ns	ns	ns	ns	ns	2,574
<i>p-value</i>								
Source	0.14	0.24	0.43	0.98	0.98	0.63	0.80	0.09

† Within columns, means followed by the same letter are not significantly different according to LSD (0.10).

‡ ns, non-significant at the 0.10 probability level.

§ na, not applicable.

Table 5.20a Most mature V6 corn leaf (MM), corn ear leaf (CE), and corn grain K concentrations as effected by potassium (K) sources K control, fluidized bed fly (FB Fly), fluidized bed bulk (FB Bulk), combustion mix (CMix), poultry litter (PL), and muriate of potash (KCl) in 2017.

Site Plant Parameters	-----Accomack-----		-----Caroline-----			-----Dinwiddie -----		
	CE	Grain	MM	CE	Grain	MM	CE	Grain
K Source	Tissue Concentrations g K kg⁻¹							
K Control	14.78c†	4.23 b	30.13 bc	18.99	3.74 c	22.75	23.85	2.03
FB Fly	17.20 a	4.25 b	29.55 c	19.69	4.33 ab	25.70	24.38	1.85
FB Bulk	17.03 a	4.13 b	29.98 bc	18.99	4.15 bc	25.38	22.35	1.83
CMix	16.65 ab	4.28 b	32.65 a	18.72	4.49 ab	24.48	25.20	2.13
PL	15.50 bc	4.75 a	31.90 ab	19.72	4.67 a	23.78	23.63	2.05
KCl	16.28 ab	4.12 b	32.38 a	19.68	4.13 bc	23.88	24.65	1.93
LSD_{0.10}	1.31	0.34	2.06	ns‡	0.48	ns	ns	ns
<i>p-value</i> Source	0.04	0.05	0.06	0.94	0.06	0.12	0.32	0.37

† Within columns, means followed by the same letter are not significantly different according to LSD (0.10).

‡ ns, non-significant at the 0.10 probability level.

Table 5.20b Most mature V6 corn leaf (MM), corn ear leaf (CE), and corn grain K concentrations as effected by potassium (K) sources K control, fluidized bed fly (FB Fly), fluidized bed bulk (FB Bulk), combustion mix (CMix), poultry litter (PL), and muriate of potash (KCl) in 2017.

Site	-----ESAREC-----			-----Essex-----		
Plant Parameters	MM	CE	Grain	MM	CE	Grain
K Source	Tissue Concentrations g K kg⁻¹					
K Control	25.48	22.28 ab	6.06	27.76	26.65	5.05
FB Fly	25.38	21.53 bc	6.02	28.66	26.57	5.05
FB Bulk	25.18	21.13 bc	5.98	29.85	28.03	5.18
CMix	27.08	23.50a	5.61	28.61	25.23	5.18
PL	26.63	20.30	5.52	29.36	26.70	5.18
KCl	26.13	22.48 ab	5.68	29.59	25.77	4.95
LSD_{0.10}	ns	1.9	ns	ns	ns	ns
<i>p-value</i>						
Source	0.36	0.10	0.37	0.25	0.28	0.95

† Within columns, means followed by the same letter are not significantly different according to LSD (0.10).

‡ ns, non-significant at the 0.10 probability level.

Table 5.21 Most mature V6 corn leaf (MM), corn ear leaf (CE), and corn grain K concentrations as effected by potassium (K) sources K control, fluidized bed fly (FB Fly), fluidized bed bulk (FB Bulk), combustion mix (CMix), poultry litter (PL), and muriate of potash (KCl) in 2018.

Site	-----Dinwiddie-----			-----ESAREC-----			-----Essex-----		
Plant Parameter	MM	CE	Grain	MM	CE	Grain	MM	CE	Grain
K Source	Tissue Concentrations g P kg⁻¹								
K Control	26.05 c†	20.73	3.85 abc	31.83	27.43	4.55	27.03	18.95	5.08
FB Fly	28.70 ab	22.30	3.23 d	32.63	27.43	4.75	29.33	20.23	5.25
FB Bulk	27.55 bc	23.33	3.90 abc	30.50	27.20	4.68	29.99	21.73	5.40
CMix	29.93 a	22.43	3.68 c	28.95	27.48	4.53	30.75	21.80	5.18
PL	28.15 b	22.18	4.08 ab	30.85	28.60	4.83	29.88	21.33	6.75
KCl	28.55 ab	22.90	4.23 a	34.00	29.13	4.75	30.08	21.03	5.48
LSD_{0.10}	1.68	ns‡	0.37	ns	ns	ns	ns	ns	ns
<i>p-value</i>									
Source	0.04	0.26	0.006	0.21	0.82	0.81	0.20	0.12	0.43

† Within columns, means followed by the same letter are not significantly different according to LSD (0.10).

‡ ns, non-significant at the 0.10 probability level.

Table 5.22 Mehlich-1 soil test (0-15 cm) potassium (K) concentrations by poultry litter ash K sources including: K control, fluidized bed fly (FB Fly), fluidized bed bulk (FB Bulk), combustion mix (CMix), poultry litter (PL), and muriate of potash (KCl).

Site	Across Site Year†		-----All Sites-----		
Year			2017	2018	
K Source			mg K kg ⁻¹		
K Control	73.3		83.8	22.4	
FB Fly	86.8		97.3	35.7	
FB Bulk	83.9		100.4	18.2	
CMix	85.0		94.6	14.7	
PL	86.6		104.7	19.9	
KCl	88.94		97.9	20.3	
LSD 0.10		13.4		10.4	ns§
<i>p-value</i>					
(Year × Site × Source)	0.81		na ¶	na	
(Year × Site)	<0.0001		na	na	
(Year × Source)	0.97		na	na	
(Site × Source)	0.92		na	na	
Year	<0.0001		na	na	
Site	0.13		<0.0001	<0.0001	
Source	0.35		0.06	0.81	

† Across Site years only includes replicated sites (ESAREC, Essex, and Dinwiddie) and excludes Accomack and Caroline.

‡ Within columns, means followed by the same letter are not significantly different according to LSD (0.10).

§ ns, non-significant at the 0.10 probability level.

¶ na, not applicable

Table 5.23 Mehlich-1 soil test (0-15 cm) potassium (K) concentrations by poultry litter ash K sources including: K control, fluidized bed fly (FB Fly), fluidized bed bulk (FB Bulk), combustion mix (CMix), poultry litter (PL), and muriate of potash (KCl).

Site	Accomack	Caroline	--Dinwiddie--		----ESAREC----		-----Essex-----	
Year	2017	2017	2017	2018	2017	2018	2017	2018
K Source	mg K kg ⁻¹							
K Control	92.2	42.4 c‡	105.6	27.3	84.4	69.5	94.6	58.5
FB Fly	96.7	57.4 bc	130.3	33.5	101.1	94.9	109.4	60.0
FB Bulk	101.6	68.4 ab	121.4	37.4	95.1	56.2	106.8	78.0
CMix	94.4	61.3 bc	130.1	38.3	92.9	77.5	94.5	76.6
PL	96.8	92.6 a	116.5	37.7	103.5	89.5	113.9	58.6
KCl	97.4	51.9 bc	120.8	36.9	103.5	75.3	116.0	81.1
LSD 0.10		ns	2.4	ns	ns	ns	ns	ns
<i>p-value</i>								
Site								
Source	0.93	0.04	0.42	0.67	0.37	0.54	0.47	0.75

† Across Site years only includes replicated sites (ESAREC, Essex, and Dinwiddie) and excludes Accomack and Caroline.

‡ Within columns, means followed by the same letter are not significantly different according to LSD (0.10).

§ ns, non-significant at the 0.10 probability level.

Table 5.24 Corn yield response to nitrogen (N) sources including: N control, ash coated urea (ACU), and urea (CO(NH₂)₂) utilized as starter and side dress N in 2017.

Site	All Sites
N Source	kg ha ⁻¹
N Control	2,082 b†
ACU	4,854 a
Urea	4,380 a
	LSD 0.10 854
<i>p-value</i>	
(Site × Source)	0.03
Site	<0.0001
Source	<0.0001

† Within columns, means followed by the same letter are not significantly different according to LSD (0.10).

‡ ns, non-significant at the 0.10 probability level.

Table 5.25 Corn yield response to nitrogen (N) sources including: N control, ash coated urea (ACU), and urea (CO(NH₂)₂) utilized as starter and side dress N in 2017 sites.

Site	Accomack	Caroline	Dinwiddie	Essex	ESAREC
N Source	kg ha⁻¹				
N Control	866 b	3,248 ab	3,073 b	2,133	1,088 b
ACU	2,998 a	4,453ba	7,117 a	3,288	6,413 a
Urea	2,854 a	2,712 b	7,165 a	3,604	5,567 a
LSD_{0.10}	1,267	1,289	2,620	ns‡	2,867
<i>p-value</i>					
Source	0.03	0.09	0.04	0.41	0.02

† Within columns, means followed by the same letter are not significantly different according to LSD (0.10).

‡ ns, non-significant at the 0.10 probability level.

Table 5.26 Corn yield response to nitrogen (N) sources including: N control, ash coated urea (ACU), urea (CO(NH₂)₂), urea starter with ACU at side dress (Urea/ACU), and ACU starter with urea at side dress (Urea/ACU) in 2018.

Sites	All Sites
N Source	kg ha ⁻¹
N Control	6,248 b†
ACU	11,206 a
Urea	11,504 a
Urea/ACU	11,032 a
ACU/Urea	10,848 a
	LSD_{0.10}
	1,114
P-Value	
(Site × Source)	0.87
Site	<0.0001
Source	<0.0001

† Within columns, means followed by the same letter are not significantly different according to LSD (0.10).

Table 5.27 Corn yield response to nitrogen (N) sources including: N control, ash coated urea (ACU), urea (CO(NH₂)₂), urea starter with ACU at side dress (Urea/ACU), and ACU starter with urea at side dress (Urea/ACU) in 2018 sites.

Sites	Dinwiddie	ESAREC	Essex
N Source			
N Control	2,093 c	9,408 b	4,668 b
ACU	5,521 a	12,982 a	10,319 a
Urea	5,468 a	12,967 a	10,773 a
Urea/ACU	5,582 a	13,405 a	9,846 a
ACU/Urea	4,995 b	12,928 a	9,808 a
LSD 0.10	411	1,049	1,843
P-Value			
Source	<0.0001	0.0001	0.0004

† Within columns, means followed by the same letter are not significantly different according to LSD (0.10).

Table 5.28a Corn plant tissue (most mature (MM), corn ear leaf (CE), and grain) response to nitrogen (N) sources including: N control, ash coated urea (ACU), and urea (CO(NH₂)₂) utilized as starter and side dress N in 2017 sites.

Site	-----Accomack-----		-----Caroline-----			-----Dinwiddie-----		
	CE	Grain	MM	CE	Grain	MM	CE	Grain
Source	g N Kg ⁻¹							
N Control	13.37	11.38 b†	43.38 b	27.78 b	13.30	26.53	24.70	10.30 a
ACU	14.00	14.00 a	45.55 a	37.28 a	15.75	24.68	24.95	9.13 b
Urea	13.00	13.18 ab	43.78 b	35.20 a	13.93	25.65	22.25	8.75 b
LSD 0.10	ns‡	1.87	1.54	3.64	ns	ns	ns	1.04
<i>p-value</i>								
Source	0.68	0.08	0.07	0.01	0.11	0.84	0.57	0.06

† Within columns, means followed by the same letter are not significantly different according to LSD (0.10).

‡ ns, non-significant at the 0.10 probability level.

Table 5.28b Corn plant tissue (most mature (MM), corn ear leaf (CE), and grain) response to nitrogen (N) sources including: N control, ash coated urea (ACU), and urea (CO(NH₂)₂) utilized as starter and side dress N in 2017 sites.

Site	-----ESAREC-----			-----Essex-----		
	MM	CE	Grain	MM	CE	Grain
Source	g N Kg ⁻¹					
N Control	28.05	19.67	11.20 b	27.36 b	17.35 b	11.93
ACU	36.03	29.20	13.85 a	33.10 a	22.70 a	14.20
Urea	35.50	28.88	13.43 a	32.25 a	22.25 a	13.65
LSD 0.10	ns	2.02	2.02	3.42	2.23	ns
<i>p-value</i>						
Source	0.12	0.15	0.01	0.03	0.01	0.14

† Within columns, means followed by the same letter are not significantly different according to LSD (0.10).

‡ ns, non-significant at the 0.10 probability level.

Table 5.29 Corn plant tissue (most mature (MM), corn ear leaf (CE), and grain) response to nitrogen (N) sources including: N control, ash coated urea (ACU), and urea (CO(NH₂)₂) utilized as starter and side dress N in 2018 sites.

Site	-----Dinwiddie-----			-----ESAREC-----			-----Essex-----		
	MM	CE	Grain	MM	CE	Grain	MM	CE	Grain
Source	g N kg ⁻¹								
N Control	29.23 b†	15.05 b	10.53 b	37.68 b	19.28 b	11.48 b	31.00 c	16.98 b	12.20
ACU	40.88 a	26.78 a	10.28 b	43.45 a	29.20 a	11.93 b	39.45 b	29.55 a	14.03
Urea	40.08 a	28.40 a	11.08 ab	43.45 a	28.88 a	11.80 b	42.45 a	28.70 a	12.78
ACU/Urea	40.53 a	28.75 a	12.05 a	43.30 a	28.40 a	13.33 b	40.35 ab	29.00 a	13.80
Urea/ACU	41.80 a	28.35 a	12.43 a	44.38 a	30.15 a	16.58 a	39.53 b	29.20 a	14.05
LSD 0.10	3.42	3.75	1.43	3.74	2.58	2.04	2.91	1.68	ns‡
<i>p-value</i>									
Source	0.0001	0.0001	0.08	0.04	<0.0001	0.003	0.0002	<0.0001	0.54

† Within columns, means followed by the same letter are not significantly different according to LSD (0.10).

‡ ns, non-significant at the 0.10 probability level

Chapter 6: Conclusions

Collectively across elemental and speciation analysis, granulation, solubility, and corn field trials, poultry litter ash (PLA) is a comparable N fortified, P, and K alternative fertilizer source to poultry litter (PL). Both P and K PLA concentrations when compared to industry fertilizers [triple superphosphate (TSP) or muriate of potash (KCl)] are considerably lower analysis fertilizer sources; therefore, higher PLA application rates will be required if substituted for TSP or KCl. Considering P solubility constraints controlled by Ca-phosphate compounds and species, monetite (CaHPO_4) and brushite ($\text{CaHPO}_4 \cdot 2\text{H}_2\text{O}$), PLA granulation improves solubility. Enhancing PLA into GPLA solves agronomic obstacles identified in the current projects and previous studies including increasing total and water soluble P, improving land application, transportation, and storage, by granulizing PLA into a convenient fertilizer granule form. Potassium provided by PLA is a readily available source and is a comparable nutrient source to PL and KCl that provided season long K availability to maintain sufficient corn growth. Ash coated urea, FB Fly coated onto a urea granule, proved to be a consistent N source. Noticeable differences due to volatility inhibitors in ACU binder had little to no effect observed on plant parameters; however, that is not to completely disqualify ACU as a controlled or volatility inhibited N source. Future laboratory and field research is needed to examine potential ACU properties, specifically PLA ability to improve volatility inhibitors effectiveness. Improving PLA P solubility and physical characteristics and inventing PLA into fortified N products alters a waste product into a value added fertilizer source. Poultry litter ash transformation into valuable and comparable nutrient sources provides an opportunity and innovative channel to catalyze PL nutrient redistribution from regions with excess nutrients to crop deficit areas within the Commonwealth of Virginia and beyond.